NBSIR 80-1987

A Mathematical Model for Use in Evaluating and Developing Impact Test Methods for Protective Headgear

Robert E. Berger

Product Safety Technology Division
Center for Consumer Product Technology
National Engineering Laboratory
National Bureau of Standards
U.S. Department of Commerce
Washington, D.C. 20234

October 1979

Issued March 1980

U.S. DEPARTMENT OF COMMERCE

NATIONAL BUREAU OF STANDARDS

NBSIR 80-1987

A MATHEMATICAL MODEL FOR USE IN EVALUATING AND DEVELOPING IMPACT TEST METHODS FOR PROTECTIVE HEADGEAR

Robert E. Berger

Product Safety Technology Division
Center for Consumer Product Technology
National Engineering Laboratory
National Bureau of Standards
U.S. Department of Commerce
Washington, D.C. 20234

October 1979

Issued March 1980

ABSTRACT

A lumped parameter mathematical model was developed to connect injury parameters in real life head impact environments to output parameters of test methods for evaluating protective headgear. Analytical/experimental schemes were developed for mathematically representing the parameters that characterize each of the three distinct elements of the model: the head or headform, the impact surface, the helmet. A comparison of the model output to experimental results showed a satisfactory agreement. The model was shown to be useful in determining test method pass/fail criteria which correspond to the threshold of injury in the real life situation.

CONTENTS

1. INTRODUCTION

This report describes a rational connection between the real life head injury environment and the method by which the impact attenuation characteristics of protective headgear are evaluated. The complexity of this problem is such that we sacrifice some rigor (e.g., we use a rather unsophisticated mathematical model) in favor of preserving the aforementioned injury/test connection. Undoubtedly, many refinements and improvements in approach will be suggested as one follows the rational development. Nevertheless, given the existing state of test methods for protective headgear and the present lack of supporting rationales, it is suggested that the methods described herein can provide a useful tool for those concerned with rational test method development and promulgation.

A one-dimensional lumped-parameter mathematical model is used to predict the linear acceleration response history of a helmeted head or headform. The model, which is described in more detail in chapter 2, is capable of simulating a range of real life situations and a range of test method configurations. The elements of the model include the head (or headform), the helmet, and the object which strikes the head. Each of these elements is composed of several parameters (modelled as masses, springs, and dash pots). The behavior of each element, and hence of the full system, depends on the parameter values which are chosen on the basis of two sets of experimental data:

1. Data which isolates some particular element so that its deformation characteristics can be chosen independent of the other elements. The use of these data in choosing values for the parameters of the model is shown in chapter 3.

2. Data which represents the response of the system as a whole. This data was gathered in a previous study 1/, which was concerned with the effect of changing test parameters on the impact response of helmeted headforms.

The ability of the model to predict these experimental results serves as measure of its validity. The comparison of the predictions of the model to the experimental behavior is shown in chapter 4.

Finally, to illustrate how the model might be used in developing test method criteria, an example for football helmets is given in chapter 5.

2. THE MODEL

Except for a few minor changes, the model is the same as that described in a previous report 2/. In that study, the model was used to illustrate quantitatively the effect of changing test parameters; however, no attempt was made to assign realistic values for parameters.

The model is used to calculate the linear acceleration response of a one-dimensional system which consists of three distinct elements (figure 1):

1. head or headform

2. helmet

3. impact surface

The representation of this system by a one-dimensional model must be regarded as a major assumption. This basic assumption underlies every existing headgear test method, all of which measure the linear acceleration in one-dimensional drop tests. The widespread adoption of linear acceleration as a head injury indicator has been based on laboratory impact experiments with cadavers, where the head was observed to move relatively independent of the body, and on the fact that, in live subjects, the duration of impact is small compared to the neck muscle reaction time 3/.

Referring to figure 1, x_1 is the instantaneous position of the head/helmet interface and x_3 is the instantaneous position of the helmet/impact surface interface . (Note: x_2 will be reserved for the humanoid headform, as discussed below. Also, $x_1 = x_3$ will represent the instantaneous position of the head/impact surface interface when there is no helmet.) In this work, we will adopt the convention that $x = 0$ represents the initial position of the head/helmet interface. Each element will now be examined in more detail:

2.1 Impacting Object

The impacting object may be of finite or infinite size. The latter condition represents a situation where a helmeted head strikes a surface such as the football field or a road. For the massive surface, the helmeted head is assumed to be traveling initially at speed V toward the impact surface. For smaller impacting objects, the object is assumed to be travelling at speed V toward the stationary helmeted head.

2.2 Impact Surface

The impact surface is considered to be rigid for small impacting objects, but may be either rigid or resilient for massive impact surfaces. When the massive impact surface is rigid, the helmet/impact surface interface remains fixed at the position $x_3 = D$, where D is the initial thickness of the helmet liner.

When the (massive) impact surface is resilient, a functional relationship is assumed between the force, F, on the helmet and the displacement, $x = x_3 - D$, of the helmet/impact surface interface:

$$F = f(x) \qquad (1)$$

For example, many surfaces can be represented by a power law function,

$$F = Bx^p \qquad (1a)$$

Where B and p are chosen to fit experimental data as described in section 3.1. In particular, if the deformation of the surface is such that theories of quasi-static, elastic impact apply, the exponent will have the value $p = 1.5$, while B depends upon the geometry and material characteristics of the impacting objects 4/. Usually, these theories are valid only if the deformation of the surface is small compared to its thickness.

In contrast, deformations for some common surfaces (such as artificial turf) may be significant compared to its thickness. For such surfaces, alternative formulations of f(x) must be generated. The following formulation was chosen to represent artificial turf:

$$f(x) = \frac{Bx}{\sqrt{d^2 - x^2}}, \qquad (1b)$$

where d is some effective thickness of the surface. In this case, B and d are chosen to fit experimental data. The formulation in (1b) was chosen because: (1) it possesses such desirable properties as $f(x) = 0$ when $x = 0$ and $f(x) \to \infty$ when $x \to d$, (2) it is easily integrable (the value of this will become evident in section 3.1), and (3) it is suitable for fitting experimental data (section 3.1).

2.3 Head or Headform

The head is considered to be resilient, but the headform may be either rigid or resilient. Rigid metal headforms are prescribed in many current impact tests for protective headgear. In the model, the metal headform is treated as a rigid body of mass, M_R. The resilient headform model (sketched in figure 2) represents the human head (in a real life injury situation) or a humanoid headform. The response of this model was shown to represent the driving point impedance response of cadaver heads 5/. The humanoid headform used in the aforementioned experimental study 1/ was also shown to exhibit a driving point impedance response which was similar to cadaver heads 3/. This model's linear acceleration response to impact also agrees well with the response of the humanoid headform (see section 3.2). The values of parameters K, C, M_1, M_2 depend on the impact location (front, top, side, back, etc.).

The deformation of the headform model is described by

$$F_H = K \quad [L - (x_1 - x_2)] \quad + C(\dot{x}_2 - \dot{x}_1) \qquad (2)$$

where F_H is the force between the masses of the headform element. (The dot notation above the symbol denotes differentiation with respect to time.) L is an arbitrary separation of the two masses; the acceleration response of the headform is independent of L.

2.4 Helmet

The mass of the helmet is assumed to have little or no influence on the impact response since: (1) only a small portion of the helmet takes part in the energy absorbing process during the impact, and (2) the kinetic energy associated with the rest of the helmet has been observed to be dissipated in flexural vibrations during impact. In figure 1, therefore, the force is depicted as the same on both sides of the helmet.

In general, the deformation of the helmet liner will be described by some functional relationship between the force, F, the compressive strain, ε, and the strain rate, $\dot{\varepsilon}$:

$$f(F, \varepsilon, \dot{\varepsilon}) = 0 \qquad (3)$$

In terms of the notation of figure 1:

$$\varepsilon = 1 - \frac{x_3 - x_1}{D} \quad \text{and} \quad \dot{\varepsilon} = \frac{\dot{x}_1 - \dot{x}_3}{D}$$

where D is the initial thickness of the helmet liner.

Two linear spring/dashpot models, the Voigt and Maxwell elements, were employed in the aforementioned study 2/ and are shown in figure 3. For each, in turn, equation 3 becomes 2/:

$$\text{Maxwell:} \quad \dot{F} = E_1 A \, \dot{\varepsilon} - \frac{E_1}{\eta} F \qquad (3a)$$

$$\text{Voigt:} \quad F = E_1 A \varepsilon + \eta A \dot{\varepsilon} \qquad (3b)$$

where A is the area of contact.

The response of these elements was unsatisfactory (see section 3.3), hence another model was constructed by adding a non-linear spring in parallel with the Maxwell element (figure 3c). The net force in the element is therefore given by

$$F = E_2 A \varepsilon^r + F_M \qquad (3c)$$

where F_M is the force in the Maxwell element. Combining with equation (3a), this new element is described by:

$$F = E_1A\dot{\varepsilon} - \frac{E_1}{\eta} F + \frac{E_1}{\eta} E_2A\varepsilon^r + E_2Ar\varepsilon^{r-1}\dot{\varepsilon} \quad (3d)$$

2.5 Equations

The system is completed by adding equations of motion for each of the masses.

$$M_1\ddot{x}_1 = F_H - F \quad (4)$$

$$M_2\ddot{x}_2 = -F_H \quad (5)$$

For the case of a resilient helmeted headform, resilient impact surface and massive impacting object, equations (1), (2), (3), (4) and (5) represent five ordinary differential equations for the five unknowns x_1, x_2, x_3, F, F_H. These equations must be supplemented by the initial conditions

$$x_1(0) = 0$$

$$\dot{x}_1(0) = V$$

$$x_2(0) = -L$$

$$\dot{x}_2(0) = V$$

$$F(0) = 0.$$

If there is no helmet, $x_1 = x_3$ and equation (3) is eliminated.

If the impact surface is rigid, x_3 is no longer a variable and equation (1) is not used. For small impacting objects, which are allowed only when the impact surface is rigid (this restriction could be easily surmounted), x_3 is again a variable and a new equation is added:

$$M_3\ddot{x}_3 = F \quad (6)$$

with initial conditions

$$x_3(0) = D$$

$$\dot{x}_3(0) = -V$$

Of course, the initial conditions for $\dot{x}_1$ and $\dot{x}_2$ then become

$$\dot{x}_1(0) = \dot{x}_2(0) = 0.$$

For a rigid headform, equation (2) and the variable F_H are eliminated and M_1 is replaced by M_R in equation (4).

2.6 Output

The system of differential equations was solved numerically on an Interdata 32 mini-computer using a modified Runga-Kutta method 6/ which computes the solution at N equally spaced time steps with interval t. The accuracy was verified by: (1) comparing the results to simple cases for which the exact solution was easily determined, and (2) computing the results for the same conditions when the time step was reduced by an order of magnitude. The output variable of most interest was the acceleration of the headform (the mass M_2 when the humanoid headform was used in the model) as a function of time. Computation runs were terminated when the acceleration dropped below zero.

Several quantities which have been advocated as being related to the likelihood of head injury were computed from the acceleration history:

1. Severity Index, SI,

$$SI = \int_0^T a(t)^{2.5} dt$$

where a(t) is the linear acceleration in g's (g = acceleration of gravity) and T is the duration of impact. Severity Index has been used as a head injury indicator based on data obtained from studies with cadavers and sub-human primates, and this use has been widely accepted. For distributed loads to the head, such as occur when wearing protective headgear, a critical value of SI = 1500 (units are seconds) has been suggested as an injury threshold 7/.

2. Head Injury Criterion, HIC,

$$HIC = \left[\frac{1}{(t_2 - t_1)} \int_{t_1}^{t_2} a(t)dt \right]^{2.5} (t_2 - t_1)$$

where t_1 and t_2 are the two times within the acceleration pulse for which the above expression is a maximum. Proponents have argued that HIC better represents the original data on which SI is based 8/ but, it has also been shown 1/ that HIC and SI are well correlated.

The integrations required for SI and HIC were computed with a library subroutine which utilizes a cubic spline fitting scheme 9/. In addition to the above output parameters, the maximum acceleration, a_{max}, the time at which the maximum acceleration occurs, t_{max}, and the ratio of final to initial velocities, V_R, were also computed. As some headgear test methods require measurements of dwell times (the time duration over which the acceleration exceeds specified levels), these were also recorded at the following g levels: 0, 50, 100, 150, 200, 250,. . .etc.

3. DETERMINING VALUES OF PARAMETERS

3.1 Impact Surface

The parameters of the force vs. displacement relationship for resilient impact surfaces, equation (1), were chosen from impact data of a bare (unhelmeted) metal headform against the impact surface. In this case, the equation of motion of the headform is

$$M_R \ddot{x} = -f(x) \qquad (7)$$

which integrates to

$$\frac{M_R}{2} (\dot{x}^2 - V^2) = -\int_0^x f(x')dx' \qquad (8)$$

where V is the initial velocity. Equation (8) is thus an energy balance. At the point of maximum displacement, $x = x_{max}$, $\dot{x} = 0$ and, from (7), $\ddot{x} = a_{max}$, so that equations (7) and (8) become:

$$M_R\, a_{max} = -f(x_{max}) \qquad (7a)$$

$$\frac{M_R}{2} V^2 = \int_0^{x_{max}} f(x)dx \qquad (8a)$$

Therefore, for any integrable functional form, f(x), equation (8a) can be solved for x_{max} and substituted into equation (7a) to obtain a relationship between a_{max} and V. For the functional forms of equations (1a) and (1b), the following relationships result:

For $f(x) = Bx^p$

$$a_{max} = CV^q \qquad (9a)$$

where

$$C = \frac{1}{g} \left(\frac{B}{M_R}\right)^{\frac{1}{p+1}} \left(\frac{p+1}{2}\right)^{\frac{p}{p+1}} \quad \text{and} \quad q = \frac{2p}{p+1} \qquad (10a)$$

In the elastic case, where p = 1.5, q = 1.2. Moreover, for no value of p can q exceed the value 2.0.

For $f(x) = Bx/(d^2 - x^2)^{\frac{1}{2}}$

$$a_{max} = \frac{h}{C} \frac{\sqrt{4V^2(h - V^2)}}{(h - 2V^2)} \tag{9b}$$

where

$$h = \frac{4Bd}{M_R} \text{ and } C = 4dg \tag{10b}$$

If a_{max} vs. V data are collected for an impact surface, the parameters of the functional relationship can be determined by fitting a curve of the functional forms derived in equations (9a) or (9b). This procedure is illustrated in figure 4 for two surfaces: (1) a cylindrical urethane pad which is manufactured for impact testing and is specified in an existing test method (ASTM F429-75) for football helmets 10/, and (2) artificial turf (5/8 inch backing material) mounted on asphalt. The data for the former surface is fit to the functional form in (9a), and the data for the latter surface is fit to the functional form in (9b). Note that the first surface appears to be well represented by the elastic theory, as q is close to 1.2.

Characterizations are also required for the hard and soft impact surfaces used in the aforementioned experimental study where the effect of changing test parameters was reported 1/. However, there is evidence (figure 5) that these surfaces have degraded in the two years since the experiment and that, therefore parameters obtained from current a_{max} vs. V data would not be useful in predicting the earlier experimental results.

Two data points for each surface were obtained at the time of the earlier experiment. Only limited confidence can be placed in the results, but it may be noted that these surfaces are quite similar to the above mentioned ASTM impact surface (having been developed for the same purpose), hence these data will be compared to curves which exactly satisfy the elastic theory (formulation (9a)). Therefore, a value of p = 1.5 (q = 1.2) will be assumed, and only the value of B will be chosen by fitting the two data points to the closest line of the family on B, as shown in figure 6:

Hard: B = 100

Soft: B = 20

where the units for B are $MN/m^{3/2}$.

3.2 Headform

The metal headform is characterized by the single value M_R. In our experiment, the mass of the headform and supporting drop apparatus was, M_R = 4.65 kg.

It is more difficult to determine values for the humanoid headform parameters K, C, M_1 and M_2. The following values for front and side impacts have been verified in the literature:

	M_1(kg)	M_2(kg)	C(N-sec/m)	K(MN/m)
Front	0.27	4.45	350	8.75
Side	0.18	4.00	420	4.55

There are no citable parametric values for back and top impacts which are required for comparison of modelling results with previously obtained experimental data (see Chapter 4). One might argue that a helmeted headform responds in a similar fashion to impacts in the anterior-posterior direction, whether the impact is to the front or back: this might justify modelling back impacts by using values cited for the front. However, no such rationale is available for choosing values to model top impacts.

Acceleration profiles were initially generated by the model using values for the parameters of the orders of magnitude shown in the table above. These were compared to acceleration profiles obtained by impacting the top of the bare humanoid headform on hard and soft surfaces. By trial and error, the parameters were adjusted to achieve a suitable match, yielding the following values:

$M_1 = 0.20$

$M_2 = 4.45$

$C = 500$

$K = 7.0$

Figure 7 presents comparisons between the predictions of the model (using the above values) and the bare headform experimental results for (a) soft and (b) hard surfaces.

The values given above will be used for top impacts, and the values in the preceding table for front/back and side.

3.3 Helmets

The properties of helmets are difficult to model due to non-linear behavior. In an earlier report it was shown that a small change in velocity (from 4.5 to 5.0 m/sec) could lead to large changes in the acceleration response of the headform. It was therefore decided to develop the needed data base exhibiting this non-linear behavior over a range of velocities. The validity of the model and of the values chosen for the parameters can now be assessed by comparison with the data base.

Twelve helmets were impact tested on the hard surface with a metal headform at the following velocities: 3.0, 3.5, 4.0, 4.5, 5.0, 5.5 and 6.0 m/sec. The experimental details were exactly the same as in the earlier study 1/. The helmets were tested at both the front and back impact sites, and the results are summarized in tables 1 and 2.

The results of this effect-of-velocity study are shown graphically in figures 8 and 9 for top and back impacts, respectively. These figures plot (a) SI and (B) a_{max}, and should be regarded as identifying a general range of behavior of football helmets as a function of velocity. It is the overall description which is considered useful here, and not the performance of any individual helmet.

Since the math model is intended to be a tool for relating a simulation of a real life impact situation to a simulation of a test method configuration, comparisons are made of these two simulated performances for a representative collection of mathematically idealized football helmets. In the present math modelling study, the range is derived from the spring/dashpot models of figure 3 with parameter values chosen by comparison with the experimental range in the effect-of-velocity study (figures 8 and 9). (In contrast, the experimental report 1/ presented comparisons involving data derived by testing actual helmets under experimentally simulated conditions.)

Other factors which influenced the selection of values included the duration of impact and the ratio of rebound velocity to impact velocity. The former was determined in the earlier experimental study 1/, and the latter in the effect-of-velocity study. The impact duration was observed to be on the order of 10 msec for top impacts and 8 msec for back impacts. The velocity ratio ranged from 0.35 to 0.70 This ratio reflects the amount of energy absorption by the helmet liner, and thus guides the values of the dashpot parameter in the model.

The model was first exercised with the linear spring dashpot elements described in equations (3a) and (3b), and the results were compared to the data with top impacts. This comparison is shown for the Maxwell element in figure 10 for both SI vs. V and a_{max} vs. V. The region which is demarked by the diamond-shaped symbols represents the range of performance of actual football helmets, taken from the data in figures 8 or 9. (This representation is also used in ensuing figures.) The curvature of the SI vs. V (figure 10(a)) response of the model is much shallower than for the experimental data. This follows from the fact that the maximum acceleration is a linear function of velocity (see figure 10(b)), which should be expected with a linear model. This is the reason that the non-linear model of figure (3c) and equation (3d) was used to describe helmet behavior. All further results pertain to this non-linear model.

The process for determining the values of the helmet parameters E_1, , E_2, r, and D was largely one of trial and error. Each set of values can be regarded as representing a "mathematical helmet." The purpose was to choose enough sets to represent the range of helmets described by the experimental results of figures 8 and 9. The procedure was to fix D at a representative value for the helmet liner thickness (top: D = 2.54 cm, back: D = 1.90 cm), and then adjust the other parameters until the response of the "mathematical helmet" appeared to fall within the experimental range as one of the family. The sets of mathematical helmets which were used in the remainder of this report are summarized in tables 3 and 4 for top and back impacts, respectively. In figures 11 and 12, the Severity Index (SI) response of these mathematical helmets, as determined by exercising the model, are compared to the experimental ranges of figures 8 and 9.

4. EFFECT OF CHANGING TEST PARAMETERS; COMPARISON OF MODEL OUTPUT TO EXPERIMENTAL DATA

Details of the experiment to determine the effect of changing test parameters have been described in a previous report 1/, where the following test parameters were considered:

Impact Surface: Hard, Soft

Headform: Humanoid, Metal

Velocity: 4.5, 5.0 m/sec

Impact Site: Top, Back

(The data in tables 1 and 2, collected for the separate purposes of the experiments conducted for this report, are now available for any desired extension of the analysis of the effect of changing velocity.)

For each impact site, six distinct impact configurations were examined with a variety of football helmets, as shown in figure 13. The six sets of experimental data permit construction of seven relationships, each of which describes the effect of changing a single test parameter (all others held constant). These seven relationships are indicated in figure 13 by the double arrows connecting the boxes.

The conditions of each box were also simulated with the math model, using the values obtained in the previous chapter. That is, the simulated conditions for each of the six boxes were run on the computer for each of the mathematical helmet representations of tables 3 and 4. The results of this computer study are summarized in tables 5 and 6.

The results of this math modelling exercise can also be used to examine the results of changing test parameters, deriving the seven relationships shown by the double arrows in figure 13 from the math model output. Lastly, the relationships obtained with the math model output can be compared to the relationships obtained with the experimental data to assess the performance of the math model in predicting the effect of changing test parameters.

These comparisons are shown in figures 14 to 20 for the top impact site. These figures show the effect of changing impact surface (figures 14-16), headform (figures 17 and 18), and velocity (figures 19 and 20). In each figure, the dashed lines represent the experimental results from the earlier study. These lines demark the 95% confidence band for a straight line fit to the experimental data. The results of the model study are represented by the set of symbols, each corresponding to a different "mathematical helmet." The test of validity of the mathematical modeling is whether or not the set of symbols suggests a similar relationship to that established by the confidence band. For the top impact site, the agreement appears to be suitable.

It was difficult to make comparisons for the back impact site. This was largely due to the scatter associated with the experimental data. This was attributed to two sources: (1) Difficulties with the experimental behavior of the humanoid headform when impacted in the back site have already been reported 1/. Namely, the headform tends to deform in the region where its "neck" attaches to the headform support. This "neck bending" phenomenon absorbs energy and leads to misleadingly low acceleration and large amounts of scatter in the data. On the other hand, as discussed in chapter 2, the model is based on the assumption that the headform exhibits linear acceleration only. (2) Another source of scatter can be attributed to the small thickness of the helmet liner at the back site. This leads to more scatter in the experimental data as the impact becomes more severe.

Of the seven relationships indicated in figure 13, for the back site, only four could be reasonably characterized by fitting straight lines. (These had correlation coefficients larger than .75; all seven relationships for the top impact surface had correlation coefficients larger than .80 1/.) That is, these four have confidence bands which were narrow enough to permit a fair comparison of the model predictions with experimental data (figures 21 - 24). While these comparisons are not quite as good as for the top site) it still appears as though the results of the math model would be useful as a first approximation.

5. USING THE MODEL TO DEVELOP PASS/FAIL CRITERIA IN A TEST METHOD FOR FOOTBALL HELMETS

In this section we will use a hypothetical example to illustrate how the model may be used. As discussed in the introduction, the model is intended to relate simulated real life injury situations to the simulation of a suggested (non-realistic) test method configuration. We will use football as the activity of interest in order to capitalize on the large body of experimental data that has already been collected on football helmets.

Several modes of head impact may be associated with any activity. For football, we will consider three distinct modes, characterized by the mass M_3 of an impacting object and the relative velocity, V, between the object and the head.

1. $M_3 = \infty$, V = 5.5 m/sec (Fall against massive impacting object, such as artificial turf.)

2. M_3 = 5 kg, V = 7 m/sec (Example: head struck by moderately large object)

3. M_3 = 2 kg, V = 10 m/sec (Example: head struck by small, fast-moving object)

The values shown above were picked arbitrarily to illustrate differences in the real life/test method relationships between small mass/high velocity impacts and large mass/low velocity impacts. The three modes were chosen to resemble several types of head impact situations which typically occur in football, as illustrated schematically in figure 25.

The first mode represents the head striking the football field surface after a fall. The formulation for resilient impact surfaces used to describe artificial turf (as described in sections 2.2, 3.1 and figure 4) were used in the computation. Modes 2 and 3 suggest lesser masses and higher velocities as may characterize impacts from knees and hands, respectively. The math model in its present formulation considers only rigid impacting objects which are non-massive, hence cannot take into account the energy which is absorbed by the impacting objects themselves. To compensate for this deficiency, velocities for impact modes 2 and 3 were intentionally chosen to be less than what might be achievable in real life.

In this example, developing a test method for football helmets, the real life situation is simulated by exercising the model for each of the three modes with parameter values that have been used to describe the human head (section 3.2). These values have only been determined for front and side impacts, and each set of values will be utilized in these examples. In addition, for purposes of illustration, the front values will also be used to describe impacts to the back site. As discussed earlier, this may be partially justified by the fact that blows to both the front or the back are in the same anterior-posterior direction (which would be in agreement with the constraints of the one dimensional model).

For both sets of "head" parameters (front/back and side) we shall use the "mathematical helmets" which were shown to describe impacts to the back site. Although side impact data was not collected, visual inspection suggested that, in many helmets, the impact attenuating features were very similar in the side and back.

The impact response in the "real life" situation can now be simulated and computed in all three modes for back and side impacts. The results of these calculations are shown in table 7. Since this exercise is aimed at illustrating use of the model to develop a connection between real life situations and a possible test method, the next step is to simulate a prospective test method.

The ASTM Test Method for Football Helmets F429-75 will be used for this purpose because it utilizes a metal headform and is readily accessible in a published document. In this test method, a helmeted metal headform is dropped in guided free fall so that it strikes a specified impact surface at 5.5 m/sec. The characterization of the impact surface was described in section 3.1 and figure 4. The results of using the mathematical helmets of tables 3 and 4 in simulating this test method configuration are also shown in table 7.

The relationships between the simulated real life situation and the test method configuration are shown for each of the impact modes in figures 26 - 33 for back site impacts, and figures 34 - 41 for side impacts. In each figure, the severity index SI is plotted on the "real life" axis (abscissa). Figures 26 - 29 and 34 - 36 show the severity index response, SI, of the test method; figures 30 - 32 and 38 - 40 show the maximum acceleration response, a_{max}, of the test method. In each figure a line has been fitted to the data by the method of least squares. For each combination of impact site and test method response parameter, the results of the three impact modes are summarized on a single graph in figures 29, 33, 37 and 41 for back/SI, back/a_{max}, side/SI, and side/a_{max} respectively.

Such graphs are useful in determining test method criteria which correspond to particular real life injury criteria. Examples of this procedure are shown in figures 29, 33, 37 and 41 for real life injury criteria of SI = 1500. It is seen that the associated test method rejection values would be SI $\cong$ 1900 and 2000 for back and side, respectively, and $a_{max} \cong$ 220 g and 230 g for back and side, respectively.

6. SUMMARY AND DISCUSSION

This report has presented a mathematical model to connect injury parameters in real life head impact environments to output parameters in test methods for evaluating protective headgear. The model may be particularly useful in determining test method pass/fail criteria which correspond to the threshold of injury in the real life injury situation.

The validity of the model depends upon the accuracy with which each element (head or headform, impact surface, range of helmets) is represented. In chapter 3, plausible parameter values were chosen for each of the elements. Notwithstanding the assertion that these were reasonable values, the true test for any model is whether or not it can usefully predict experimental results. The comparison of the model output to experimental results was presented in chapter 4 and, in general, the results were within acceptable limits.

The ability of the model to represent real life head impact situations is valid only for front and side impacts since the parameter values for the "head" element have only been experimentally determined at these sites. Nevertheless, the close agreement in pass/fail criteria for front and side impacts (compare figures 33 and 41) indicates that the application of the model does not depend strongly upon the values of the "head" parameters. Therefore, until more cadaver data for back impacts is available, the same test method pass/fail criteria should also be used for impacts to the back.

The model should not be applied to represent top impacts in the real life situation. (They were required in validating the model, however, because the experimental program contained top impacts.) In the real life situation, an impact to the top of the head is not accompanied by the nearly free-body linear acceleration as with other sites. Because such blows are directed parallel to the neck axis rather than perpendicular to it. Consequently, different injuries (often to the neck and spine) manifest themselves. For completeness in evaluating the helmet by the test method, it is suggested that the top site should still be tested with the same criteria as for the other sites (helmets generally perform best at the top site), at least until such time as real life neck injury criteria can be related to the test method.

For other types of headgear, the step-by-step procedure in applying the model to develop acceptance/rejection criteria for test methods is:

1. Determine a helmet behavior envelope by collecting injury response vs. velocity data for representative helmets, as in section 3.3.

2. Determine parameter values for "mathematical helmets" to represent the range determined in step 1 (section 3.3).

3. Determine modes of impact considered to be significant for this activity.

4. Determine parameter values to characterize typical impact surfaces for each mode, as in sections 2.2 and 3.1.

5. Apply the model, using "mathematical helmets" from step 2 and impact surfaces from step 4 to each mode of step 3 with the "head" parameters for front and side impact (chapter 5).

6. Characterize the headform and impact surface of the test method configuration in like fashion and apply model using the same "mathematical helmets."

7. Construct curves as in figures 26 to 41 to identify the relationship between the real life injury situation and the test method.

8. Use these graphs to determine test method pass/fail criteria that correspond to the onset of injury as in figures 29, 33, 37 and 41.

Finally, the model may have limited application in suggesting design improvements for protective headgear. If the helmet is characterized mathematically as in section 2.4, and if material parameters can be related to particular spring/dashpot components, then a parameter variation analysis can be performed to indicate which material changes offer the greatest potential for improved safety.

Table 1. Effect of Velocity Data for Top Impacts

Velocity (m/sec)

	A_{max}							SI						
Helmet	3.0	3.5	4.0	4.5	5.0	5.5	6.0	3.0	3.5	4.0	4.5	5.0	5.5	6.0
AP-4	66	88	100	160	215	417	439	179	348	495	976	1556	3939	4231
BP-4	102	220	205	325	415	449	456	272	1165	1172	2841	3995	4216	4363
EF-4	74	100	125	159	197	235	252	184	326	515	860	1362	1905	2377
DC-4	51	102	-	103	112	142	188	95	369	290	428	679	1048	1708
BC-4	52	78	94	122	208	338	415	132	237	393	646	1404	3289	4243
CS-4	51	79	111	135	168	194	264	102	223	395	624	1128	1520	2523
BP-4A	64	78	89	97	125	150	228	166	266	345	491	868	1269	2124
CP-4	52	66	87	116	156	162	192	102	189	288	458	929	1171	1675
DC-4A	51	66	114	134	154	169	206	93	177	569	789	1193	1514	2169
CH-4	64	77	93	105	134	164	179	146	262	393	585	941	1386	1837
AT-4	67	76	94	108	131	146	208	165	253	389	606	924	1230	1900
RS-4	65	71	91	109	122	241	300	139	200	326	470	626	1516	2674

Table 2. Effect of Velocity Data for Back Impacts

Velocity (m/sec)

	A_{max}							SI						
Helmet	3.0	3.5	4.0	4.5	5.0	5.5	6.0	3.0	3.5	4.0	4.5	5.0	5.5	6.0
AP-4	101	124	166	199	320	393	407	302	511	819	1178	2667	3997	4142
BP-4	104	198	296	328	422	454	445	307	875	2035	2607	4145	4420	4621
EF-4	127	159	179	197	229	238	293	463	763	1002	1295	1813	2158	3243
DC-4	85	121	166	215	271	347	-	210	395	760	1327	2135	3604	-
BC-4	77	130	196	290	378	390	437	197	470	1098	2120	3822	4036	4742
CS-4	117	174	236	289	354	411	438	343	766	1427	2400	3652	4586	4935
BP-4A	92	157	126	287	395	426	449	265	638	812	2066	3559	4147	4613
CP-4	92	119	134	195	243	323	391	254	413	586	1081	1740	3164	4578
DC-4A	92	132	144	228	286	356	404	275	469	660	1369	2256	3628	4463
CH-4	69	112	209	238	264	362	397	148	333	1121	1554	1935	3714	4175
AT-4	93	123	147	212	220	278	413	265	462	656	1288	1501	2491	4197
RS-4	160	224	284	350	386	426	435	679	1350	2170	3607	4462	4922	5184

Table 3. Parameters of Mathematical Helmets Chosen to Fit Effect of Velocity Data: Top Impacts

$E_1\left(\frac{MN}{m^2}\right)$	η(Kpoise)	R	$E_2\ \frac{MN}{m^2}$	Symbols Used Fig. 14 - 20
5	20	6	20 50 100 200	◇ (small)
		8	20 50 100 200	□ (small)
		10	200 500 1000 2000	○ (small)
5	10	6	20 50 100 200	◇ (medium)
		8	20 50 100 200	□ (medium)
		10	200 500 1000 2000	○ (medium)
10	10	6	20 50 100 200	◇ (large)
		8	20 50 100 200	□ (large)
		10	200 500 1000 2000	○ (large)

Table 4. Parameters of Mathematical Helmets Chosen to Fit Effect of Velocity Data: Back Impacts

$E_1 \left(\frac{MN}{m^2}\right)$	η(Kpoise)	R	$E_2 \frac{MN}{m^2}$	Symbols Used Fig. 21 - 24
5	20	6	20 100 200 500 1000	◇
		8	200 500 1000	□
		10	200 500 2000	○
5	10	6	20 100 200 500 1000	◇
		8	200 500 1000	□
		10	200 500 2000	○
10	10	6	20 100 200 500 1000	◇
		8	200 500 1000	□
		10	200 500 2000	○

Table 5. Results of Simulating Experimental Conditions - Top Impacts

Velocity:	V_L = 4.5 m/sec								V_H = 5.0 m/sec			
Headform:	Humanoid				Metal				Metal			
Impact Surface:	Hard		Soft		Hard		Soft		Hard		Soft	
Mathematical Helmet(E_1-n-R-E_2)	A_{max}	SI	A_{max}	SI	A_{max}	SI	A_{max}	SI	A_{max}	SI	A_{max}	SI
5-20-6-20	118	619	107	552	123	645	110	569	150	964	132	830
-50	137	777	120	663	145	831	125	693	182	1294	152	1040
-100	156	954	133	779	169	1049	139	826	212	1655	170	1248
-200	177	1178	146	918	197	1341	155	988	246	2109	189	1489
8-20	106	513	98	469	109	526	101	480	128	754	117	678
-50	113	575	103	516	117	596	106	531	146	912	128	786
-100	123	656	110	573	130	692	114	595	167	1106	141	907
-200	138	773	120	652	148	836	125	684	193	1375	156	1061
10-200	114	582	103	519	119	607	106	535	155	978	132	818
-500	129	694	112	594	138	743	117	620	186	1264	149	980
-1000	145	814	123	670	159	897	129	708	213	1552	164	1130
-2000	162	965	133	760	182	1099	141	814	242	1899	179	1300
5-10-6-20	108	507	98	463	112	523	101	475	145	854	127	746
-50	136	725	118	622	145	776	123	650	186	1270	153	1016
-100	160	941	134	767	174	1041	141	815	220	1684	174	1258
-200	182	1194	149	927	204	1370	159	1000	255	2174	193	1520
8-20	86	367	81	350	88	371	83	354	119	622	107	570
-50	107	492	97	448	112	510	100	460	152	885	129	752
-100	126	625	110	543	135	667	115	566	181	1159	147	922
-200	147	792	124	655	161	872	130	693	212	1497	165	1114
10-200	119	559	104	492	127	594	108	510	178	1085	143	859
-500	144	742	120	613	158	821	127	648	215	1475	163	1073
-1000	162	906	132	717	183	1036	141	768	242	1822	178	1251
-2000	180	1089	144	828	207	1287	154	898	270	2207	193	1438
10-10-6-20	87	359	81	353	88	356	83	353	103	548	99	536
-50	101	482	95	458	104	486	97	465	135	783	122	722
-100	122	624	110	568	128	644	114	584	166	1051	143	909
-200	146	811	126	700	156	865	132	732	201	1409	163	1132
8-20	85	283	79	281	87	280	81	280	97	414	90	416
-50	86	335	80	332	87	332	81	332	99	527	96	518
-100	87	401	84	390	88	400	85	393	122	665	112	627
-200	105	495	97	466	108	503	99	474	149	859	129	764
10-200	85	354	79	349	87	350	81	350	112	592	104	567
-500	97	447	91	426	100	451	93	431	144	798	124	712
-1000	115	544	103	499	121	562	106	511	170	1007	140	845
-2000	133	666	115	583	144	708	120	606	197	1265	155	994

Table 6. Results of Simulating Experimental Conditions - Back Impacts

Velocity:	V_L = 4.5 m/sec								V_H = 5.0 m/sec			
Headform:	Humanoid				Metal				Metal			
Impact Surface:	Hard		Soft		Hard		Soft		Hard		Soft	
Mathematical Helmet(E_1-n-R-E_2)	A_{max}	SI	A_{max}	SI	A_{max}	SI	A_{max}	SI	A_{max}	SI	A_{max}	SI
5-20-6-20	152	934	131	774	161	991	136	807	198	1503	153	1181
-100	200	1439	160	1069	220	1615	168	1140	273	2503	203	1691
-200	224	1733	173	1228	251	2006	184	1324	308	3083	220	1952
-500	254	2160	190	1449	293	2605	204	1584	355	3929	242	2306
-1000	274	2494	202	1615	323	3096	218	1783	388	4600	257	2567
8-200	185	1231	149	933	202	1367	156	988	259	2218	191	1506
-500	212	1539	164	1098	239	1776	174	1178	301	2852	212	1786
-1000	233	1801	176	1234	267	2141	187	1338	333	3386	227	2009
10-200	156	939	131	759	167	1007	136	792	220	1674	169	1219
-500	178	1143	143	872	196	1266	150	920	258	2134	187	1431
-2000	216	1548	164	1084	246	1814	174	1165	316	2995	215	1796
5-10-6-20	145	818	125	689	153	859	129	712	195	1386	159	1096
-100	202	1420	161	1055	224	1599	170	1123	279	2516	205	1689
-200	227	1738	175	1231	257	2020	186	1326	314	3120	223	1966
-500	257	2181	192	1463	298	2639	206	1600	361	3980	245	2329
-1000	278	2517	204	1632	328	3135	220	1801	393	4651	259	2592
8-200	193	1263	153	943	214	1418	161	998	274	2343	198	1551
-500	221	1606	169	1131	252	1876	180	1216	316	3014	219	1851
-1000	241	1881	181	1276	280	2261	193	1386	346	3557	233	2080
10-200	167	961	135	755	181	1045	141	787	243	1834	179	1272
-500	193	1224	150	904	215	1384	158	957	281	2364	198	1518
-2000	229	1675	172	1146	266	2002	183	1238	336	3269	224	1906
10-10-6-20	112	564	103	528	115	565	106	534	142	375	129	805
-100	161	966	137	810	170	1012	142	838	217	1626	174	1276
-200	187	1223	153	967	203	1325	160	1014	255	2111	194	1531
-500	221	1622	172	1192	247	1844	182	1273	305	2878	219	1891
-1000	245	1953	186	1367	280	2301	199	1479	343	3528	236	2168
8-200	143	803	125	695	150	825	128	712	201	1389	162	1117
-500	173	1056	143	852	187	1129	148	886	244	1888	185	1379
-1000	196	1283	156	984	216	1419	164	1036	277	2337	201	1593
10-200	113	587	104	543	114	584	106	547	161	999	138	874
-500	138	743	120	651	143	758	122	663	198	1324	158	1063
-2000	177	1069	144	849	193	1155	149	884	256	1990	188	1397

Table 7. Results of Simulating Real Life Impact Modes in Football and ASTM Test Method

Mathematical Helmet (E_1-n-R-E_2)	Real Life Simulations - Back						Real Life Simulations - Side						Test Method Simulation - Metal Headform	
	V=5.5 m/sec Artificial Turf, $M_3=\infty$		V=7 m/sec M_3=5 kg		V=10 m/sec M_3=2 kg		V=5.5 m/sec Artificial Turf, $M_3=\infty$		V=7 m/sec M_3=5 kg		V=10 m/sec M_3=2 kg		V=5.5 m/sec ASTM Surface	
	A_{max}	SI	A_{max}	SI	A_{max}	SI	A_{max}	SI	A_{max}	SI	A_{max}	SI	A_{max}	SI
5-20-6-20	183	1522	224	1325	274	1510	175	1466	217	1391	268	1632	217	1949
-100	236	2227	306	2201	380	2453	215	2013	280	2080	342	2375	283	3015
-200	260	2603	344	2717	427	2978	234	2298	308	2462	372	2758	312	3560
-500	293	3140	392	3468	477	3718	259	2693	344	2992	405	3264	348	4306
-1000	317	3560	425	4055	511	4279	276	2991	369	3386	423	3622	372	4864
8-200	224	2016	295	1952	370	2240	203	1804	264	1825	329	2144	274	2761
-500	253	2421	340	2523	424	2827	225	2106	298	2237	366	2564	307	3363
-1000	274	2754	372	3001	462	3299	241	2351	322	2571	389	2890	331	3838
10-200	198	1643	252	1468	319	1746	180	1496	229	1428	291	1732	243	2221
-500	222	1946	295	1879	375	2198	198	1717	259	1721	328	2057	274	2699
-2000	260	2482	356	2658	449	2990	227	2109	304	2265	376	2609	318	3500
5-10-6-20	183	1475	216	1155	263	1346	171	1371	206	1187	257	1435	218	1872
-100	242	2272	309	2135	379	2377	218	2015	279	1983	339	2270	288	3043
-200	267	2668	348	2676	426	2923	238	2321	309	2392	369	2675	317	3605
-500	300	3217	395	3444	477	3678	262	2729	345	2942	402	3199	352	4357
-1000	323	3637	428	4035	511	4246	279	3030	370	3344	421	3566	376	4912
8-200	236	2132	303	1959	374	2222	210	1853	268	1775	329	2075	286	2895
500	265	2564	349	2563	428	2832	232	2183	302	2221	366	2520	318	3515
-1000	287	2906	380	3051	464	3312	248	2438	327	2568	389	2856	341	3990
10-200	213	1781	264	1484	327	1741	189	1546	234	1367	294	1661	262	2414
-500	239	2125	309	1957	384	2234	209	1810	267	1717	331	2026	291	2927
-2000	277	2693	368	2775	456	3048	238	2236	312	2302	377	2604	333	3738
10-10-6-20	150	1106	169	750	216	929	144	1072	171	845	214	1069	168	1259
-100	204	1740	228	1282	296	1486	188	1590	217	1303	275	1551	239	2171
-200	231	2092	268	1676	344	1893	208	1868	249	1618	310	1874	271	2678
-500	266	2611	322	2334	408	2561	235	2265	290	2117	356	2375	311	3414
-1000	292	3033	365	2907	453	3133	255	2576	320	2529	385	2777	339	3994
8-200	193	1563	206	1050	266	1243	175	1412	194	1080	248	1319	227	1941
-500	222	1926	253	1436	322	1644	198	1694	230	1382	290	1634	263	2476
-1000	245	2232	289	1811	369	2028	215	1928	258	1664	321	1922	289	2919
10-200	167	1255	162	757	214	931	152	1146	165	827	208	1048	195	1501
-500	191	1515	198	964	252	1148	171	1349	183	990	235	1223	227	1893
-2000	230	1986	264	1473	331	1678	201	1709	233	1375	292	1624	274	2593

CAPTIONS TO FIGURES

1. Elements of mathematical model

2. Humanoid headform model

3. Mathematical helmet models: (a) Maxwell, (b) Voight, (c) Maxwell plus non-linear spring.

4. Examples of fitting a_{max} vs. V data:

   (a) Urethane impact surface of ASTM test method F427-75. Values of C and q correspond to F = B x P where p = 1.76 and B = 144.6 $MN/m^{1.76}$.

   (b) Representation of artificial turf (data from ref. 11). Values of h and C correspond to $F = Bx/(d^2 - x^2)^{1/2}$ where d = .008 m and B = 6539 N.

5. Static force displacement curves showing degradation of soft impact surface.

6. Determination of parameter B for hard and soft surfaces.

7. Comparison of acceleration profiles of bare humanoid headform and model.

8. Effect of velocity data for top impacts: (a) SI (b) a_{max}

9. Effect of velocity data for back impacts: (a) SI (b) a_{max}

10. Comparison of Maxwell model to effect-of-velocity data (a) SI (b) a_{max}; E_1=30 MN/m^2, η=15 -, 20·····, 30 ---.

11. Comparison of mathematical helmet model response to effect-of velocity data for top impacts; a) E_1=5, η=20, b) E_1=5, η=10, c) E_1=10, η=10.

12. Comparison of mathematical helmet model response to effect-of-velocity for back impacts; a) E_1=5, η=20, b) E_1=5, η=10, c) E_1=10, η=10.

13. Experimental configurations examined in previous study 1/.

14. Comparison of model (symbols) and experiment (envelope) for effect of changing impact surfaces (metal headform, v = 4.5 m/sec, top).

15. Comparison of model (symbols) and experiment (envelope) for effect of changing impact surface (humanoid headform, v = 4.5, top).

16. Comparison of model (symbols) and experiment (envelope) for effect of changing impact surface (metal headform, v = 5.0, top).

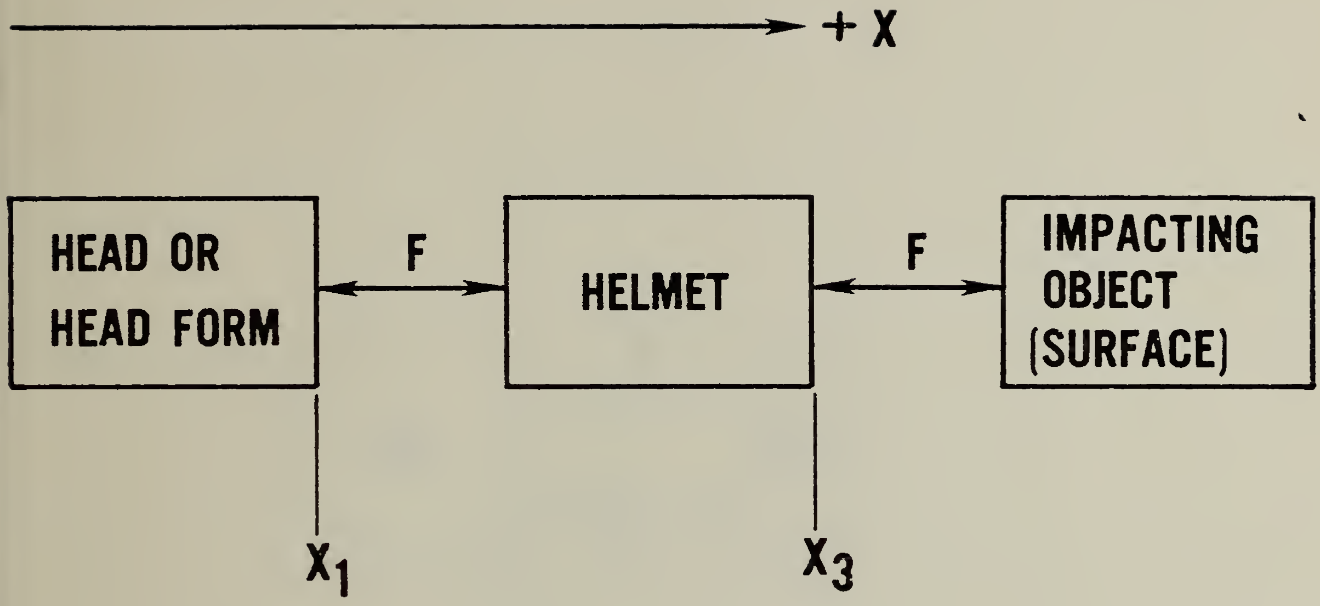

FIGURE 1

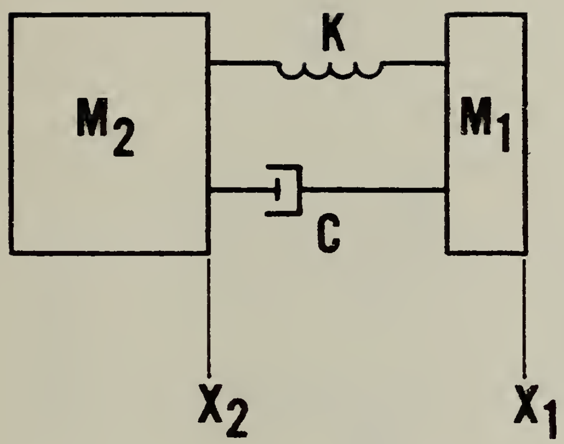

FIGURE 2

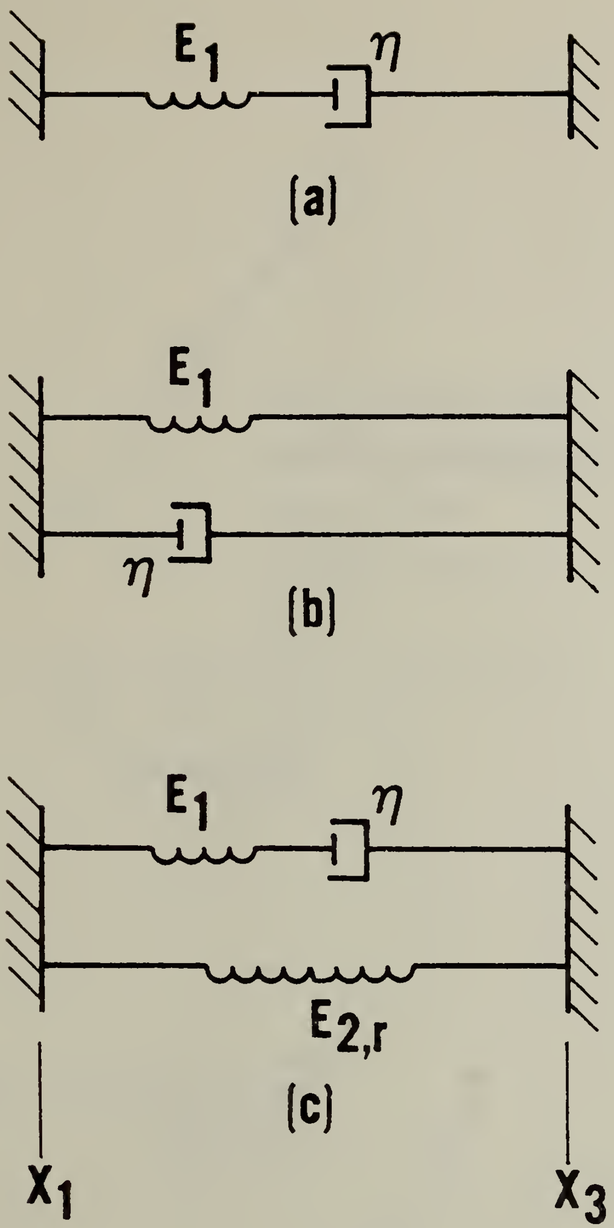

FIGURE 3

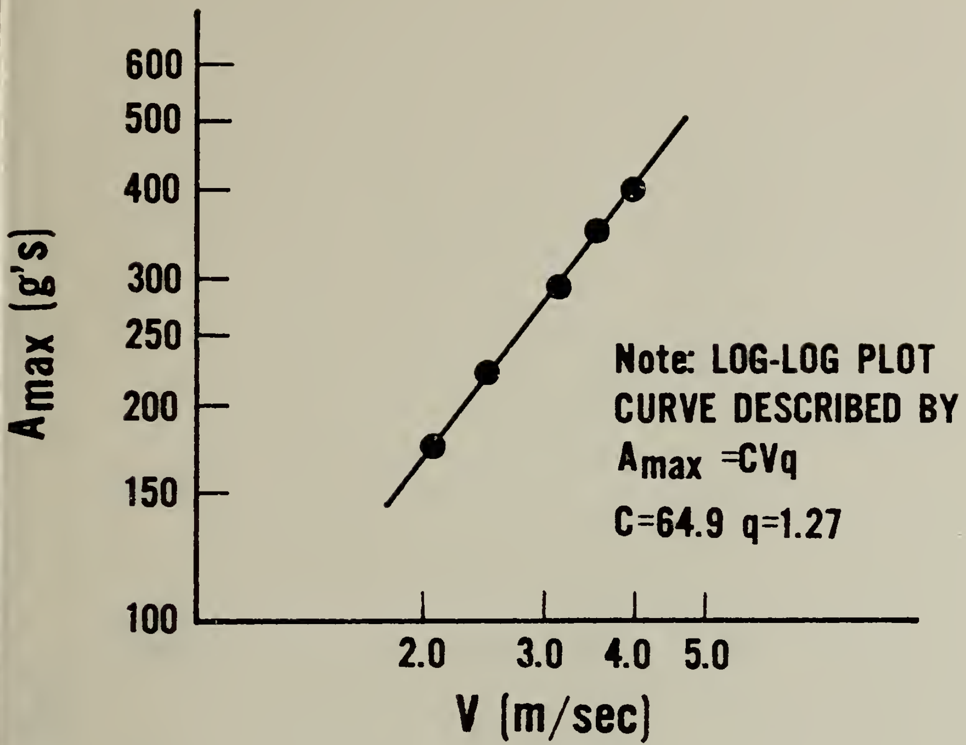
Amax (g's)
600
500
400
300
250
200
150
100
Note: LOG-LOG PLOT
CURVE DESCRIBED BY
Amax =CVq
C=64.9 q=1.27
2.0
3.0
4.0
5.0
V (m/sec)

(a)

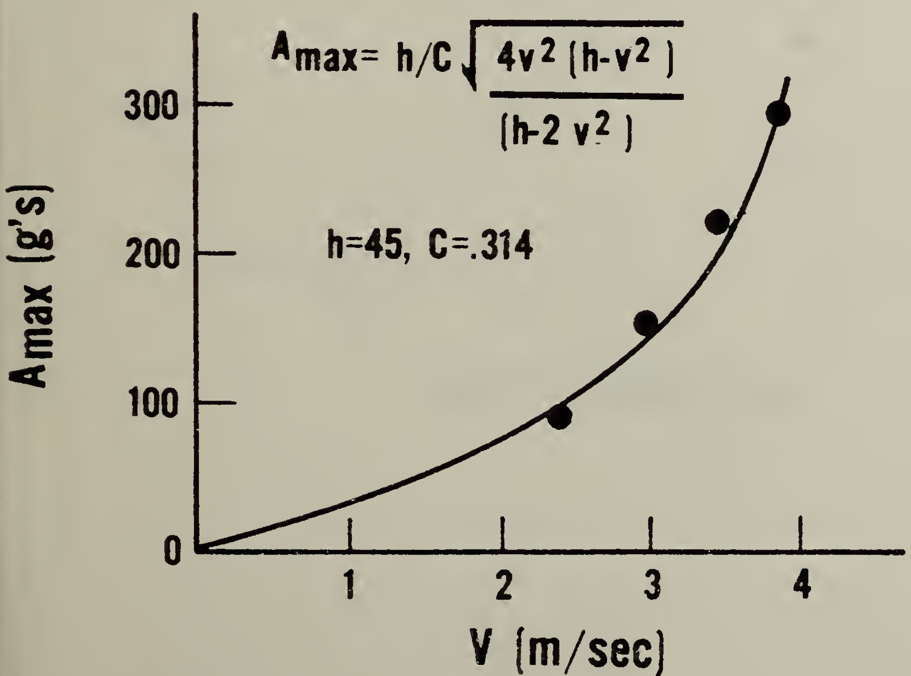
Amax= h/C √ 4v2 (h-v2) / (h-2 v2)
300
200
100
0
Amax (g's)
h=45, C=.314
1
2
3
4
V (m/sec)

(b)

FIGURE 4

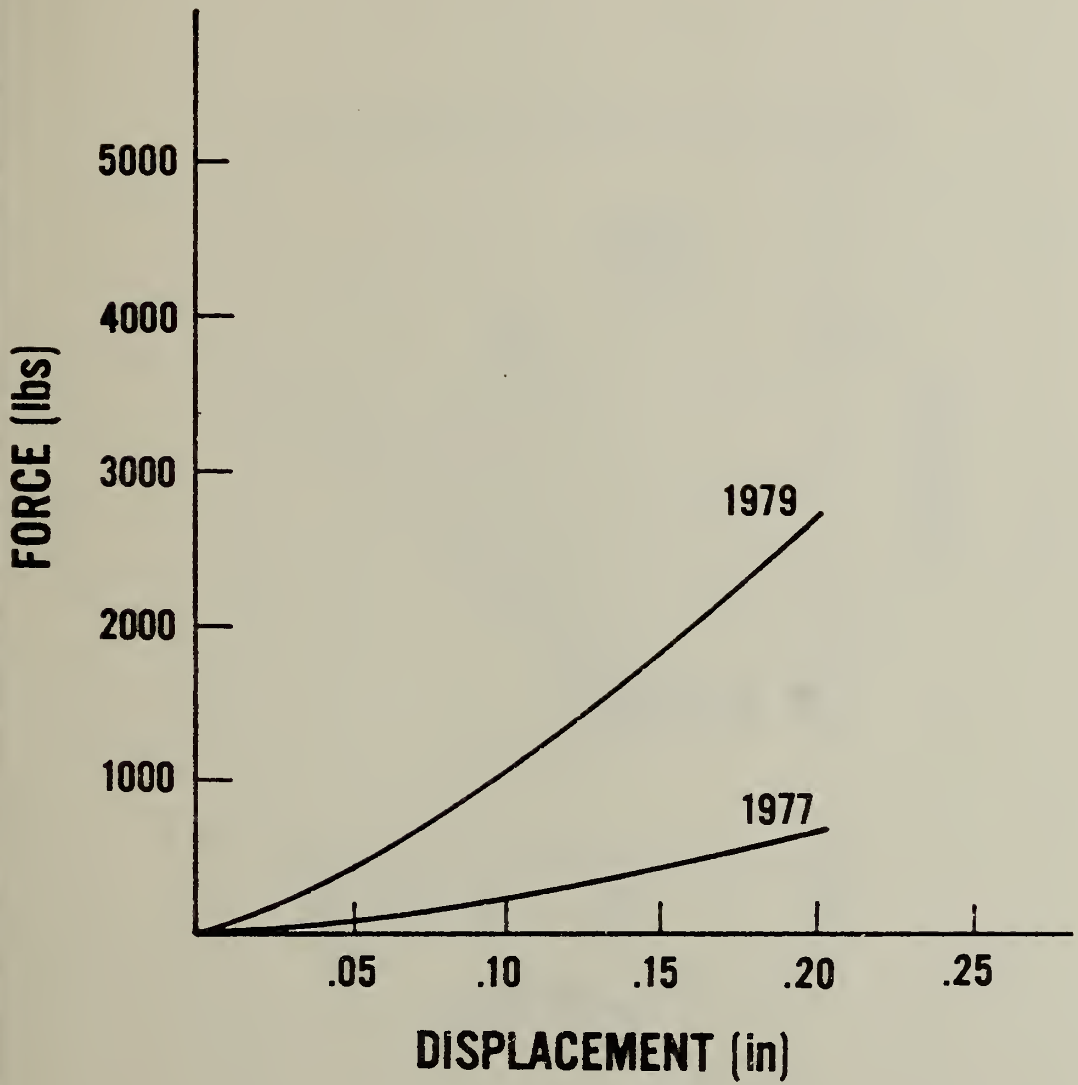
5000
4000
3000
2000
1000
FORCE (lbs)
1979
1977
.05
.10
.15
.20
.25
DISPLACEMENT (in)

FIGURE 5

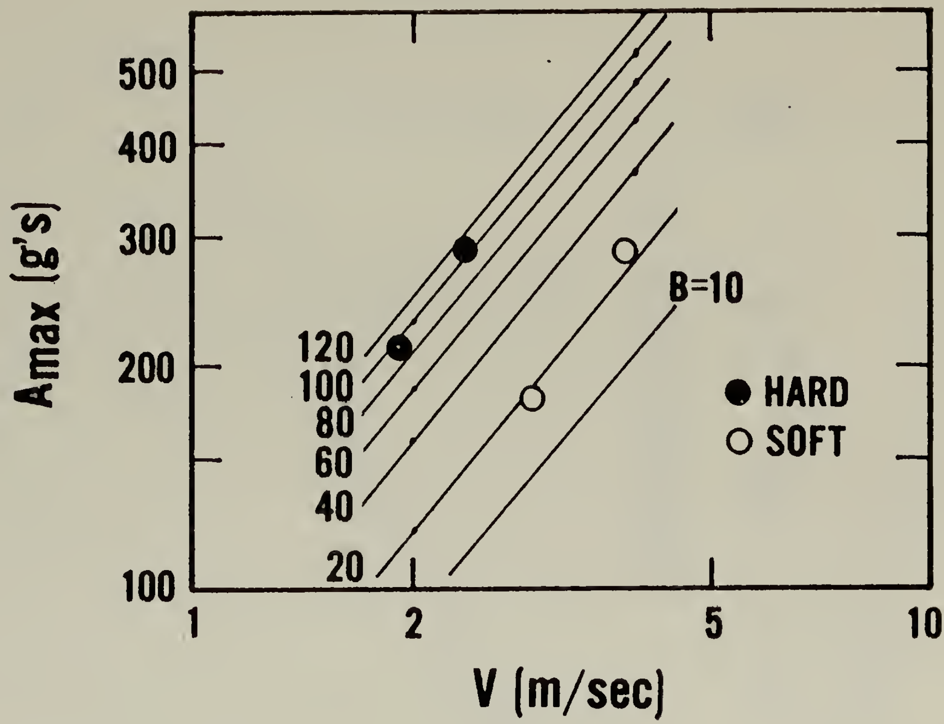
Amax (g's)
500
400
300
200
100
1
2
5
10
V (m/sec)
120
100
80
60
40
20
B=10
HARD
SOFT

FIGURE 6

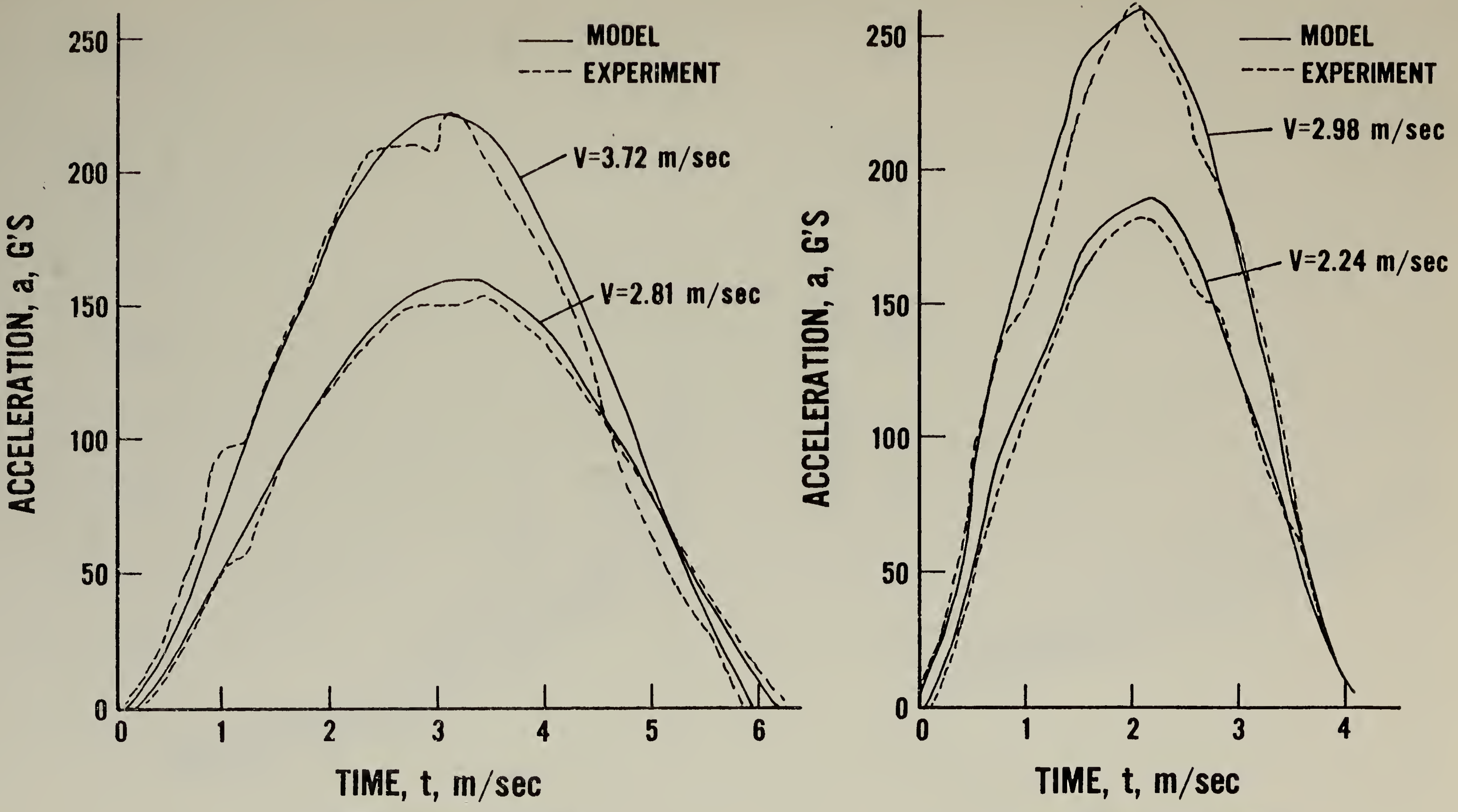

(a) SOFT IMPACT SURFACE

(b) HARD IMPACT SURFACE

FIGURE 7

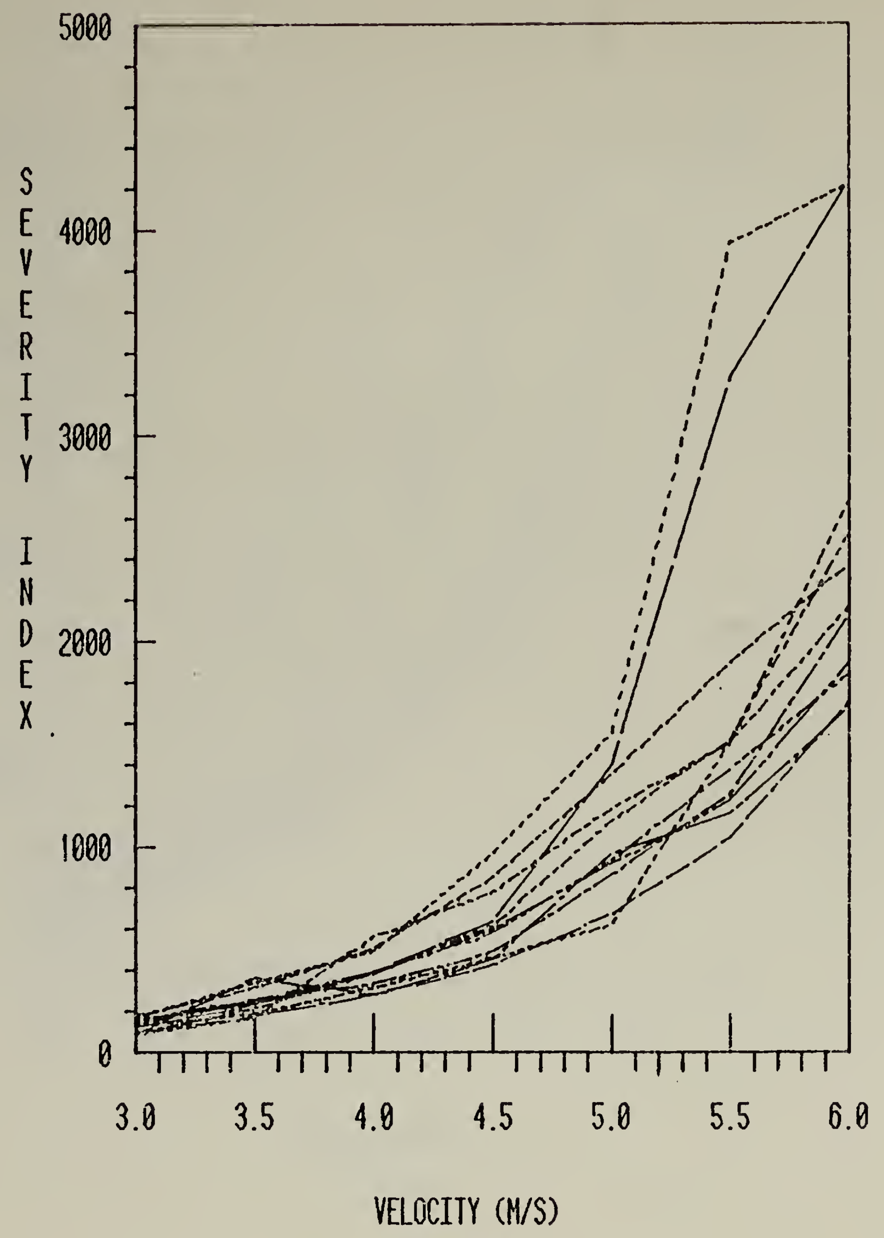

FIGURE 8a

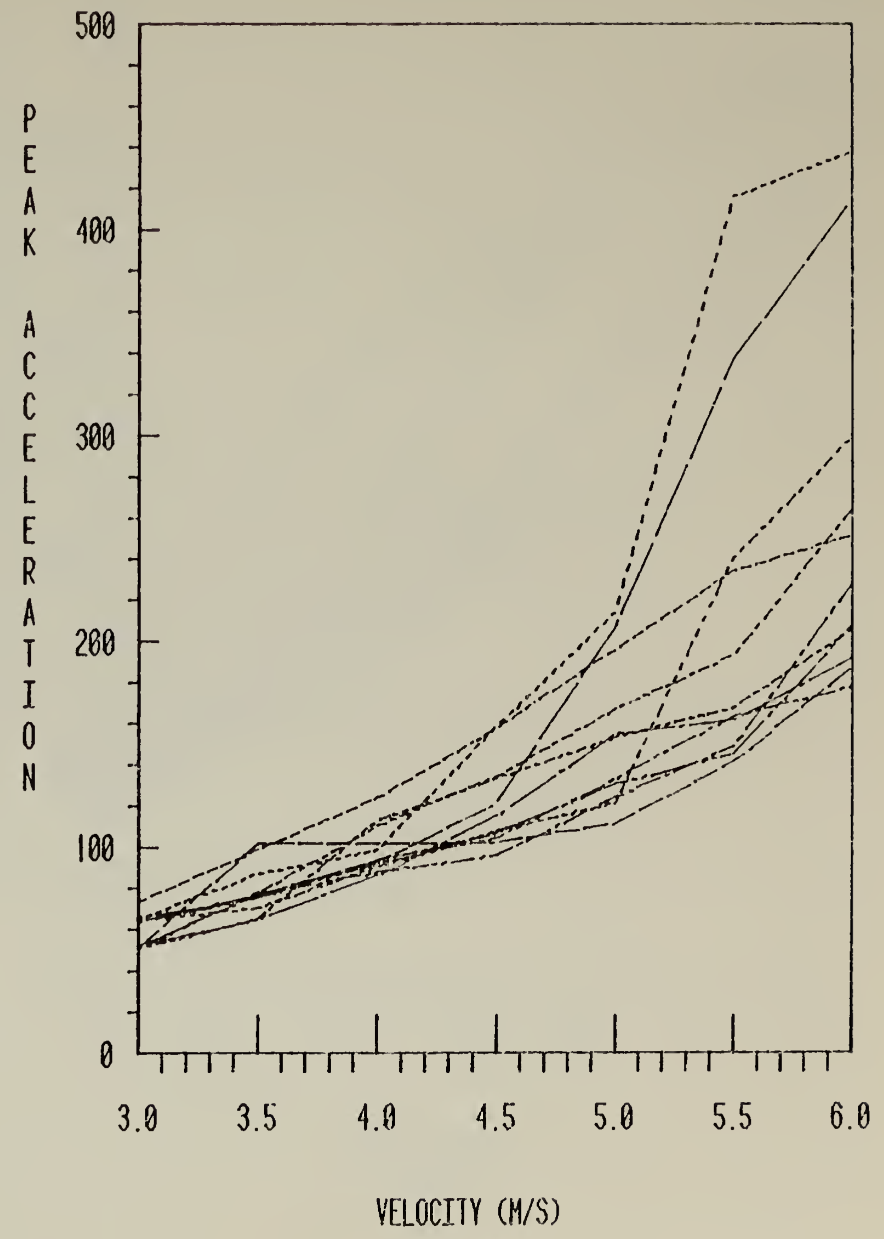

FIGURE 8b

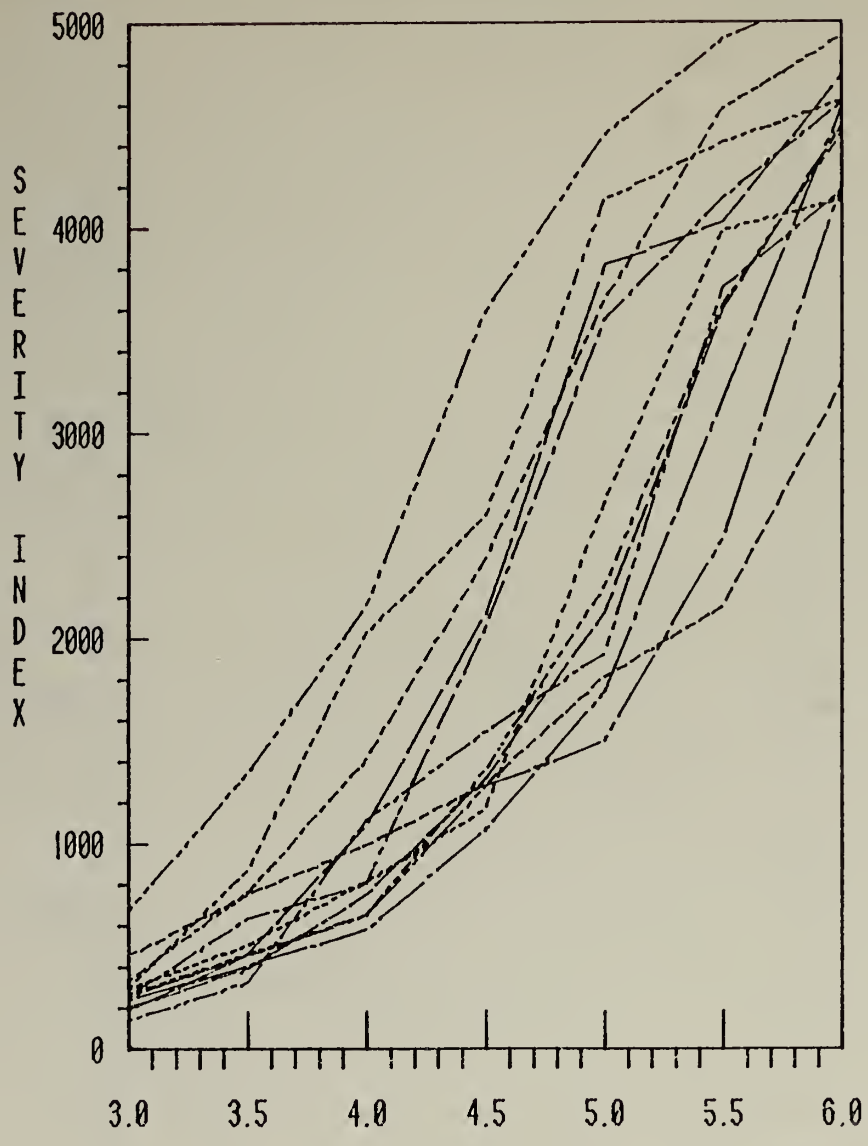

FIGURE 9a

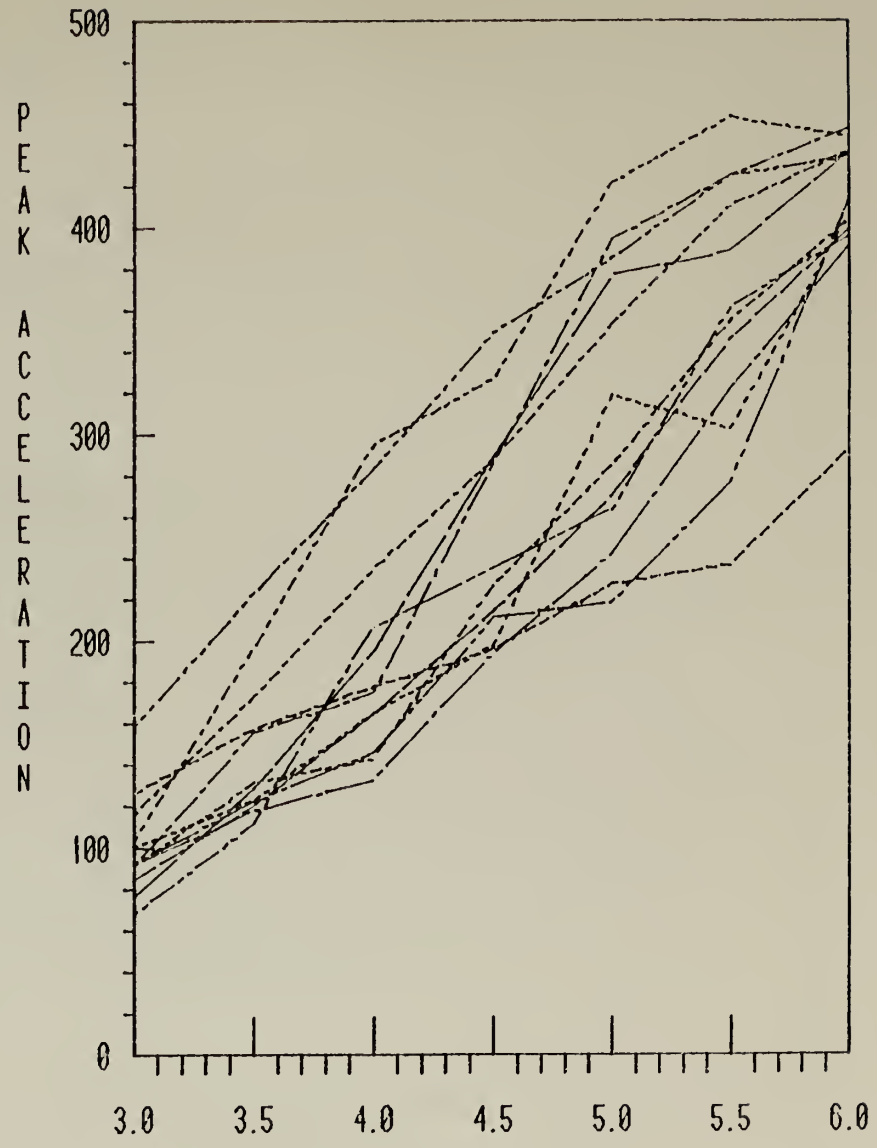

FIGURE 9b

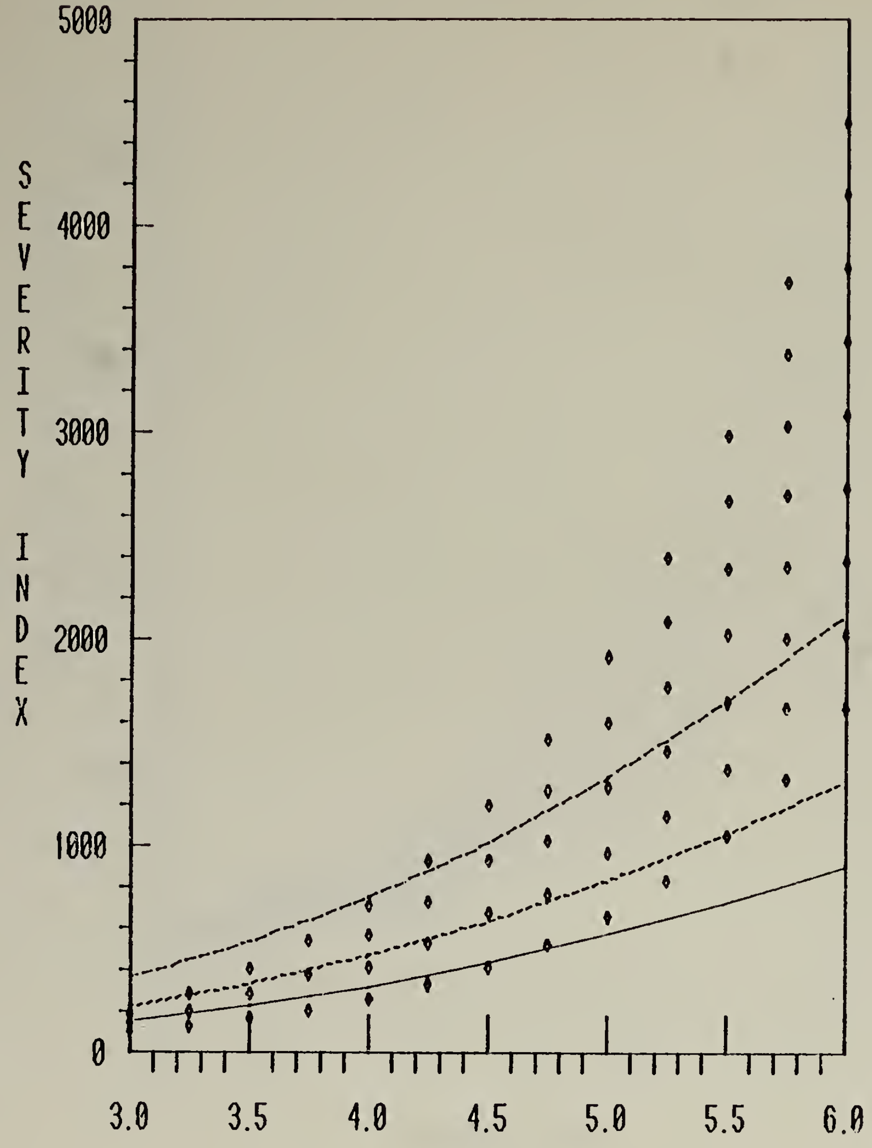

FIGURE 10a

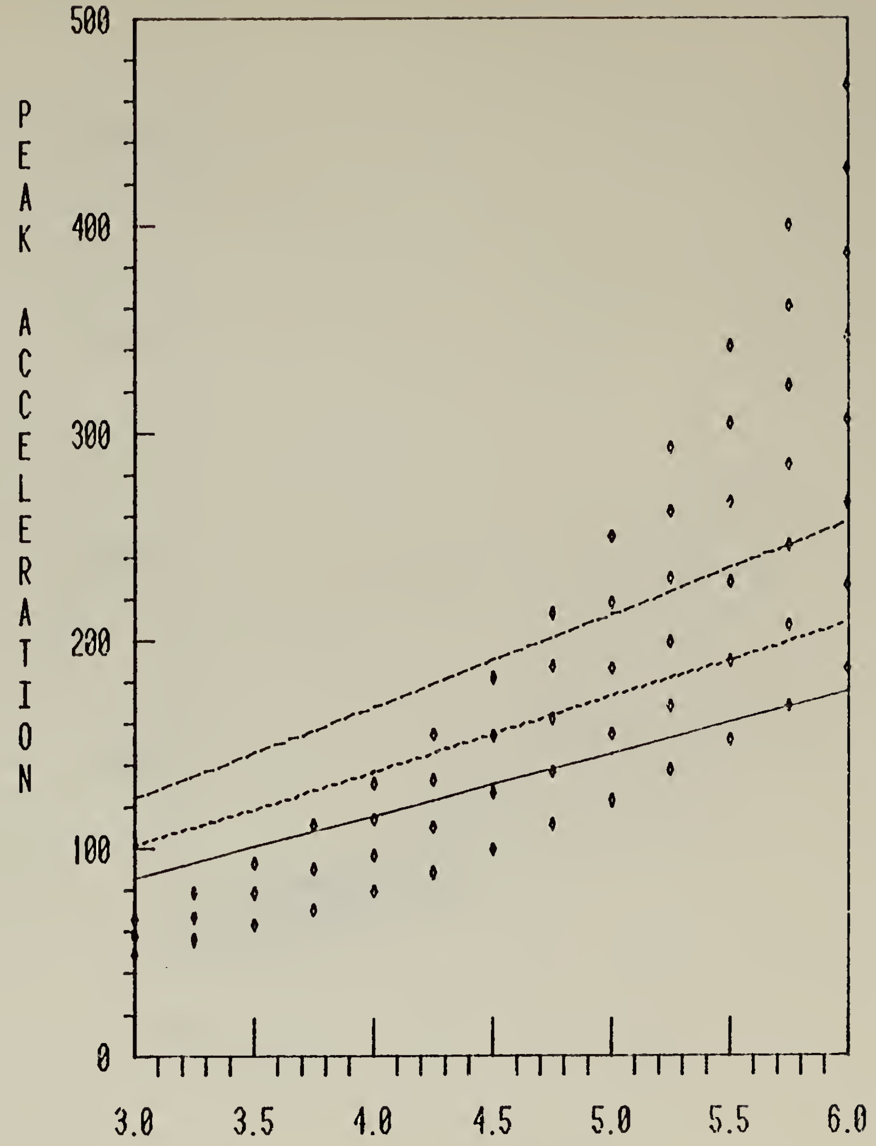

FIGURE 10b

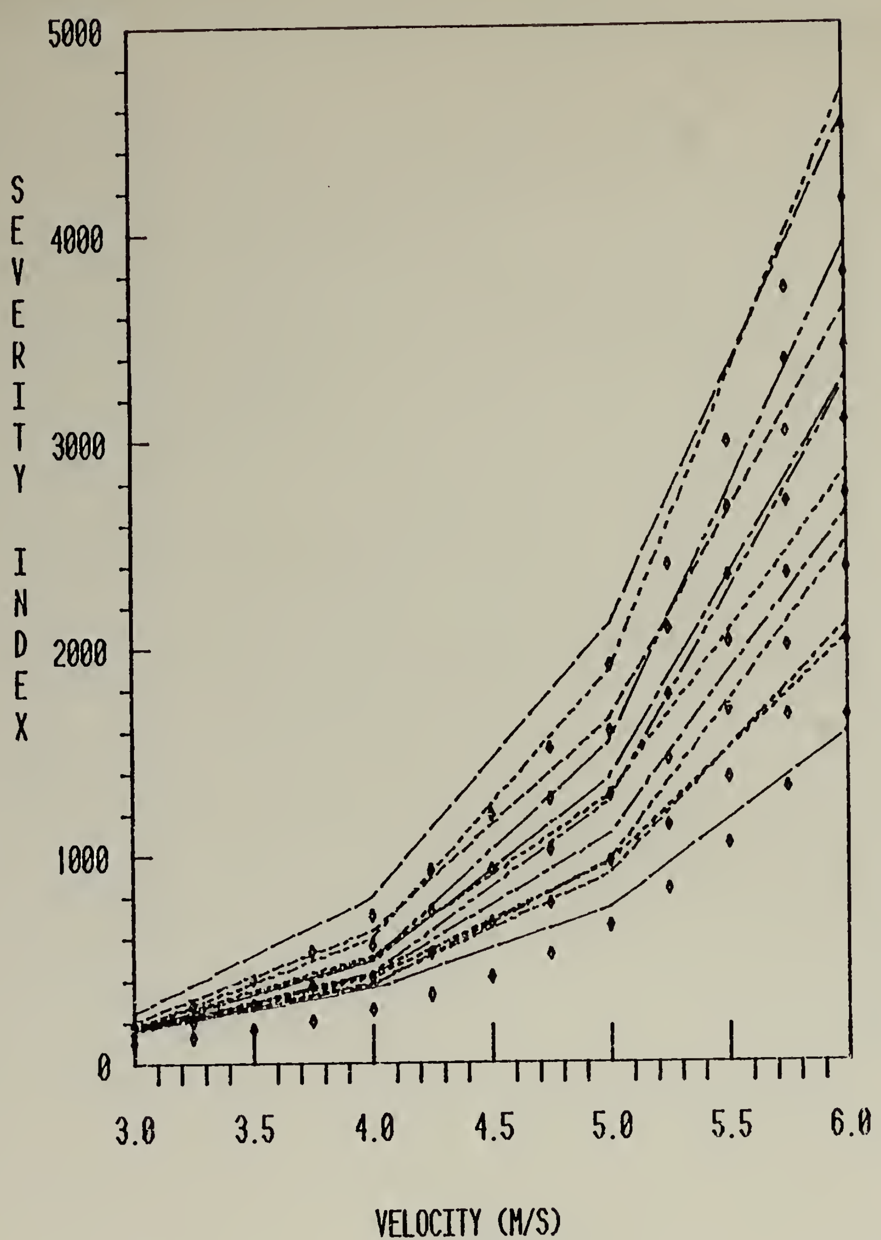

FIGURE 11a

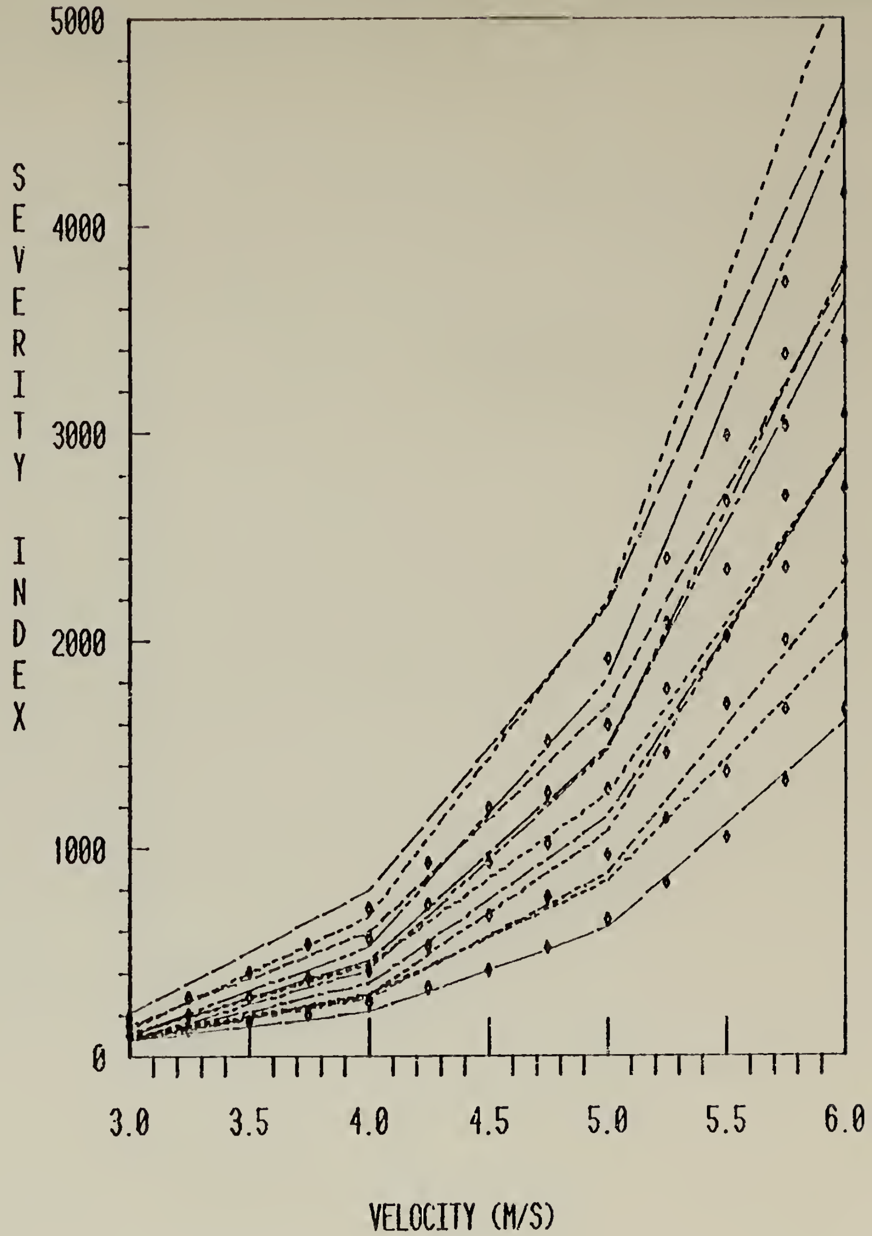

FIGURE 11b

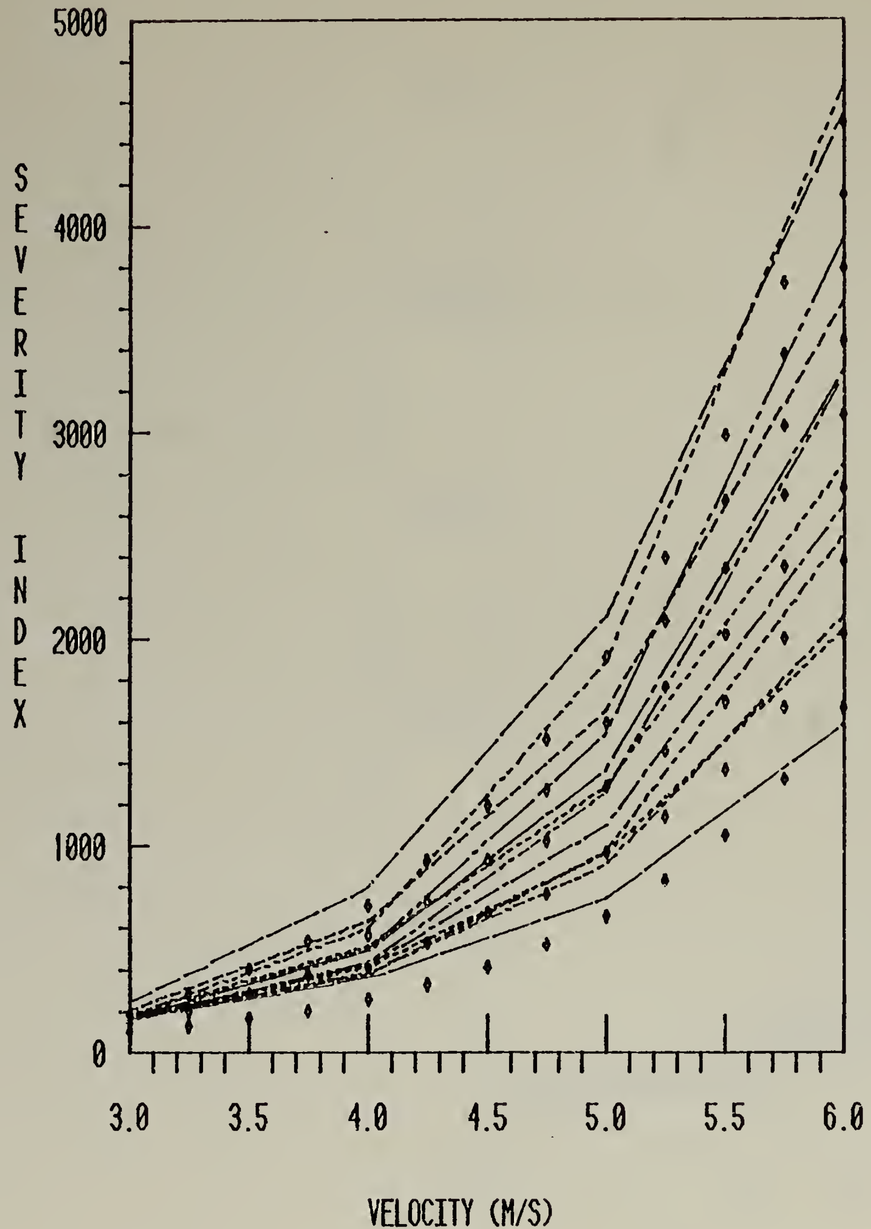

FIGURE 11a

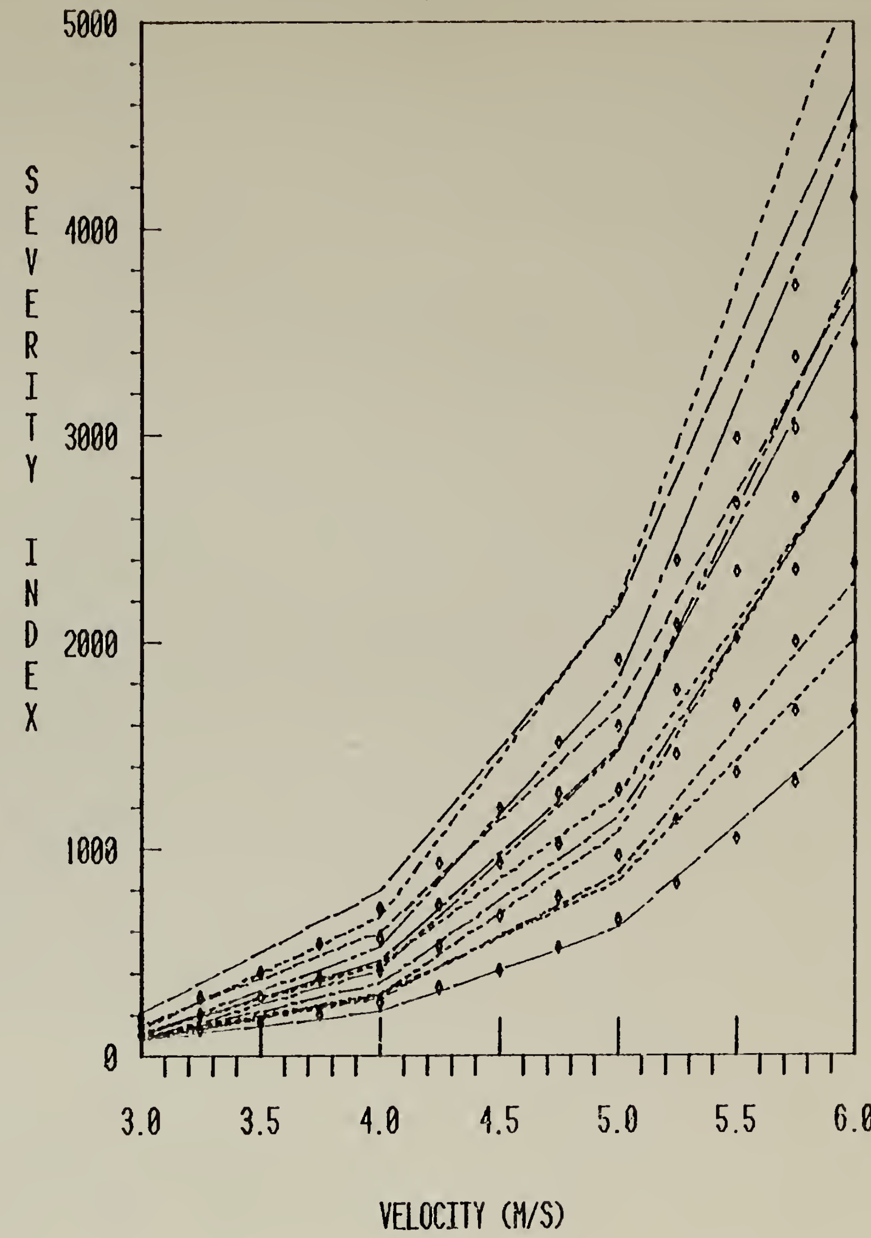

FIGURE 11b

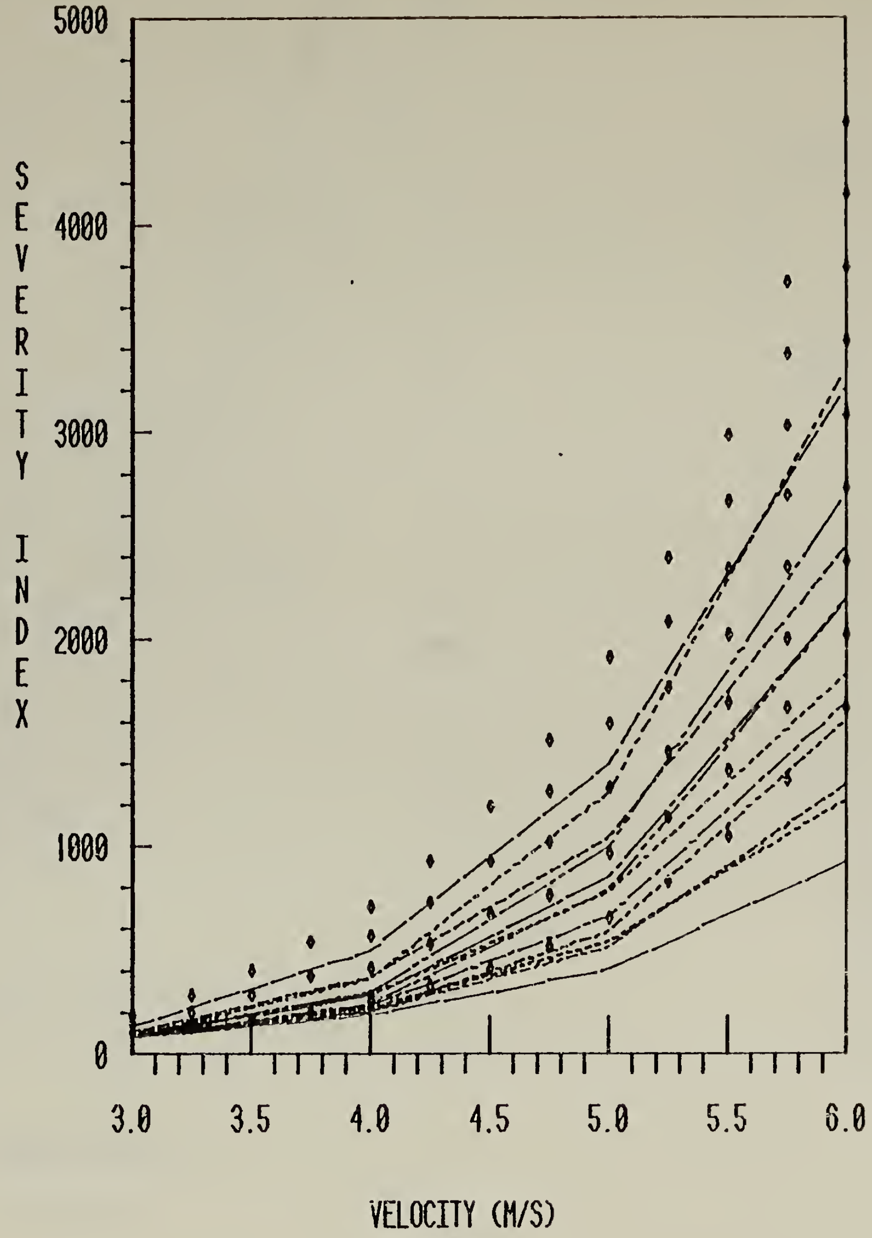

SEVERITY INDEX
5000
4000
3000
2000
1000
0
3.0
3.5
4.0
4.5
5.0
5.5
6.0
VELOCITY (M/S)

FIGURE 11c

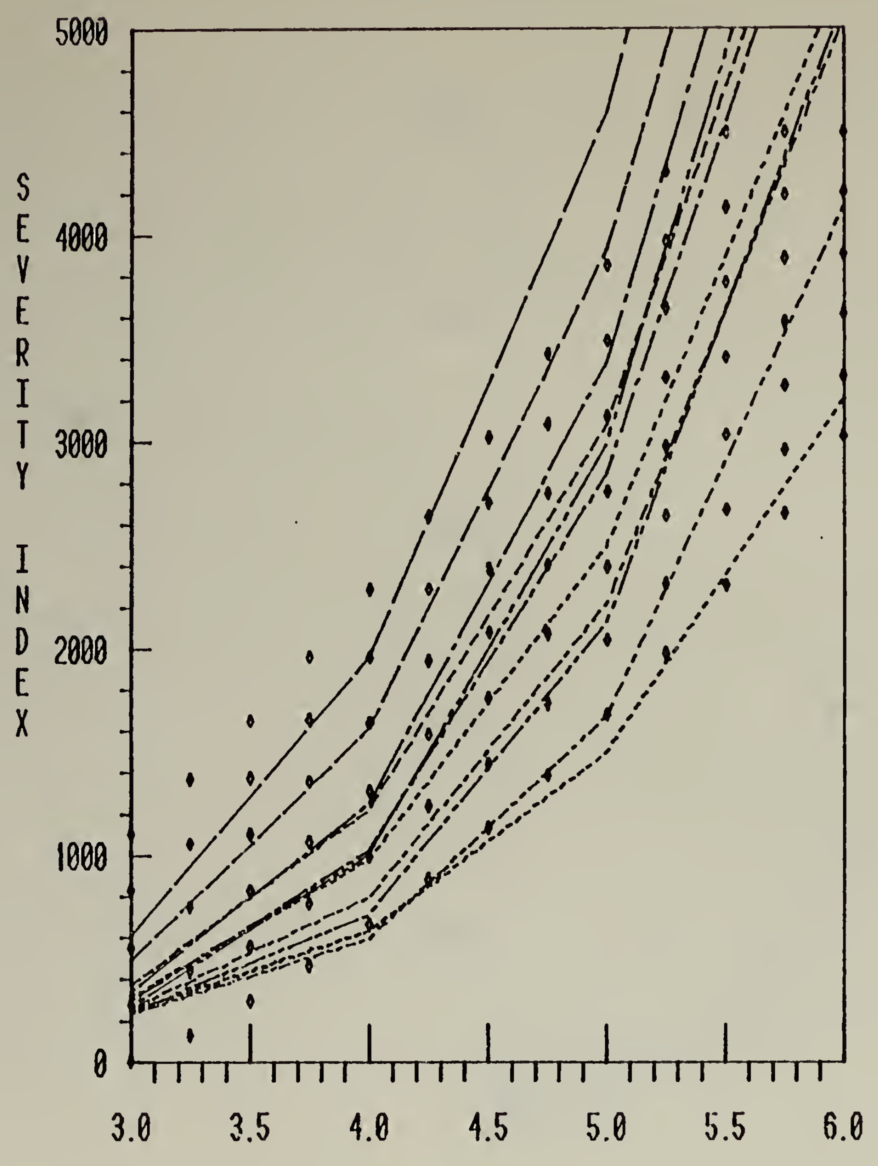

FIGURE 12a

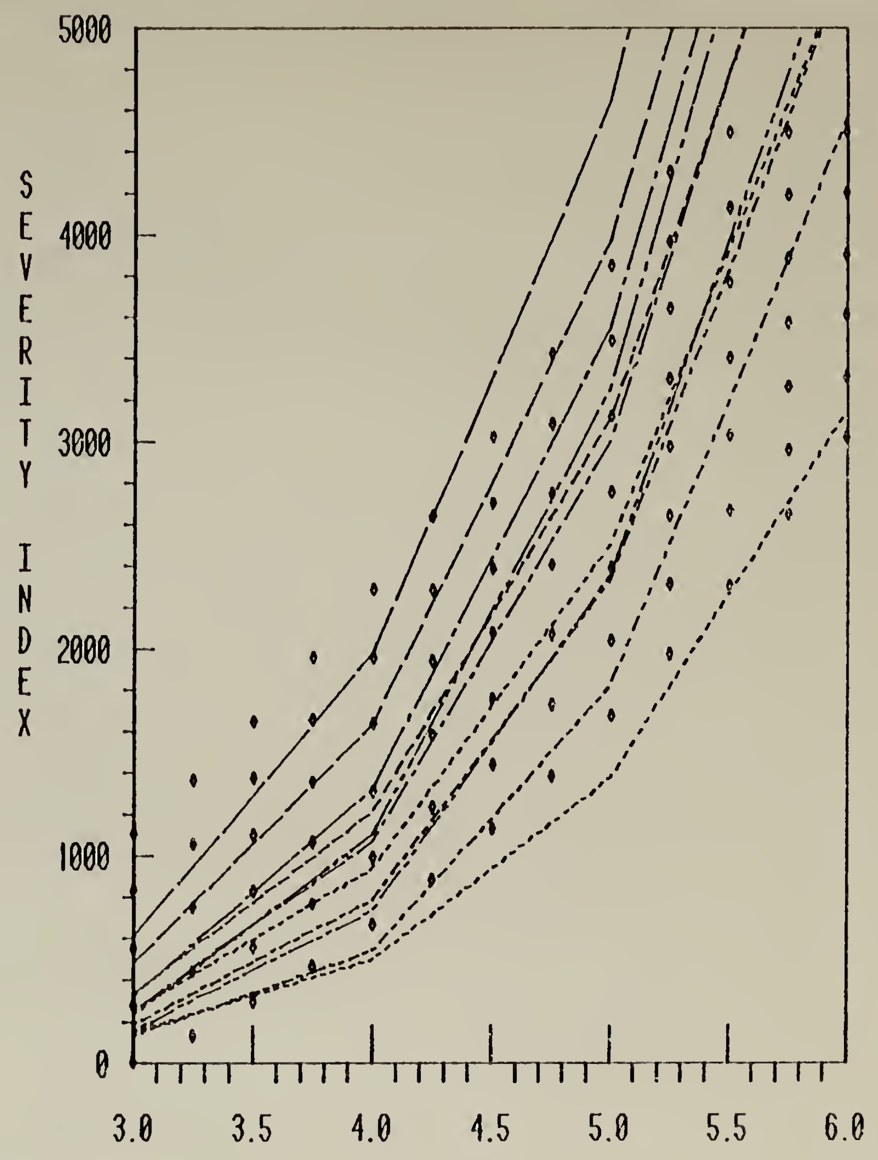

FIGURE 12b

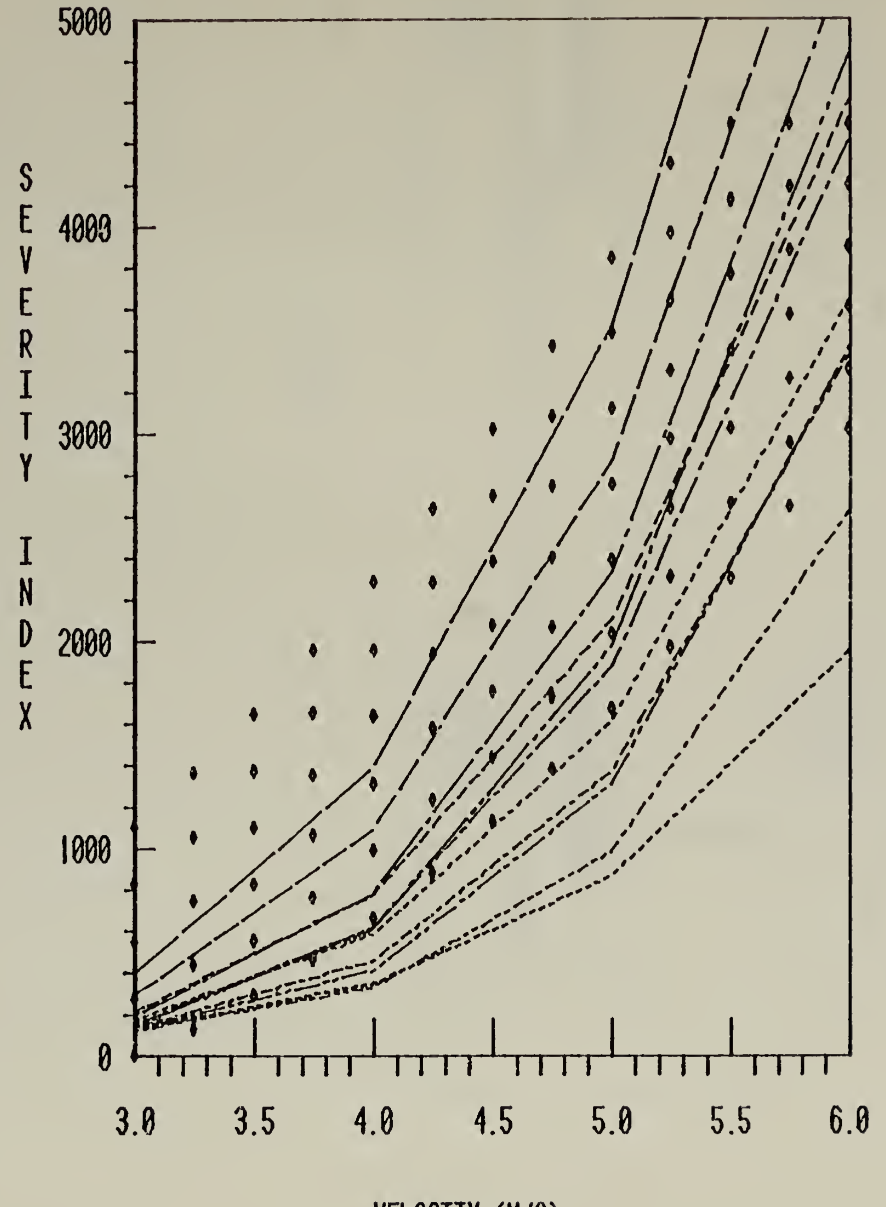
SEVERITY INDEX
5000
4000
3000
2000
1000
0
3.0
3.5
4.0
4.5
5.0
5.5
6.0
VELOCITY (M/S)

FIGURE 12c

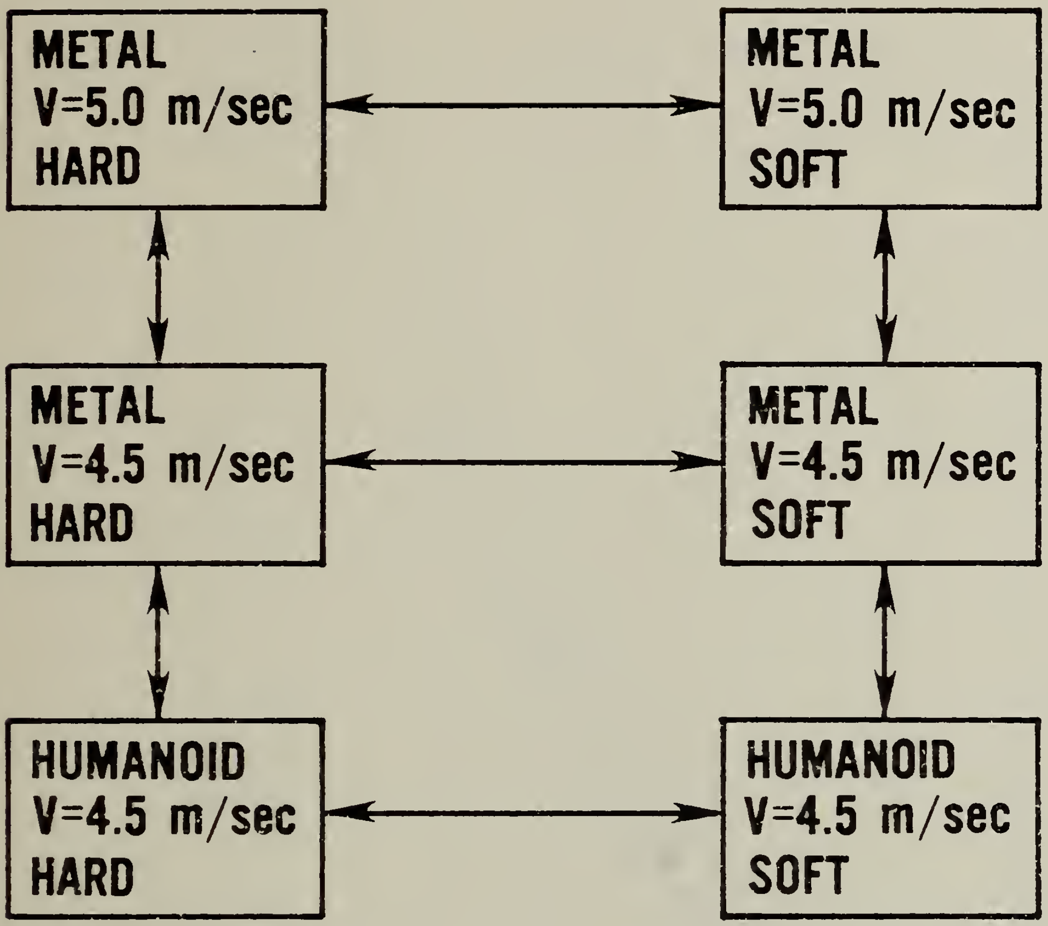
METAL
V=5.0 m/sec
HARD
METAL
V=5.0 m/sec
SOFT
METAL
V=4.5 m/sec
HARD
METAL
V=4.5 m/sec
SOFT
HUMANOID
V=4.5 m/sec
HARD
HUMANOID
V=4.5 m/sec
SOFT

FIGURE 13

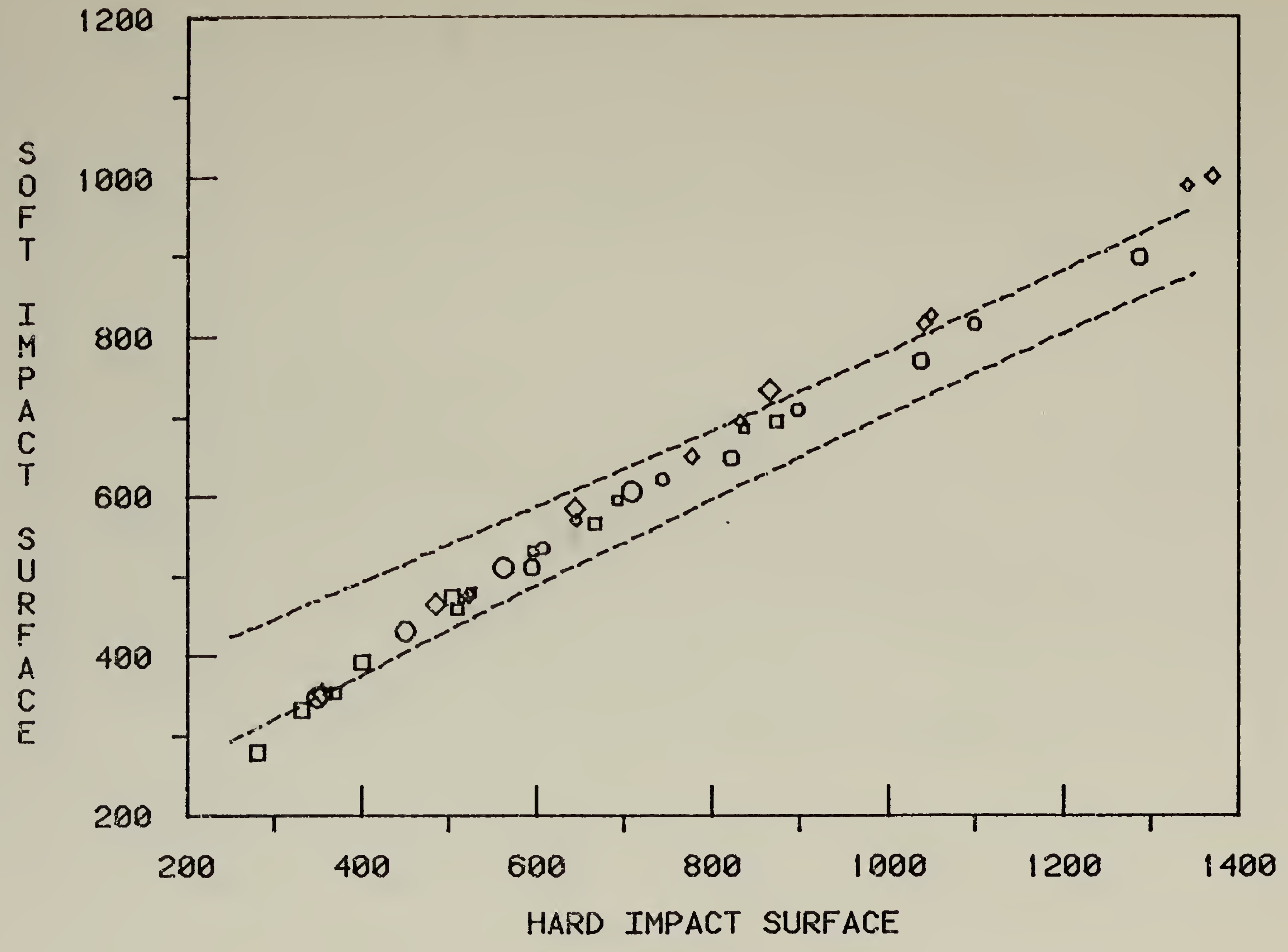

SOFT IMPACT SURFACE
1200
1000
800
600
400
200
200
400
600
800
1000
1200
1400
HARD IMPACT SURFACE

FIGURE 14

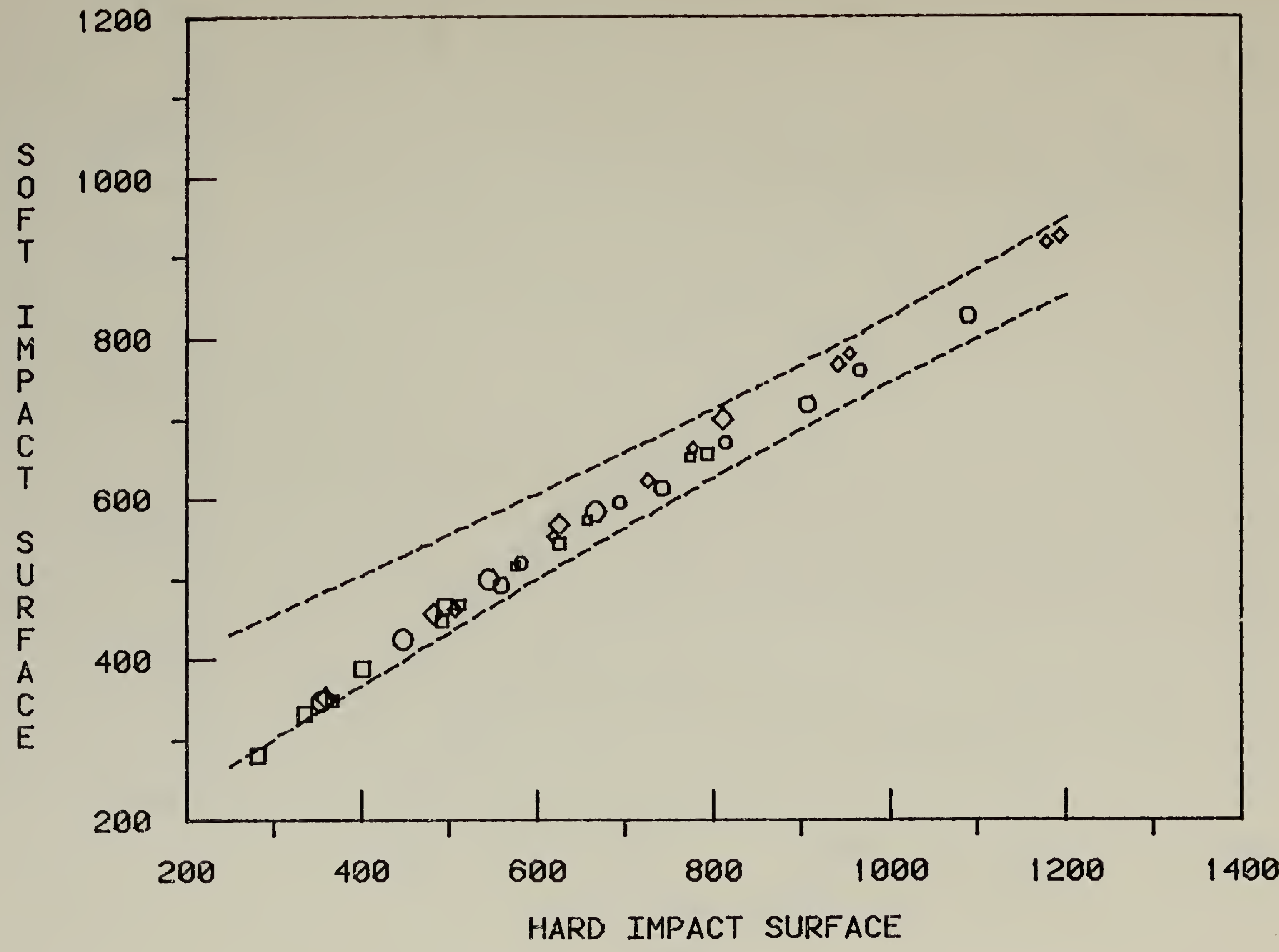

SOFT IMPACT SURFACE
1200
1000
800
600
400
200
200
400
600
800
1000
1200
1400
HARD IMPACT SURFACE

FIGURE 15

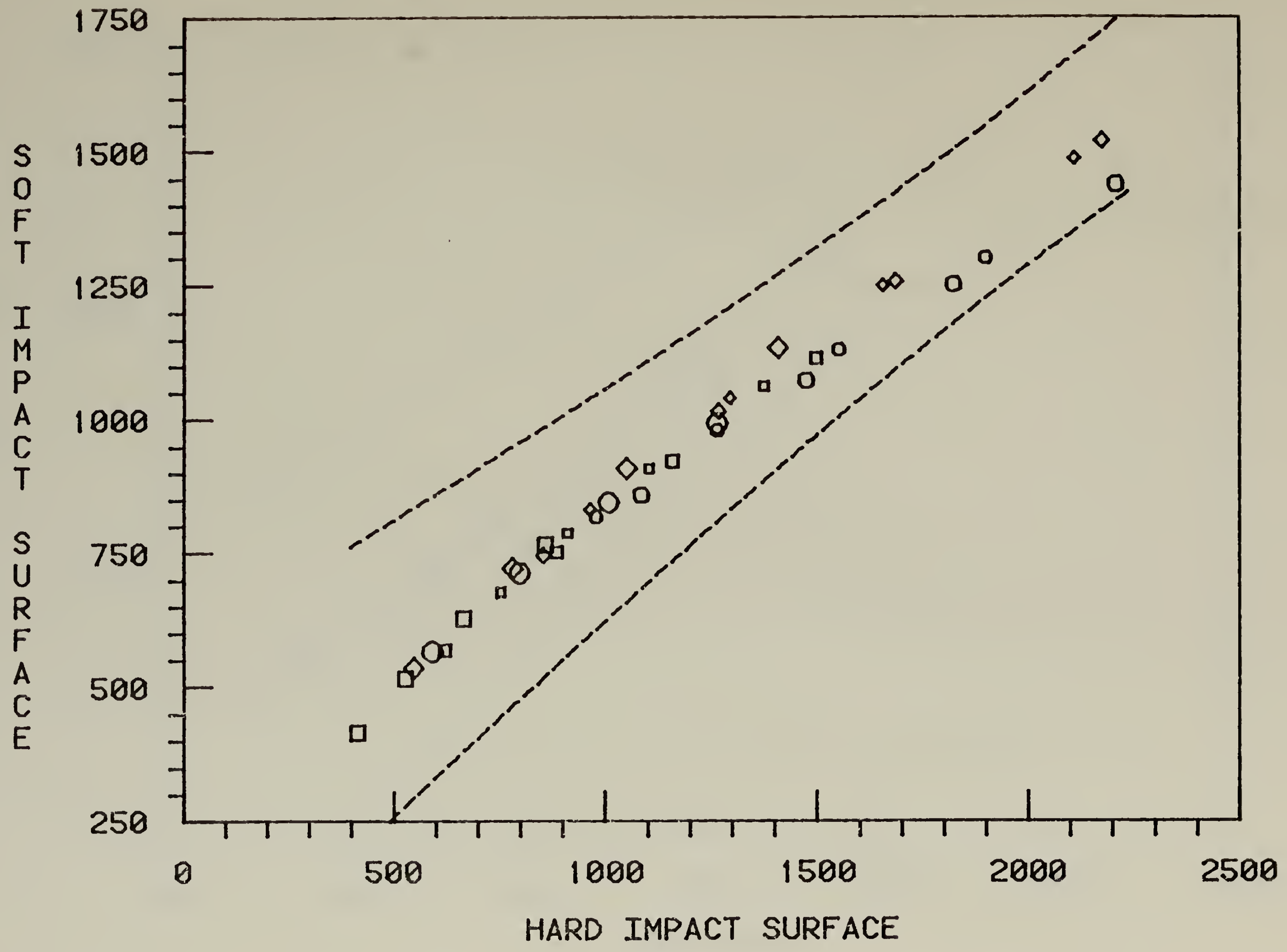
SOFT IMPACT SURFACE
1750
1500
1250
1000
750
500
250
0
500
1000
1500
2000
2500
HARD IMPACT SURFACE

FIGURE 16

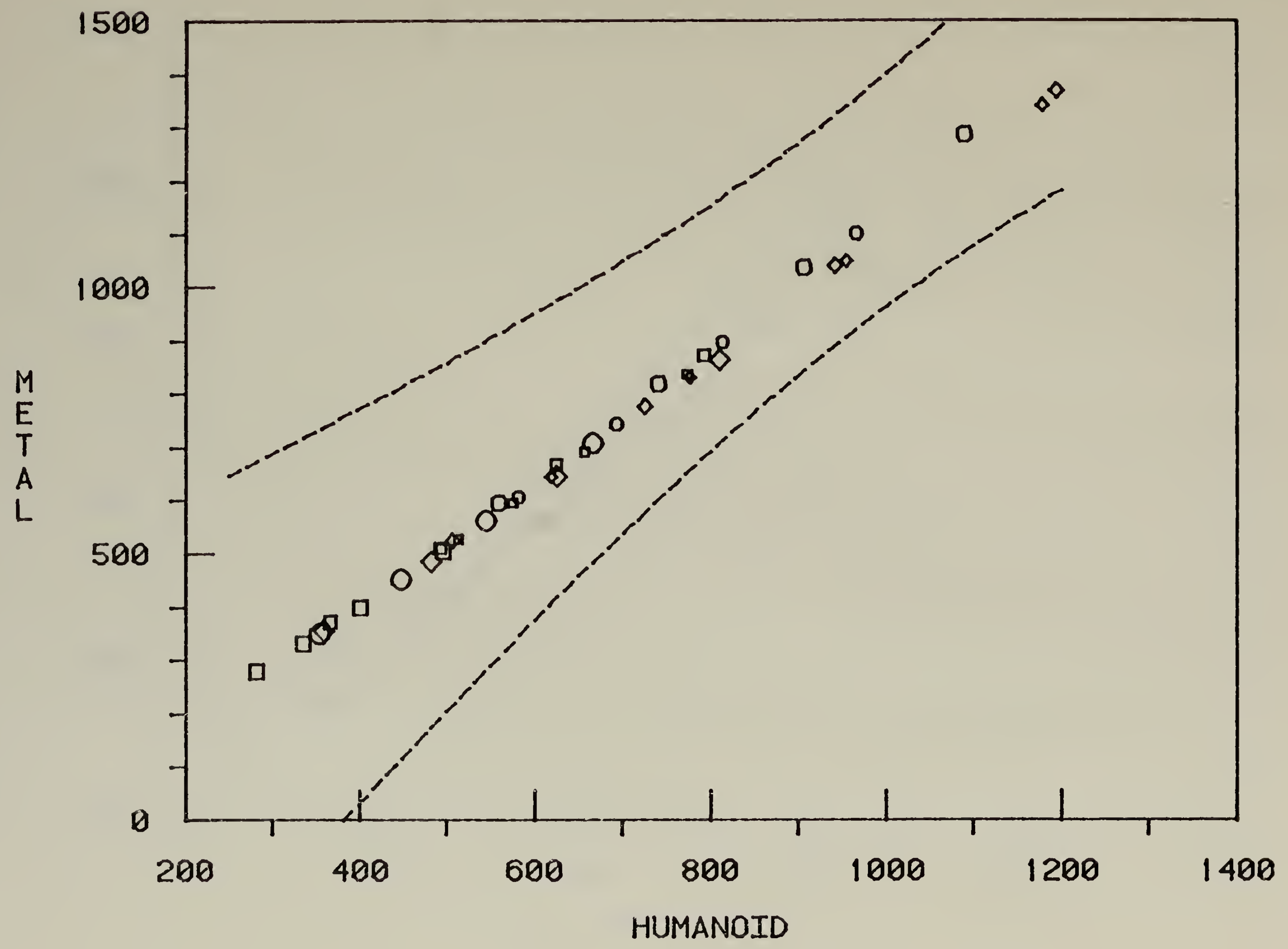

FIGURE 17

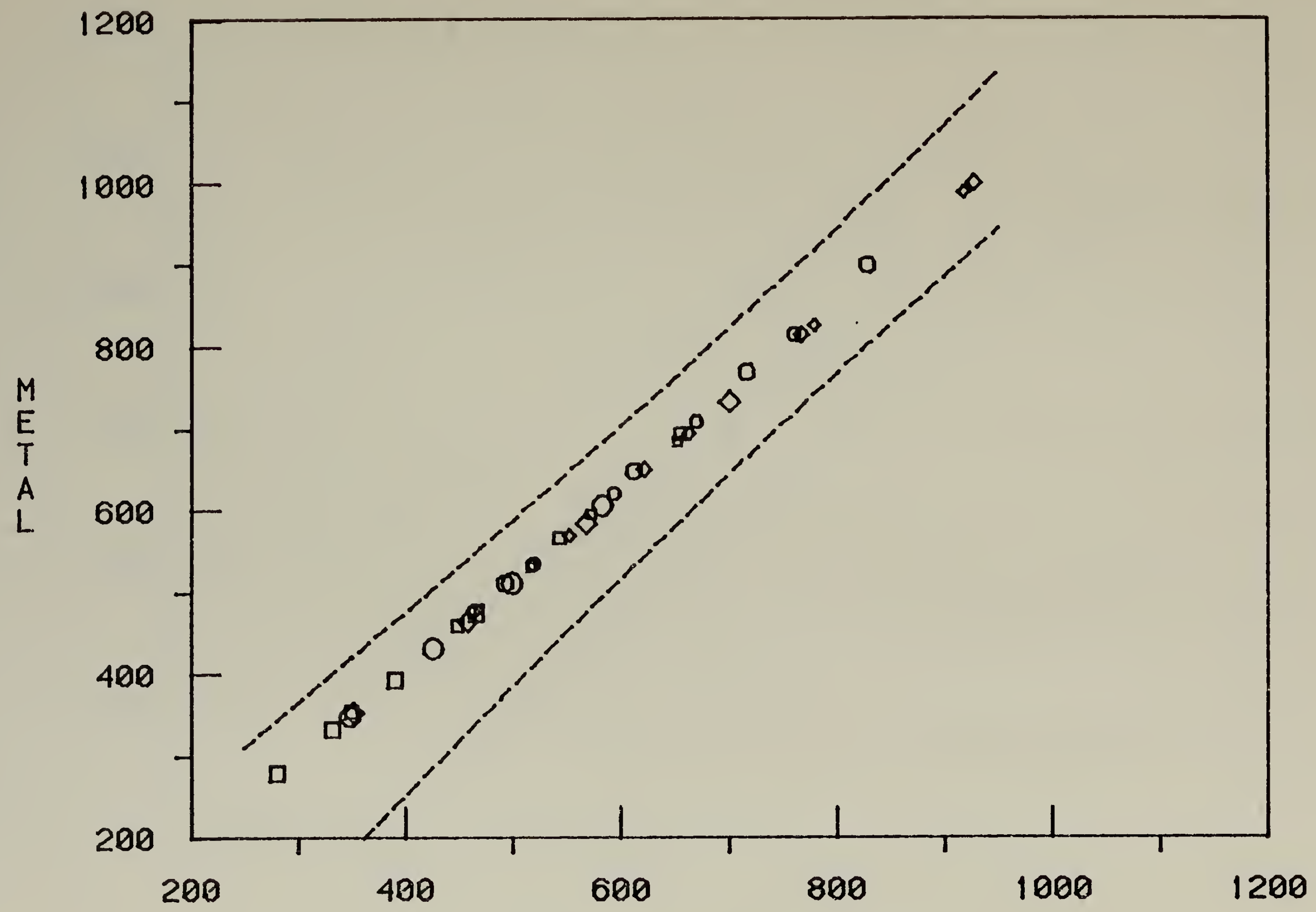
1200
1000
800
600
400
200
METAL
200
400
600
800
1000
1200
HUMANOID

FIGURE 18

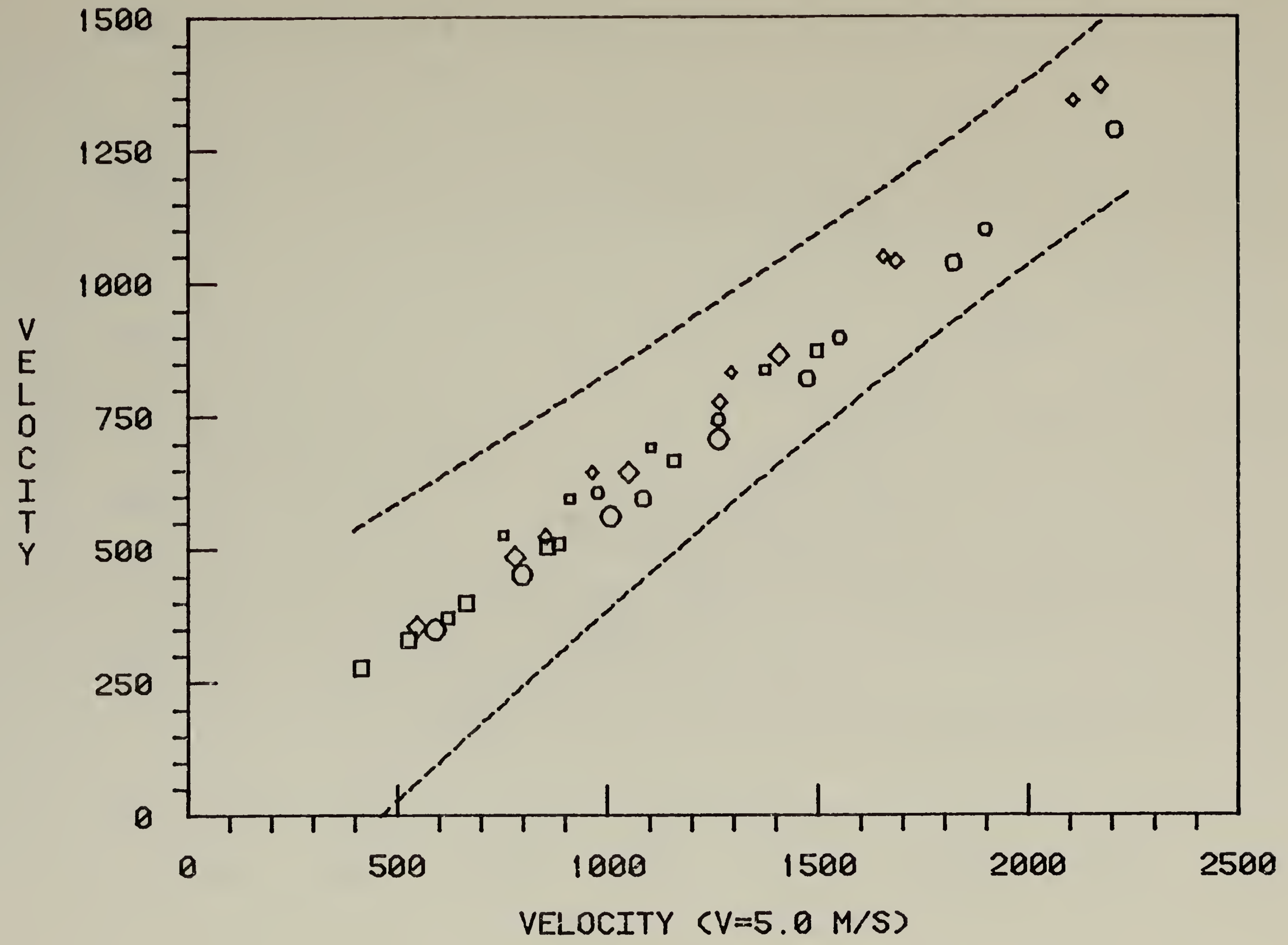
1500
1250
1000
750
500
250
0
VELOCITY
0
500
1000
1500
2000
2500
VELOCITY (V=5.0 M/S)

FIGURE 19

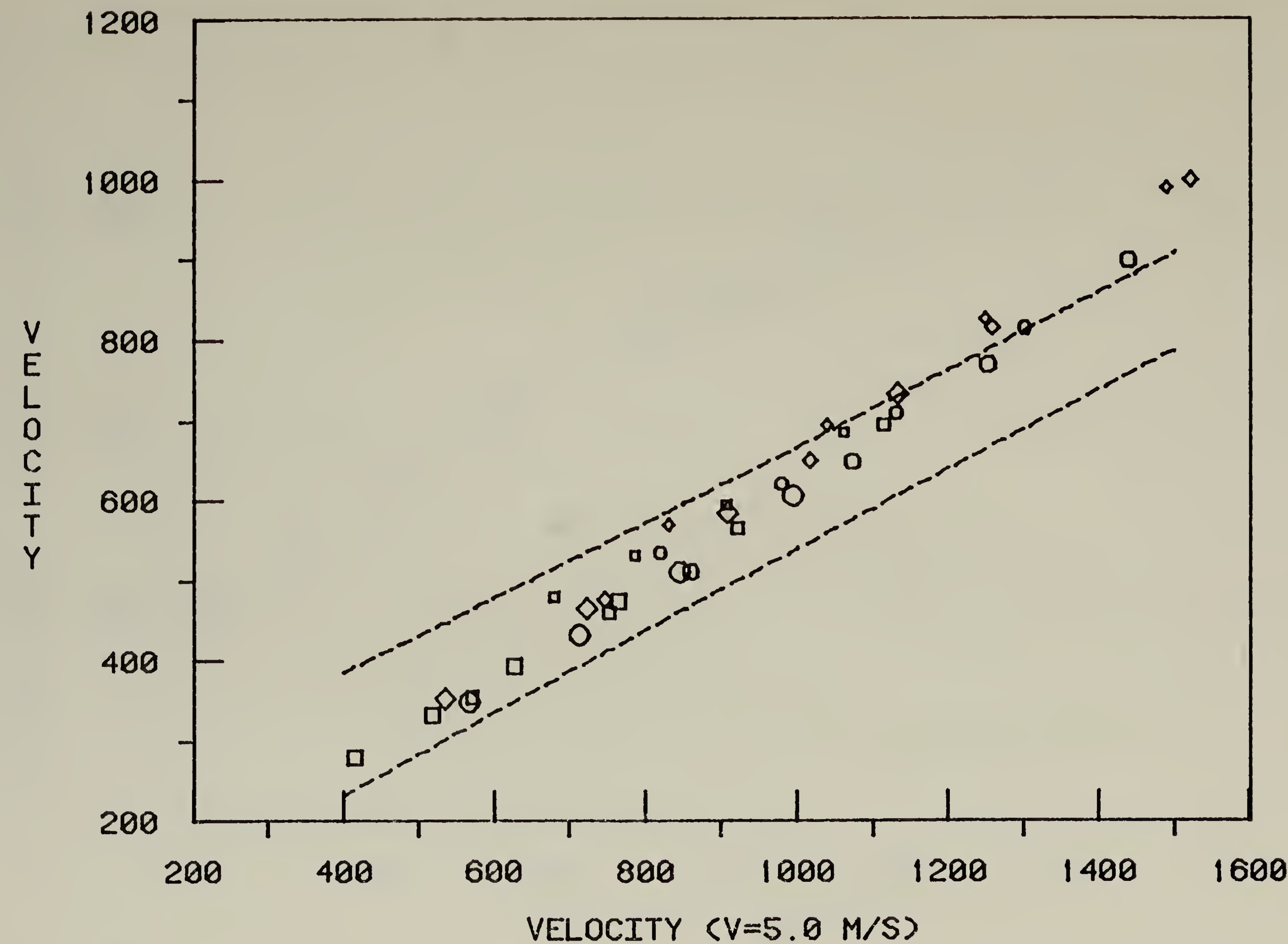
1200
1000
800
600
400
200
VELOCITY
200
400
600
800
1000
1200
1400
1600
VELOCITY (V=5.0 M/S)

FIGURE 20

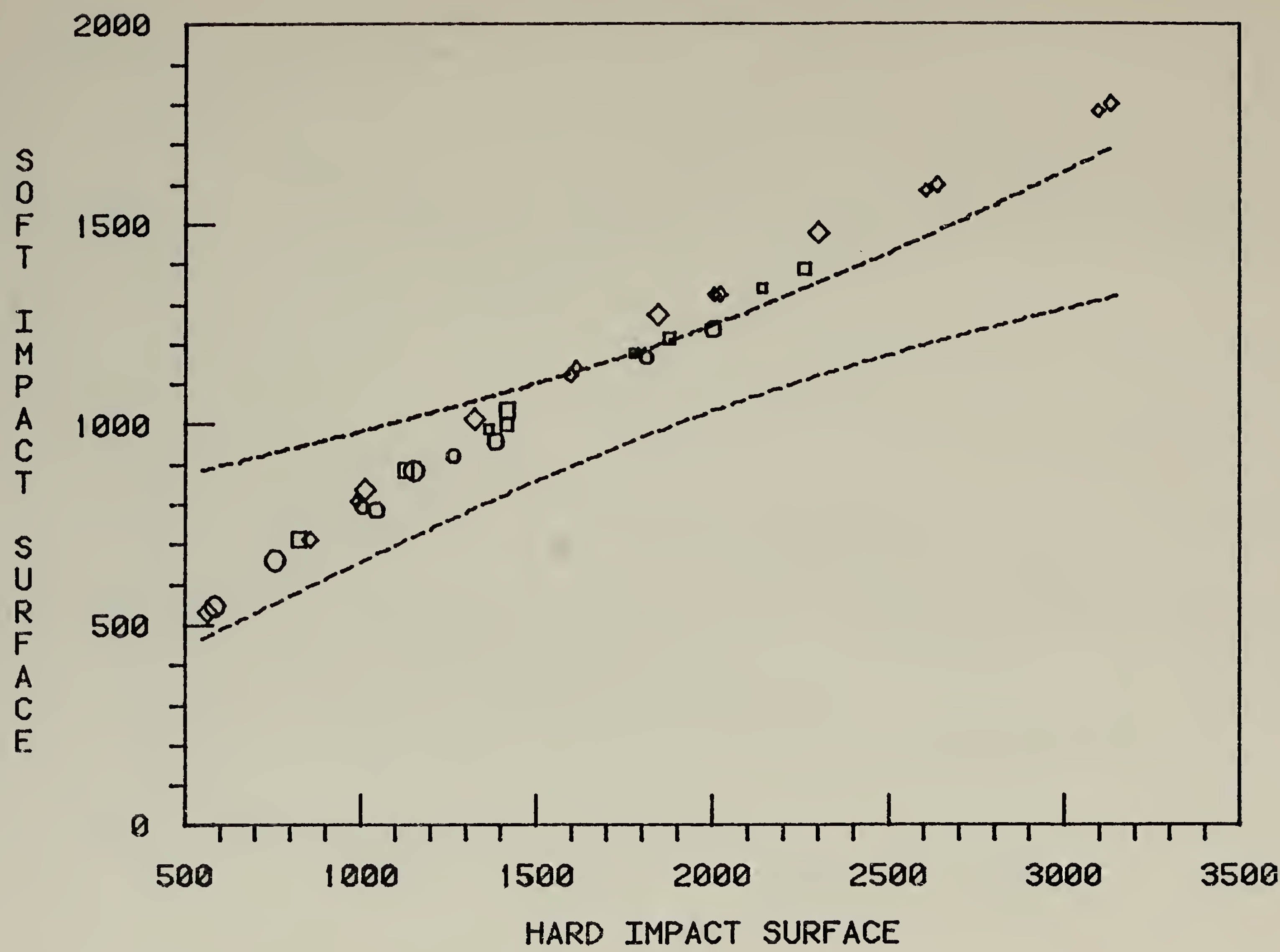
SOFT IMPACT SURFACE
2000
1500
1000
500
0
500
1000
1500
2000
2500
3000
3500
HARD IMPACT SURFACE

FIGURE 21

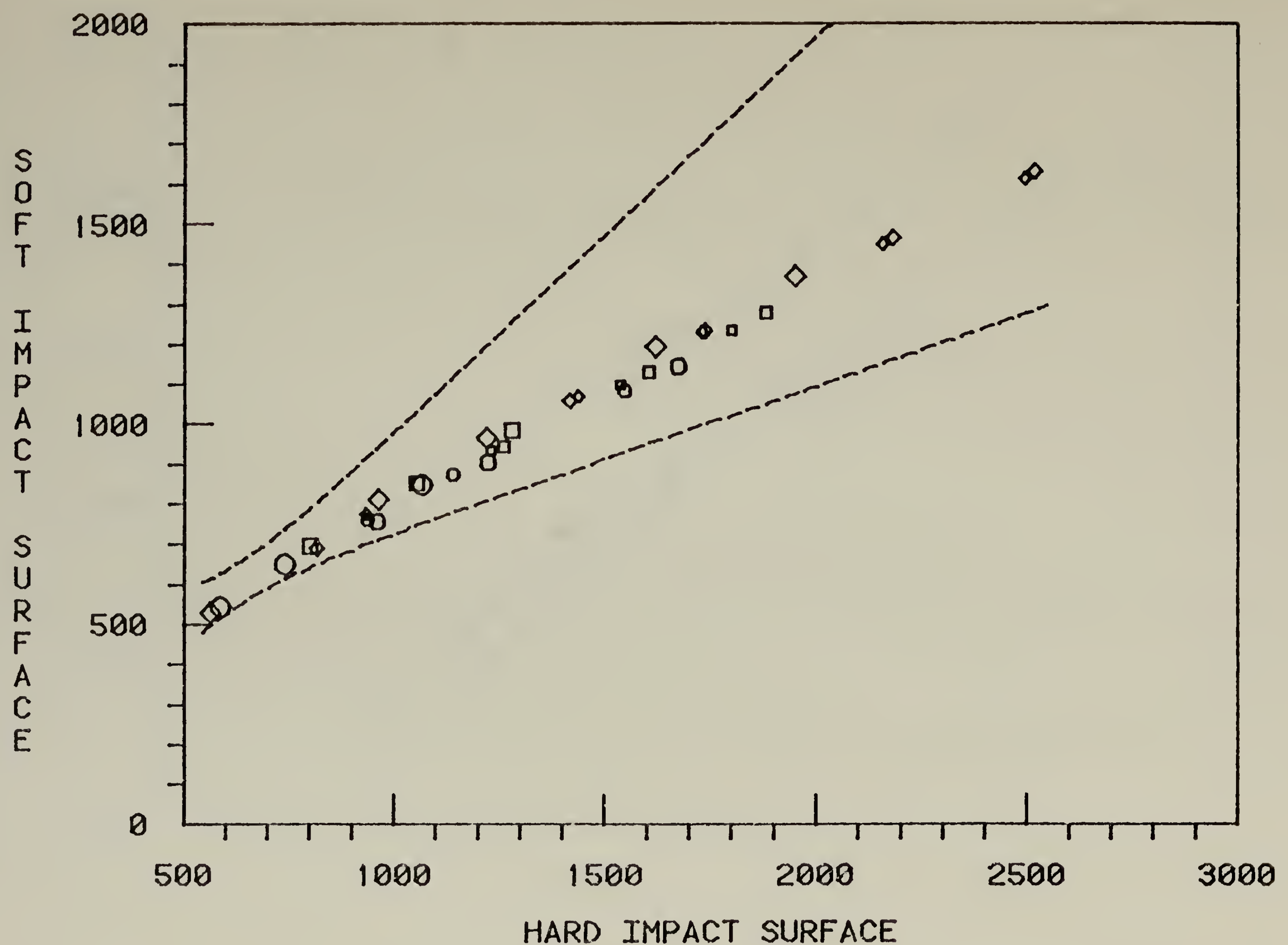
2000
1500
1000
500
0
SOFT IMPACT SURFACE
500
1000
1500
2000
2500
3000
HARD IMPACT SURFACE

FIGURE 22

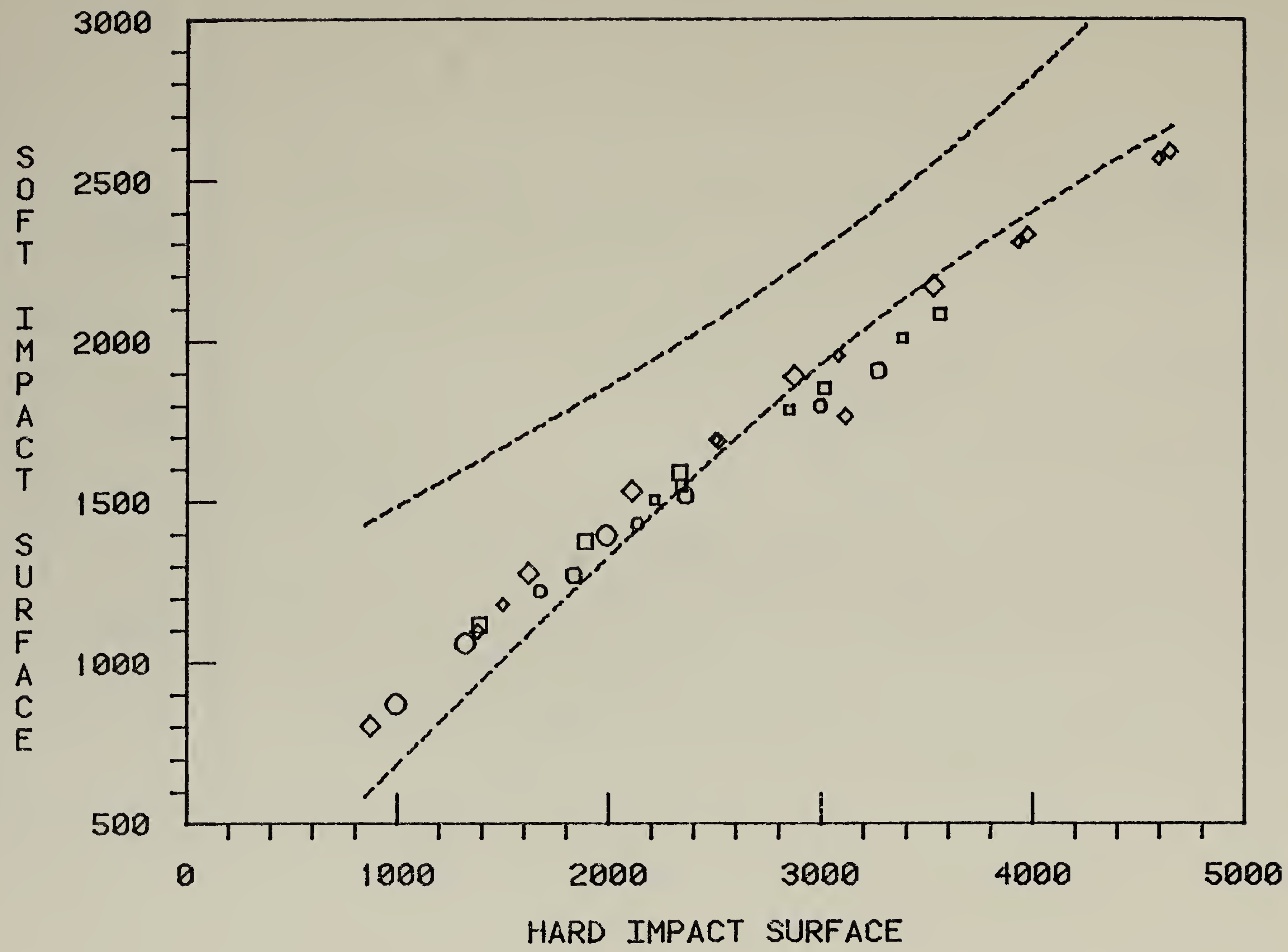

SOFT IMPACT SURFACE
3000
2500
2000
1500
1000
500
0
1000
2000
3000
4000
5000
HARD IMPACT SURFACE

FIGURE 23

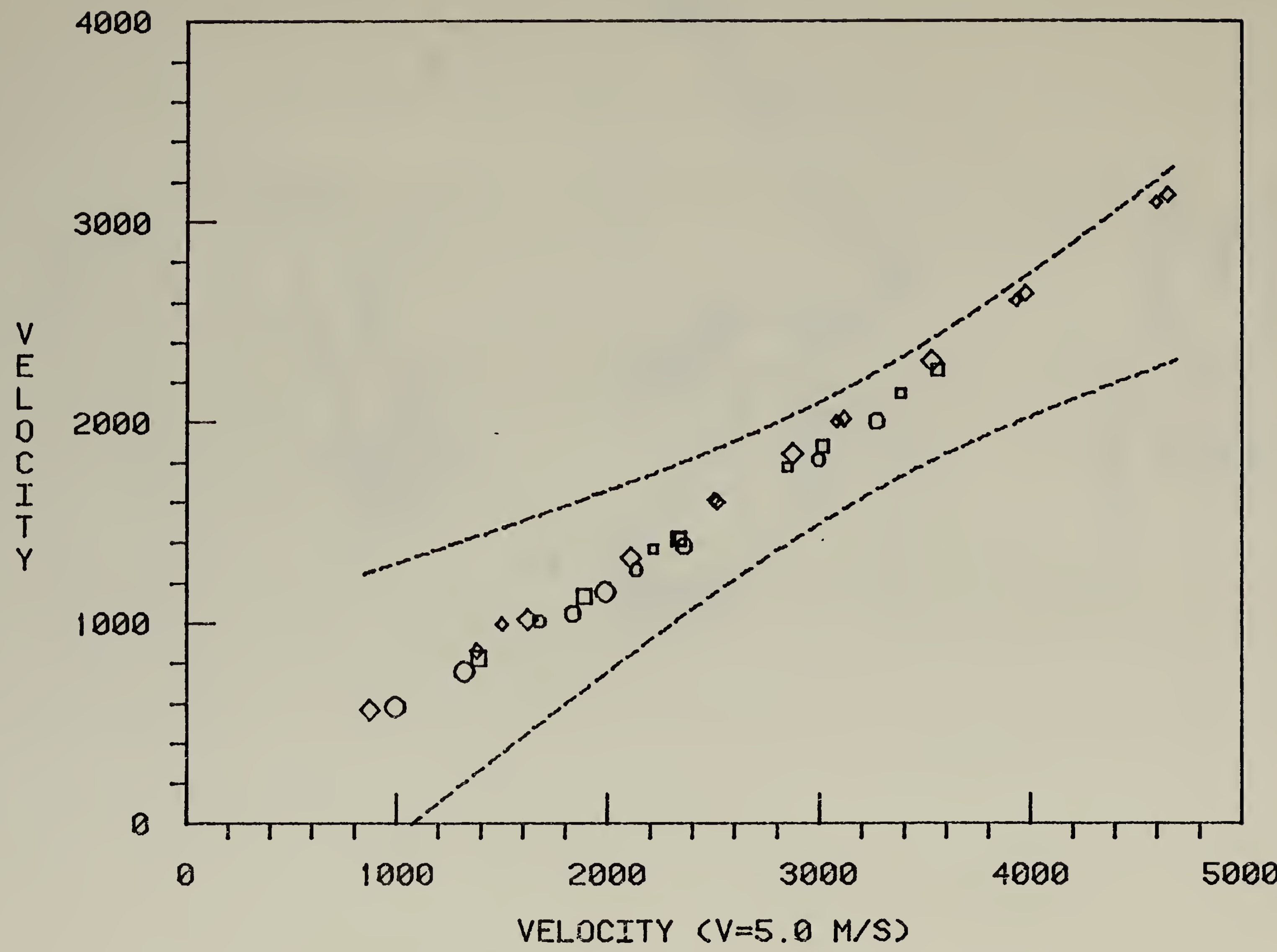
4000
3000
2000
1000
0
VELOCITY
0
1000
2000
3000
4000
5000
VELOCITY (V=5.0 M/S)

FIGURE 24

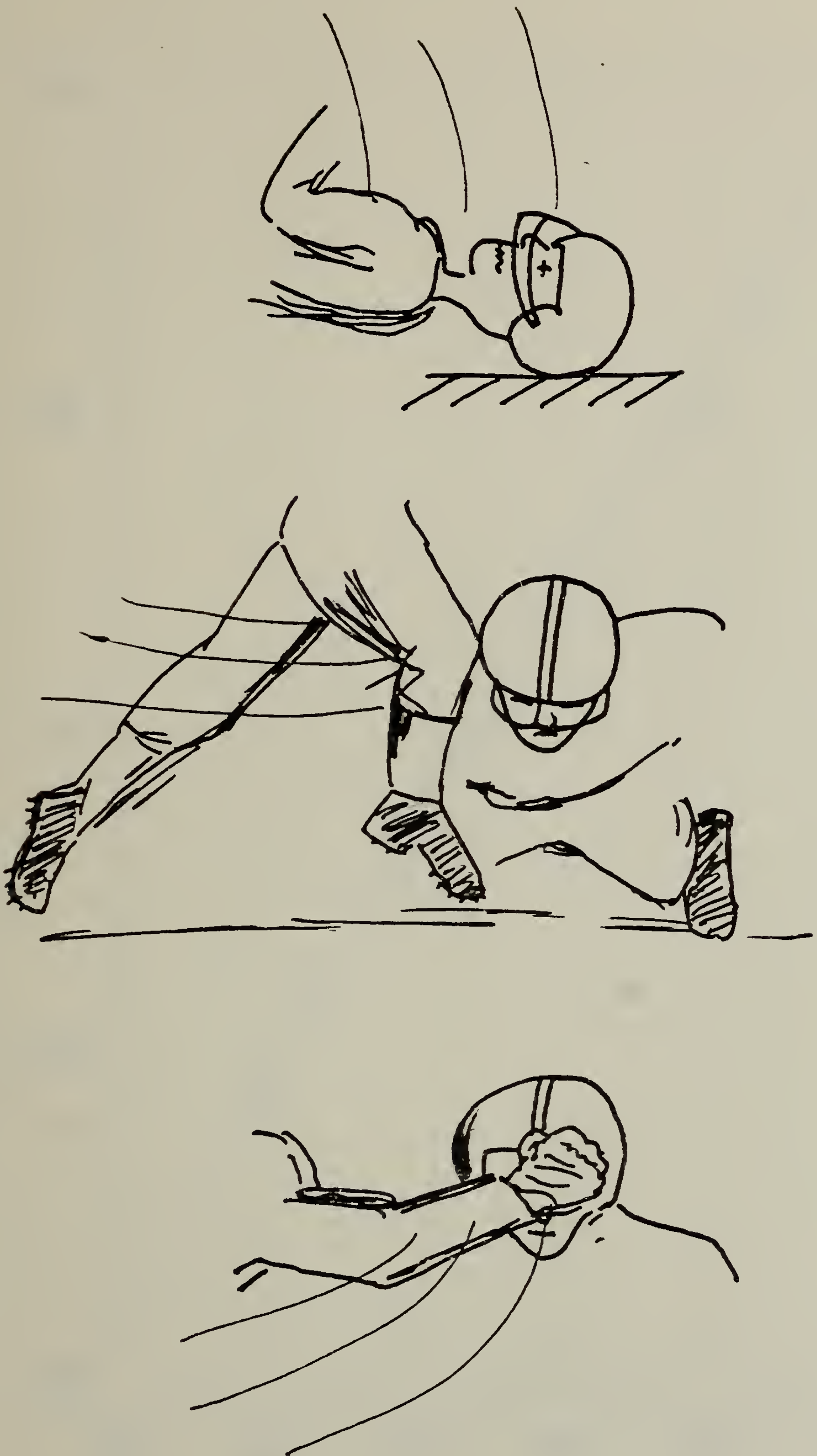

FIGURE 25

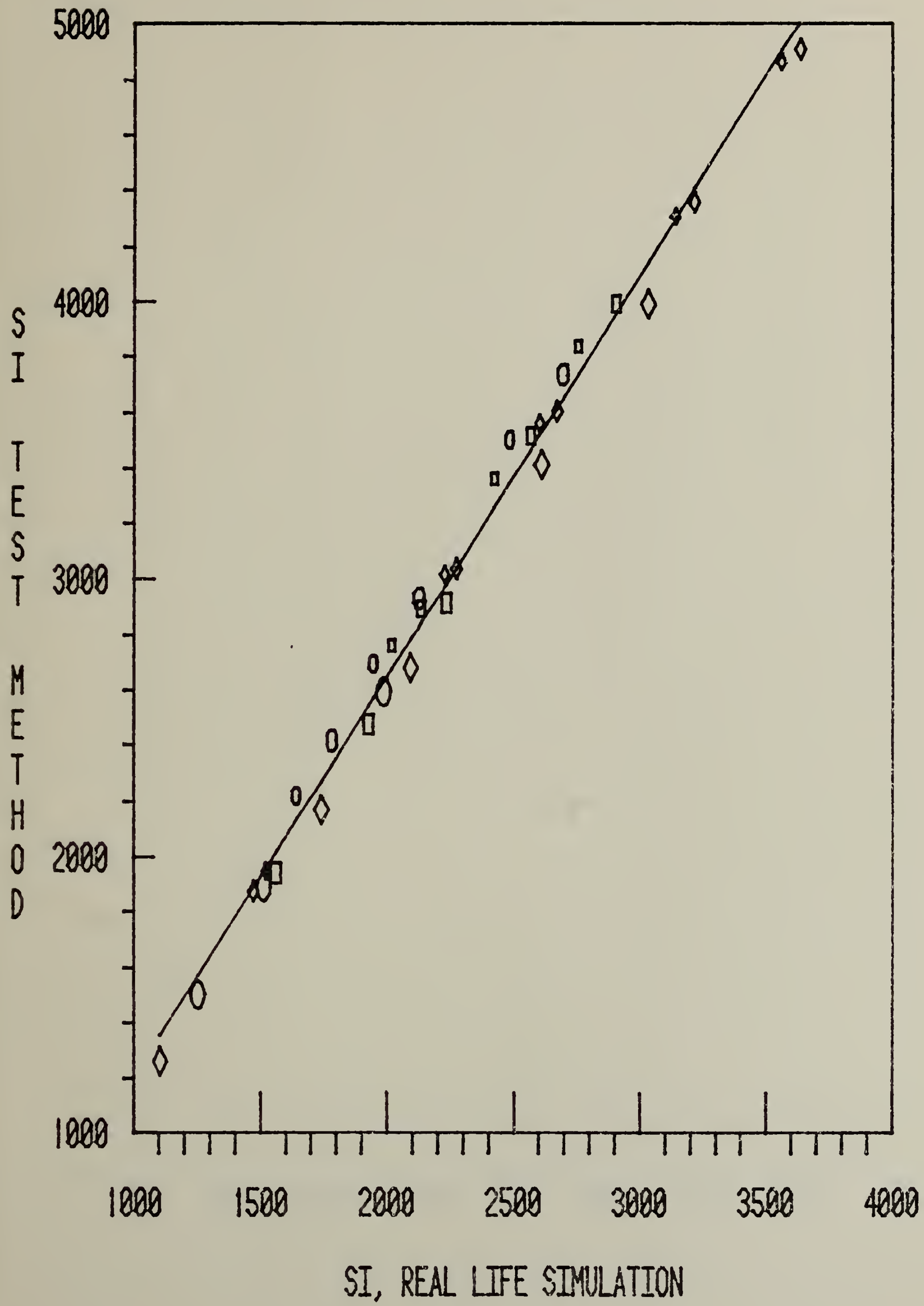
5000
4000
3000
2000
1000
S I   T E S T   M E T H O D
1000
1500
2000
2500
3000
3500
4000
SI, REAL LIFE SIMULATION

FIGURE 26

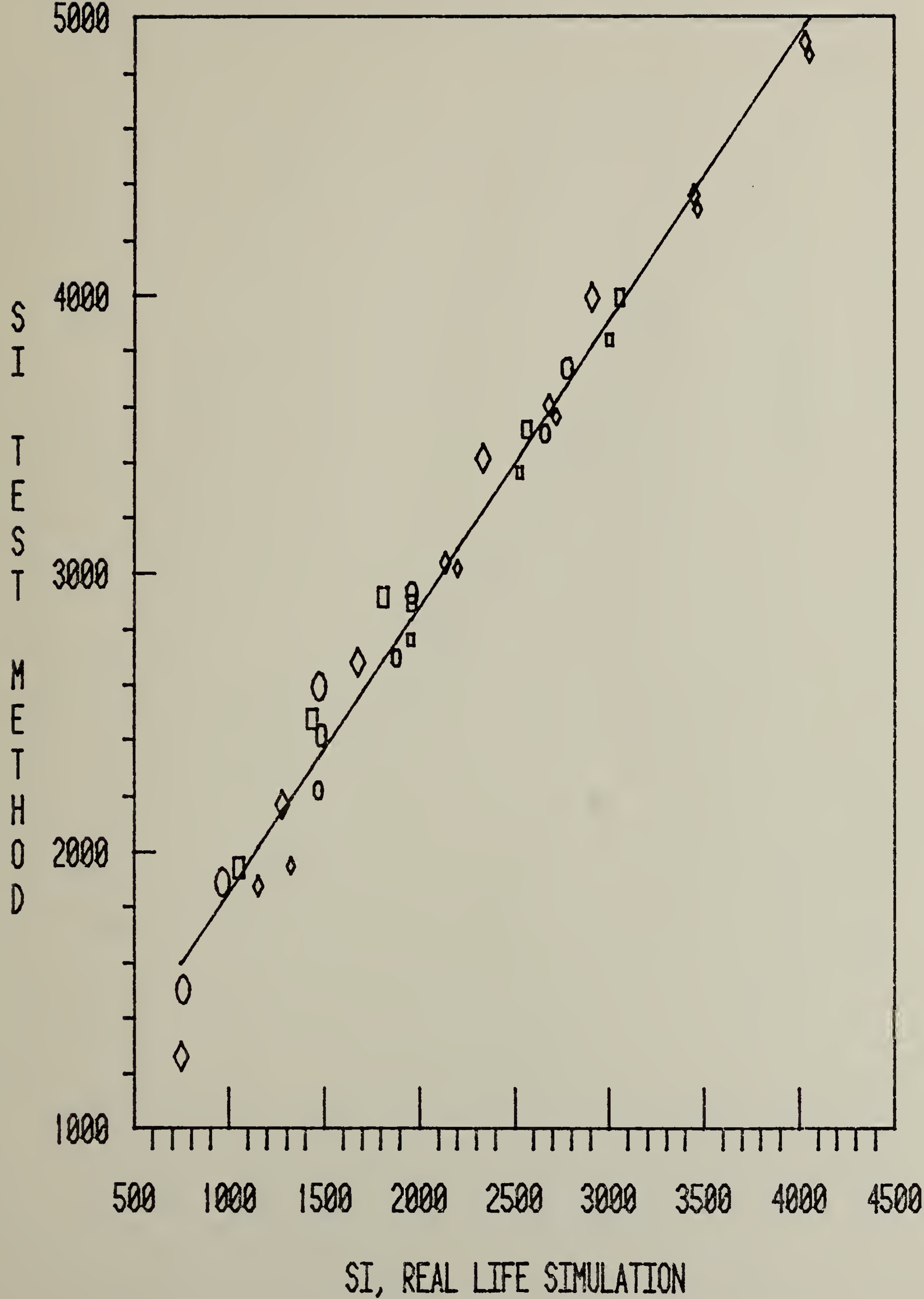
5000
4000
3000
2000
1000
S I T E S T M E T H O D
500
1000
1500
2000
2500
3000
3500
4000
4500
SI, REAL LIFE SIMULATION

FIGURE 27

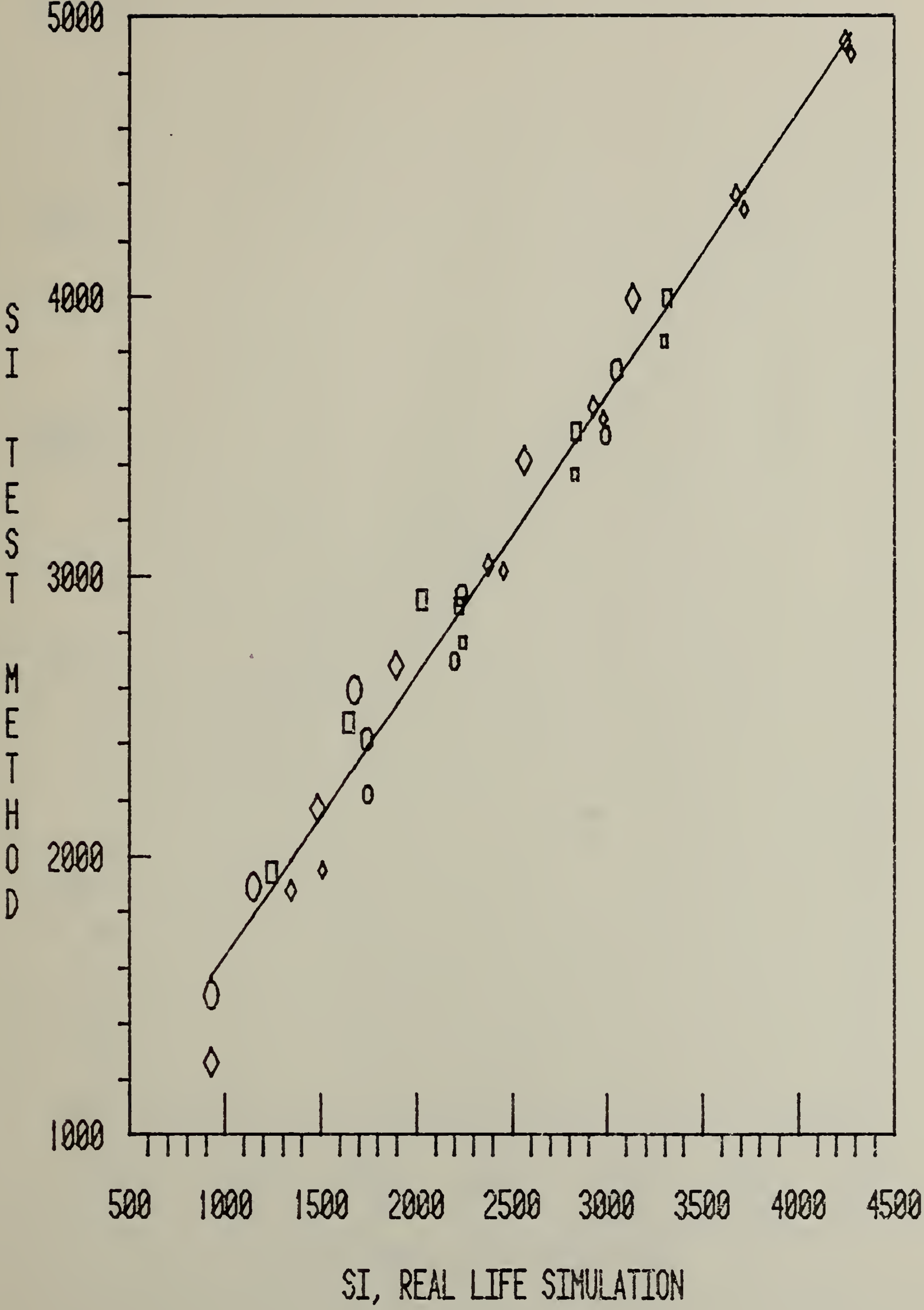

5000
4000
3000
2000
1000
S I TEST METHOD
500
1000
1500
2000
2500
3000
3500
4000
4500
SI, REAL LIFE SIMULATION

FIGURE 28

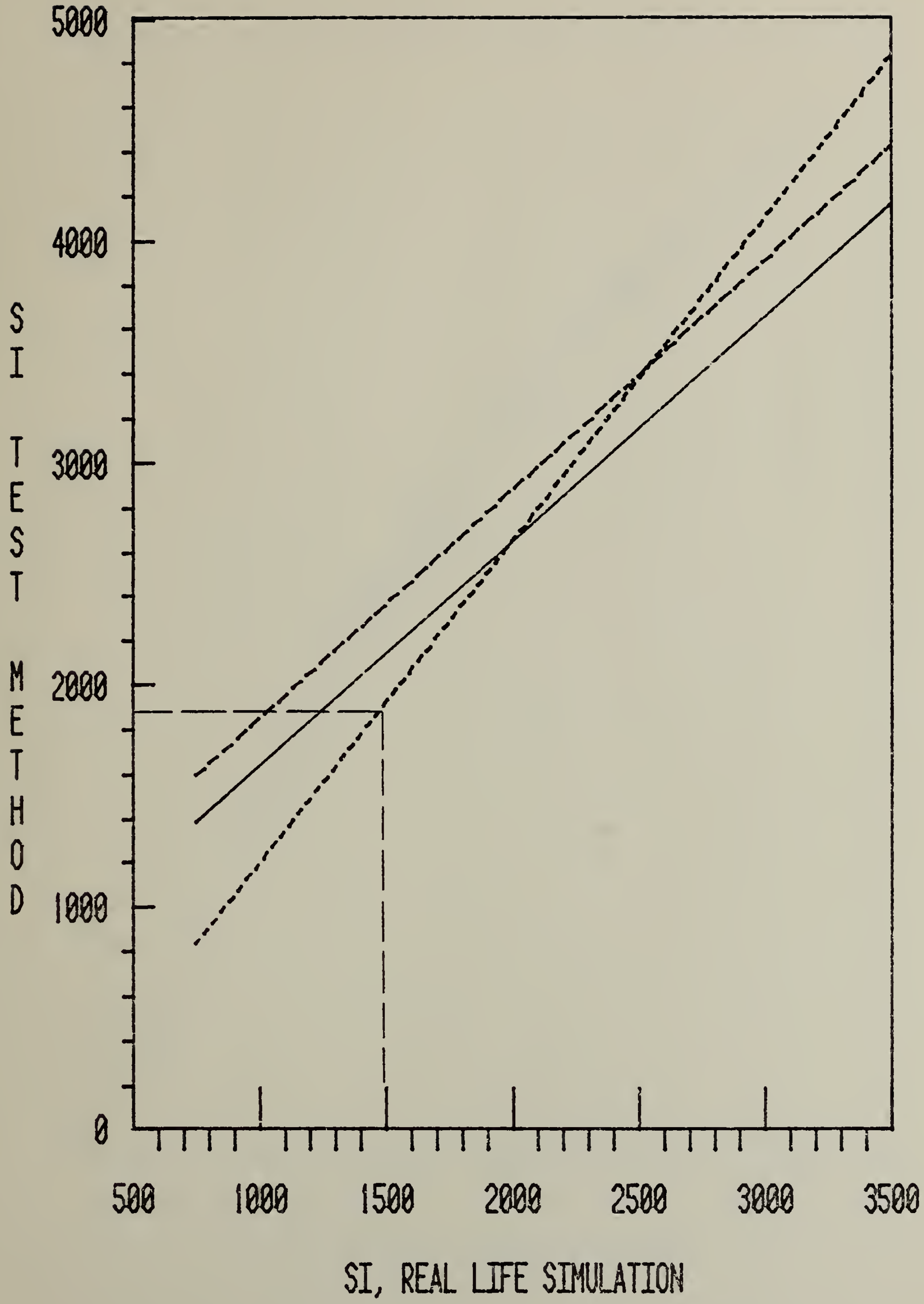
5000
4000
3000
2000
1000
0
SI TEST METHOD
500
1000
1500
2000
2500
3000
3500
SI, REAL LIFE SIMULATION

FIGURE 29

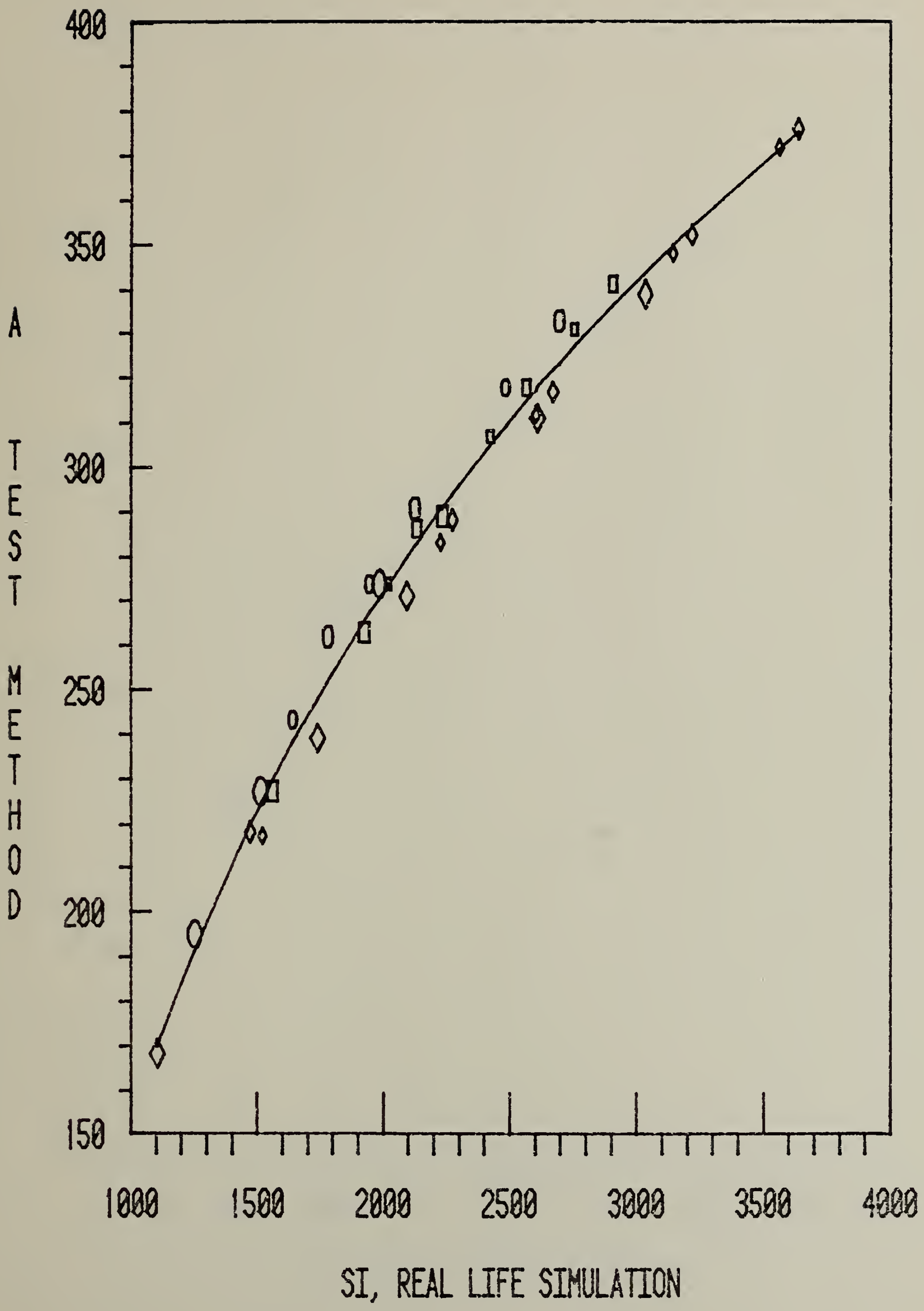

400
350
300
250
200
150
A TEST METHOD
1000
1500
2000
2500
3000
3500
4000
SI, REAL LIFE SIMULATION

FIGURE 30

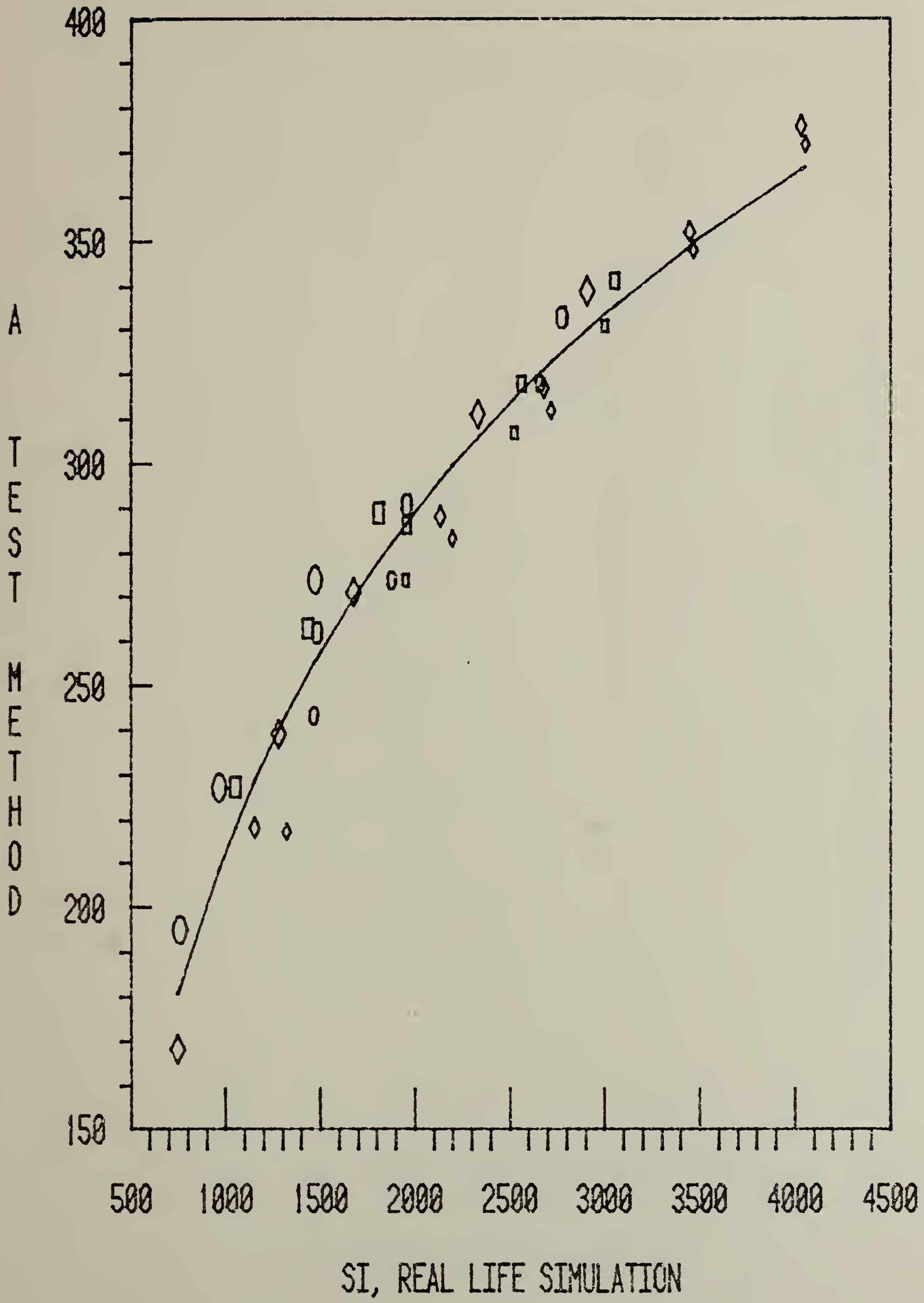
400
350
300
250
200
150
A TEST METHOD
500
1000
1500
2000
2500
3000
3500
4000
4500
SI, REAL LIFE SIMULATION

FIGURE 31

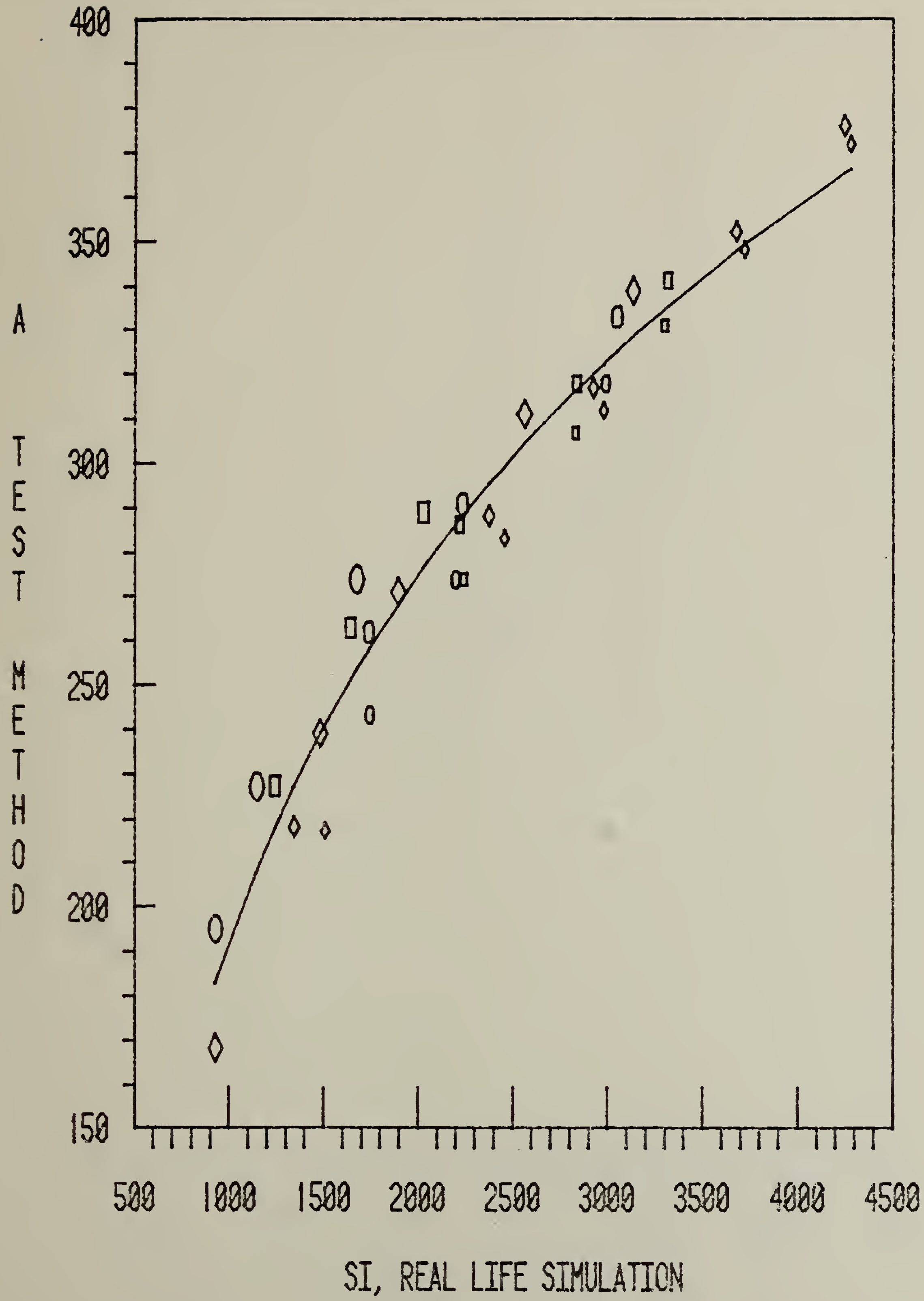

400
350
300
250
200
150
A TEST METHOD
500
1000
1500
2000
2500
3000
3500
4000
4500
SI, REAL LIFE SIMULATION

FIGURE 32

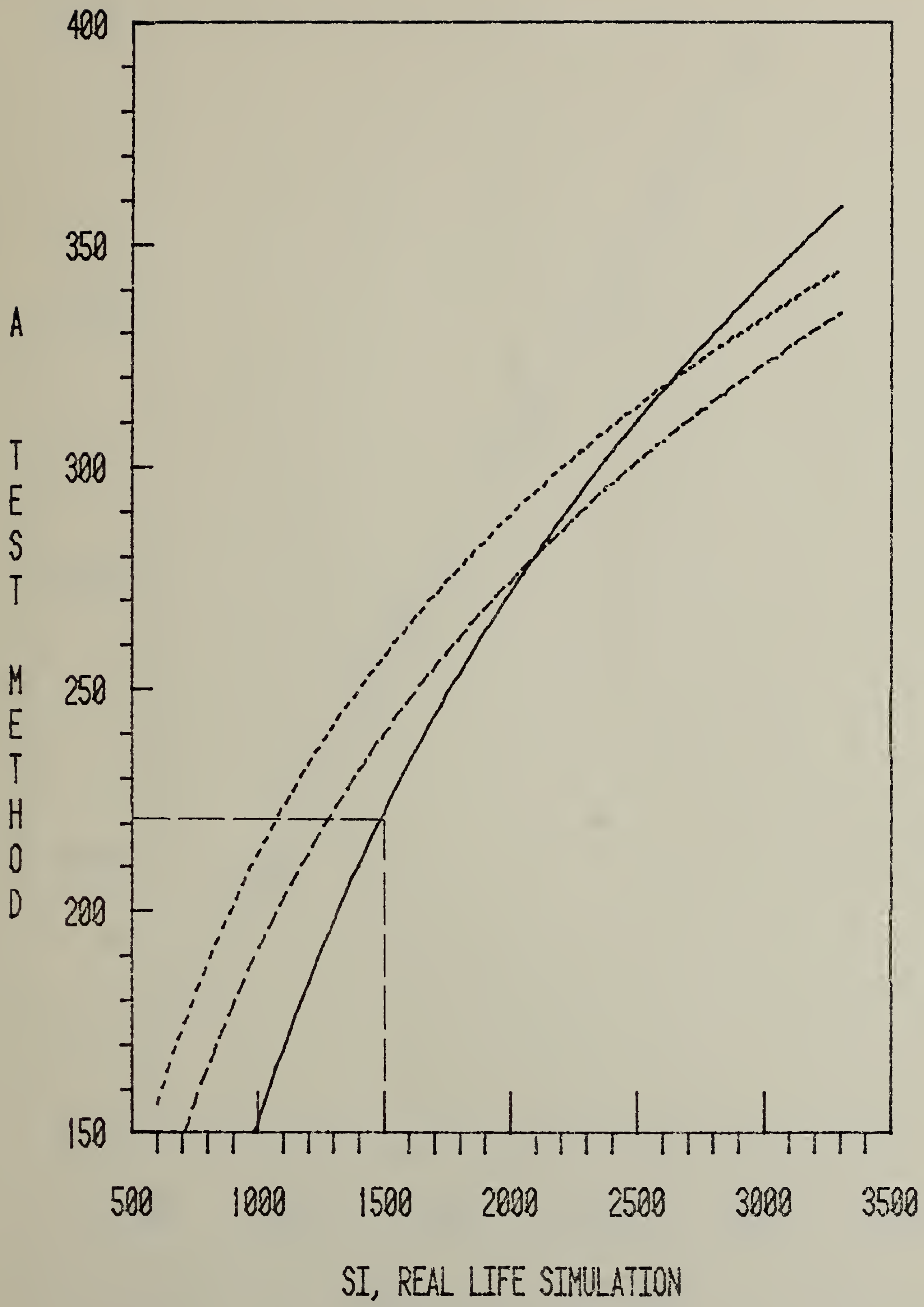

400
350
300
250
200
150
A TEST METHOD
500
1000
1500
2000
2500
3000
3500
SI, REAL LIFE SIMULATION

FIGURE 33

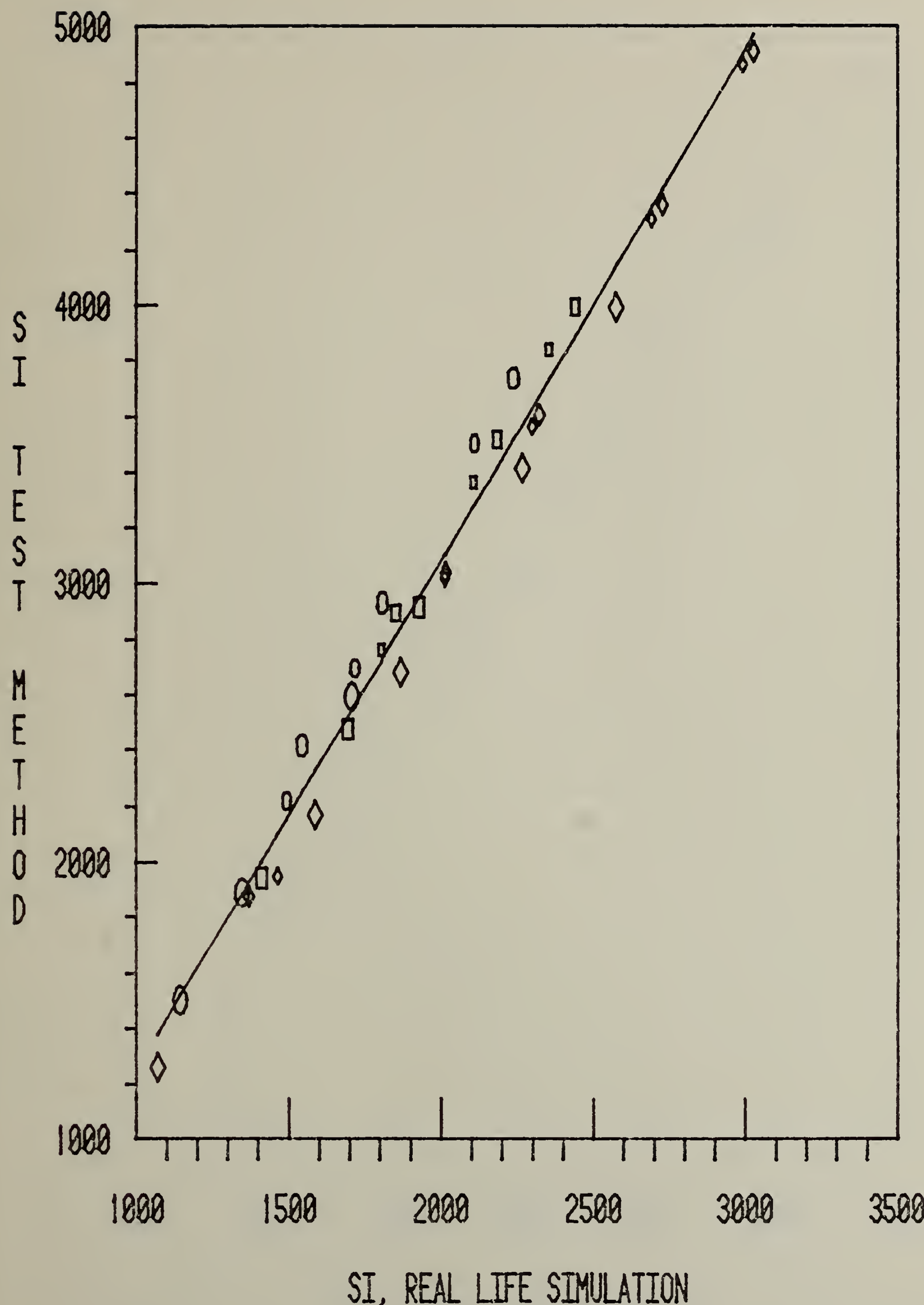
5000
4000
3000
2000
1000
SI TEST METHOD
1000
1500
2000
2500
3000
3500
SI, REAL LIFE SIMULATION

FIGURE 34

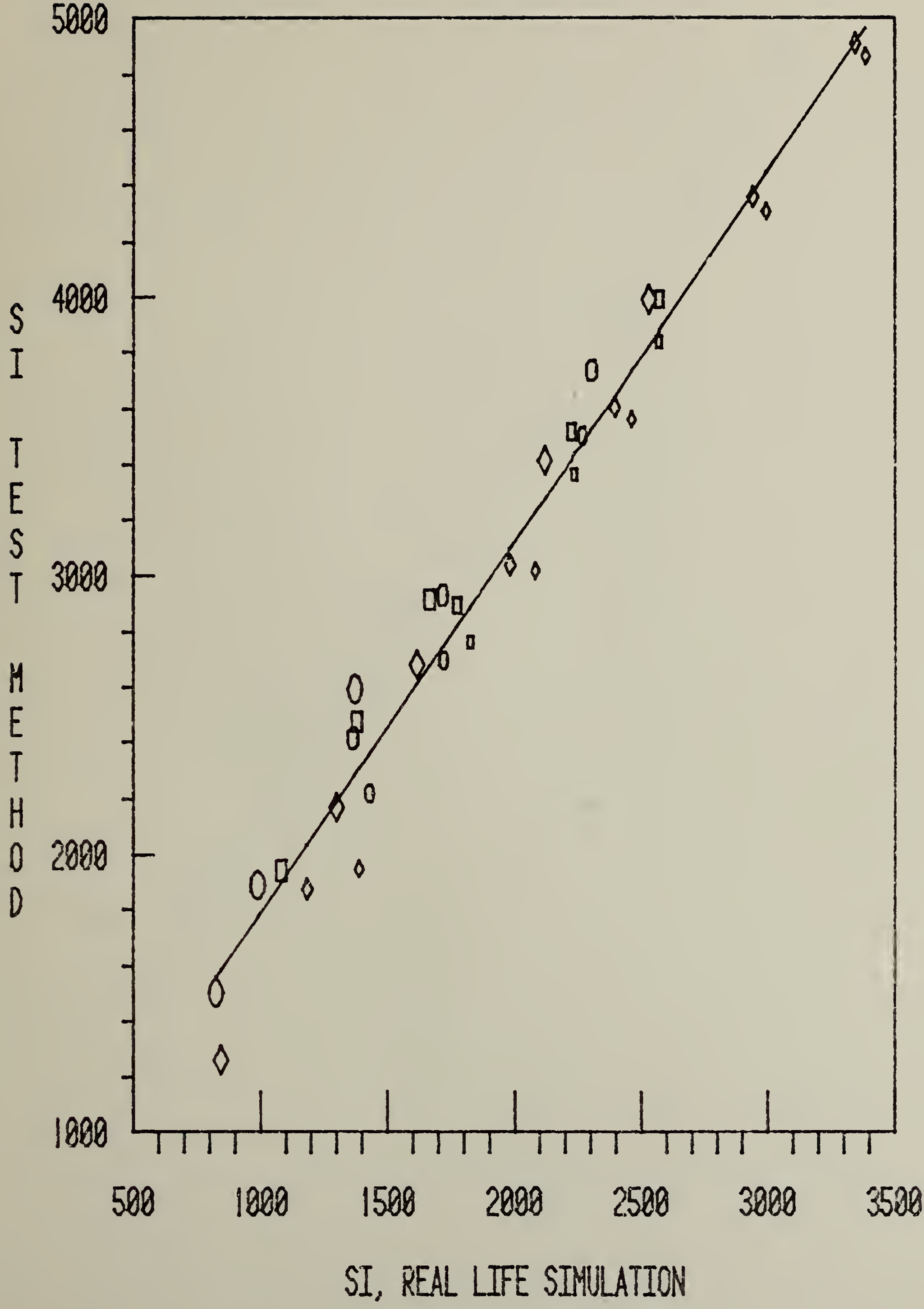
5000
4000
3000
2000
1000
SI TEST METHOD
500
1000
1500
2000
2500
3000
3500
SI, REAL LIFE SIMULATION

FIGURE 35

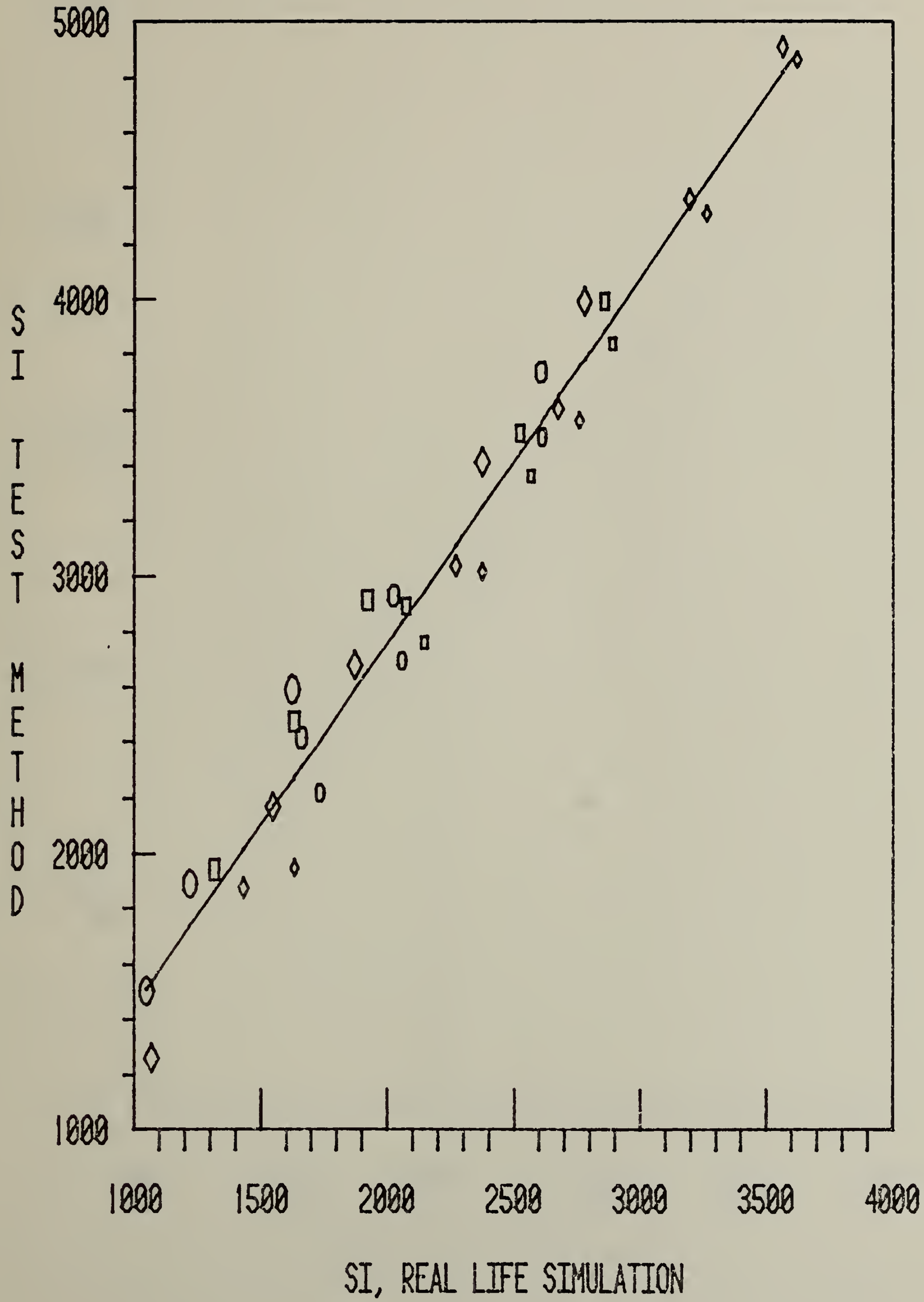

5000
4000
3000
2000
1000
SI TEST METHOD
1000
1500
2000
2500
3000
3500
4000
SI, REAL LIFE SIMULATION

FIGURE 36

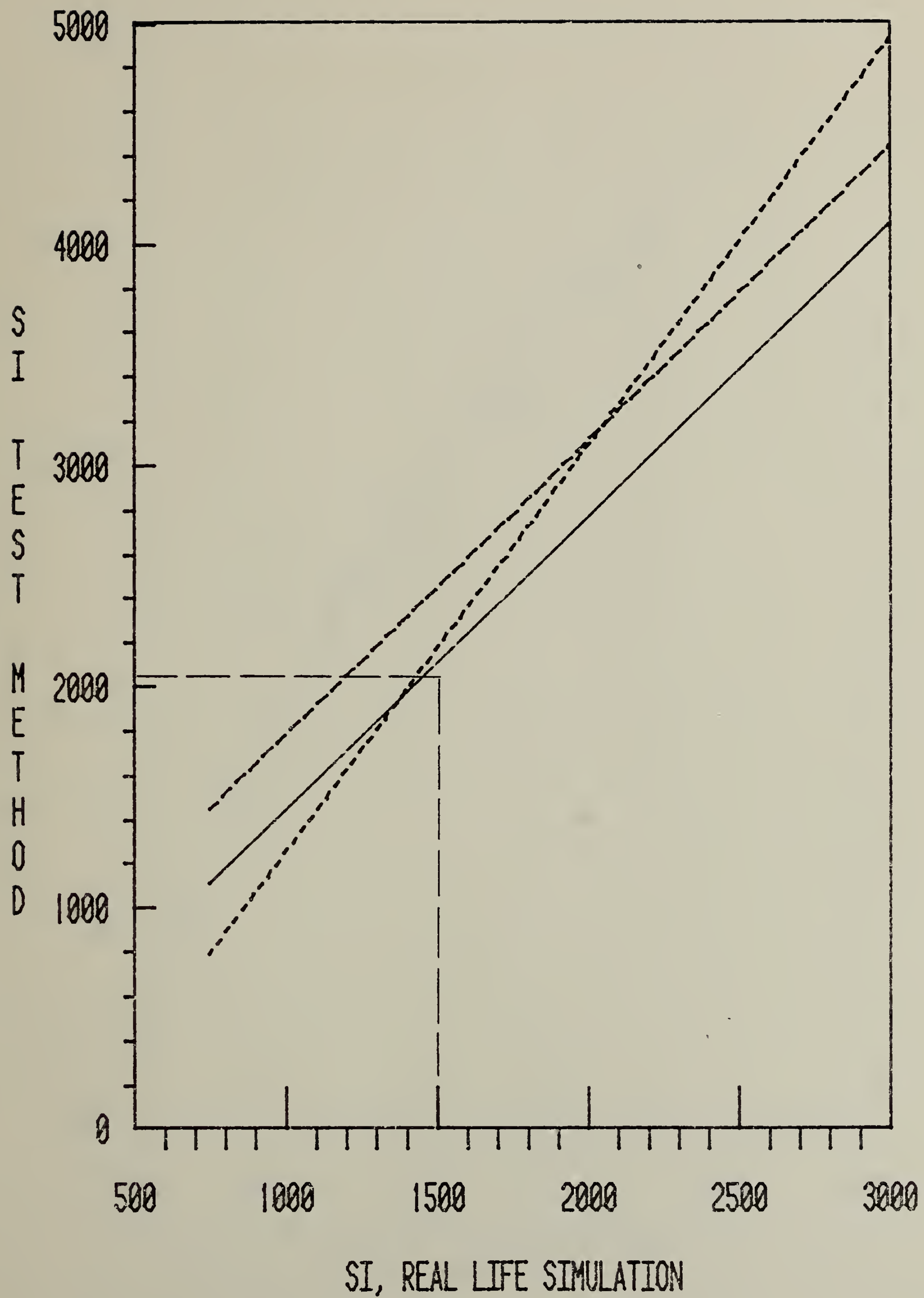
5000
4000
3000
2000
1000
0
SI TEST METHOD
500
1000
1500
2000
2500
3000
SI, REAL LIFE SIMULATION

FIGURE 37

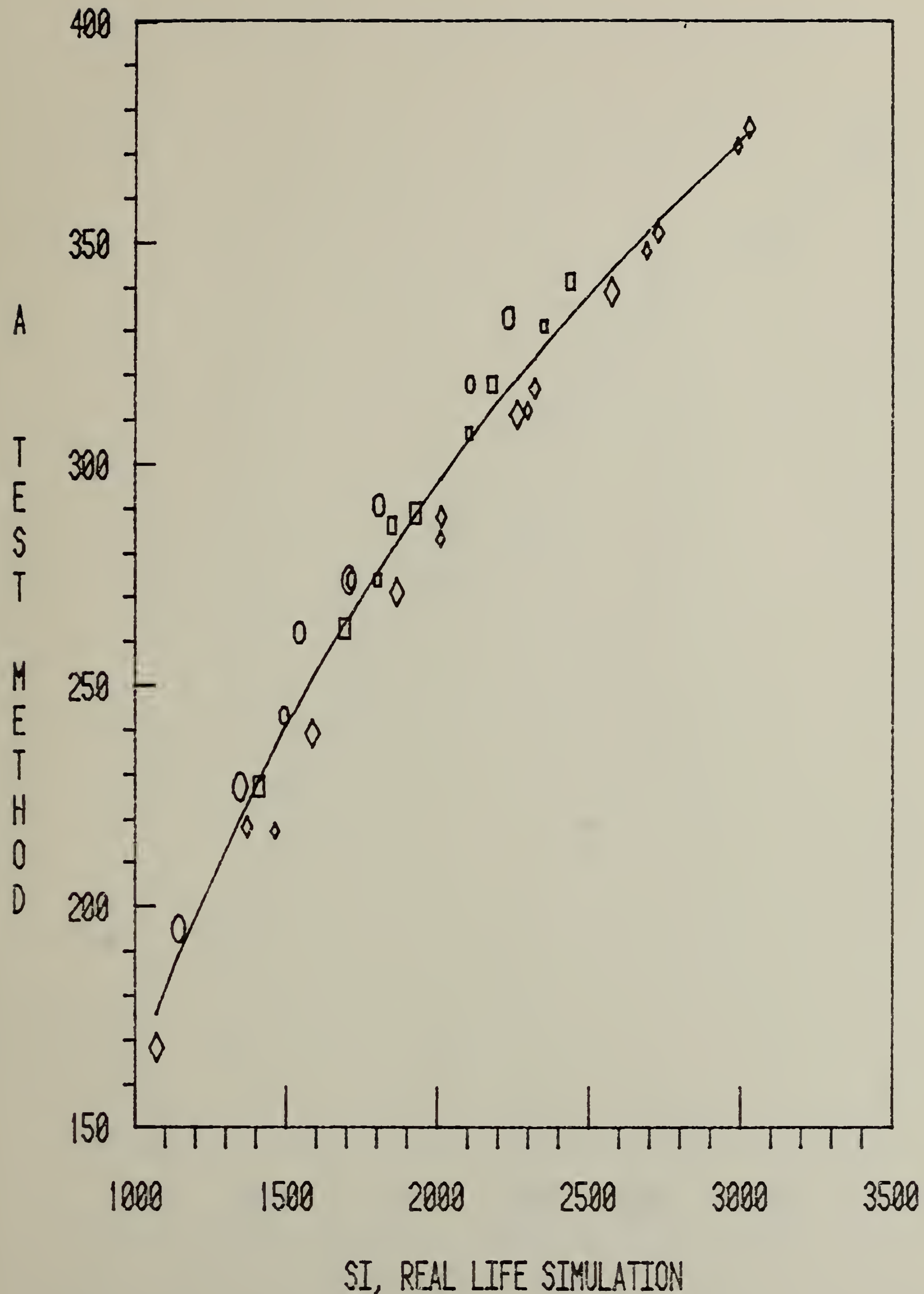
400
350
300
250
200
150
A TEST METHOD
1000
1500
2000
2500
3000
3500
SI, REAL LIFE SIMULATION

FIGURE 38

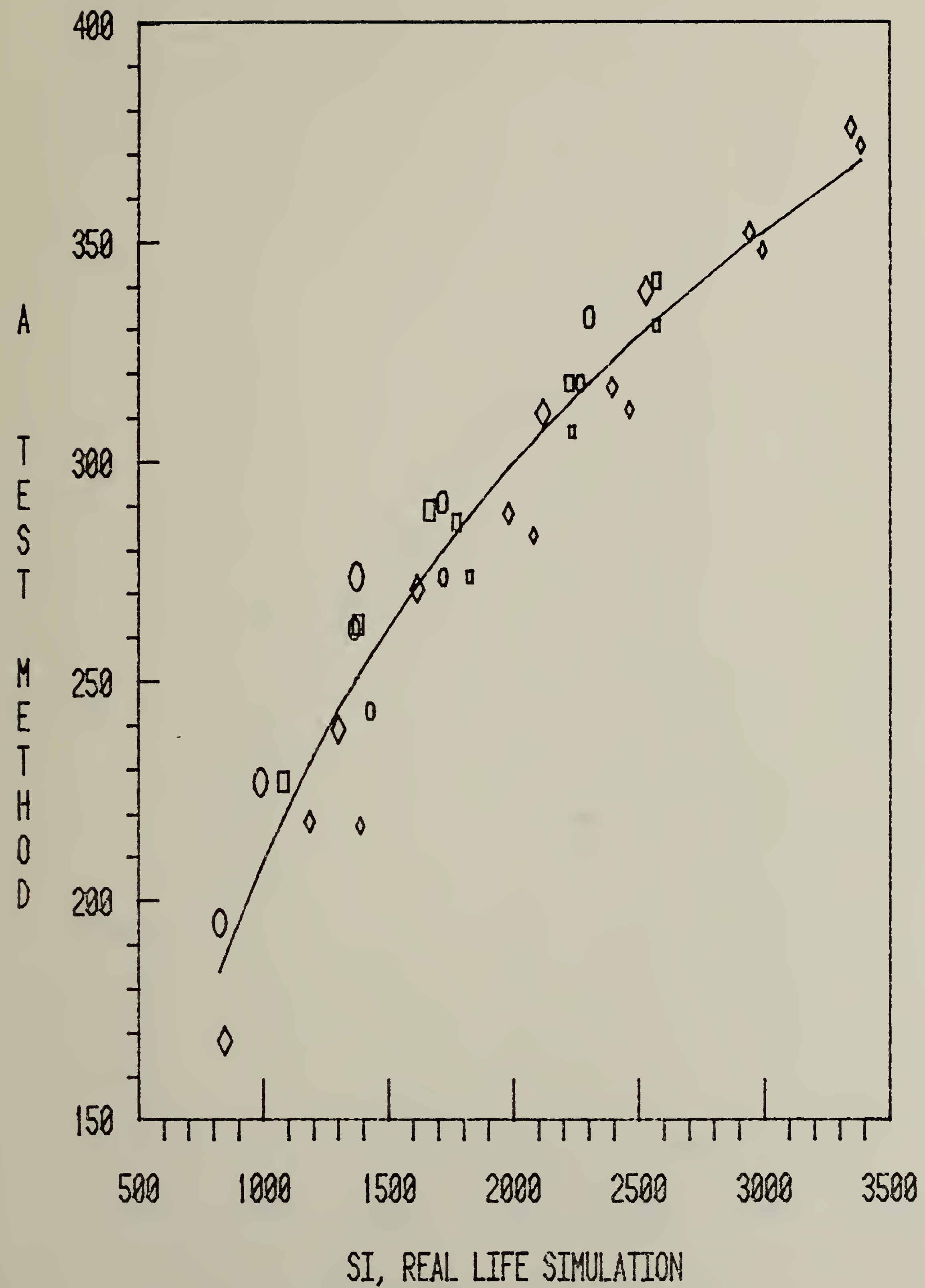
400
350
300
250
200
150
A TEST METHOD
500
1000
1500
2000
2500
3000
3500
SI, REAL LIFE SIMULATION

FIGURE 39

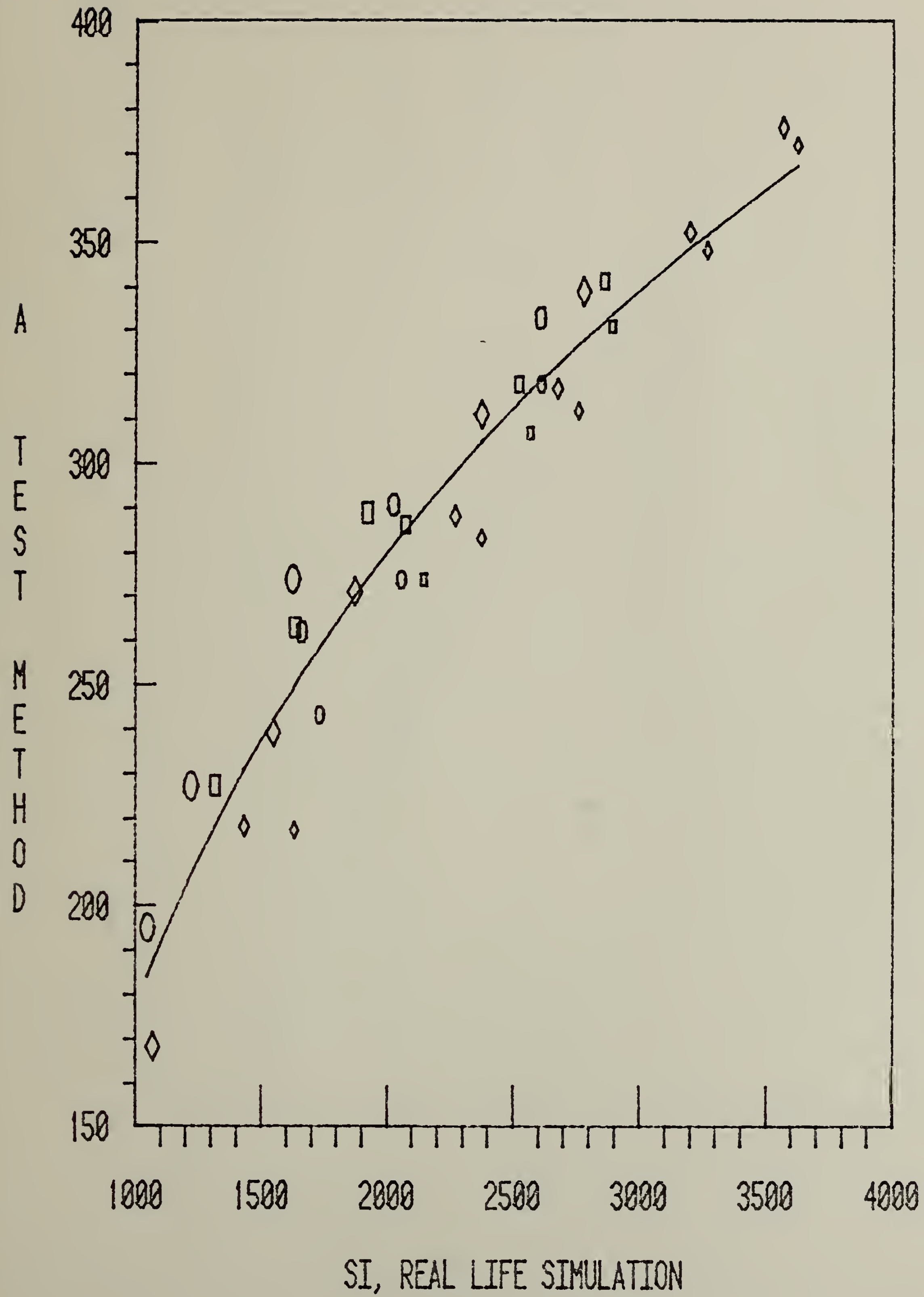
400
350
300
250
200
150
A TEST METHOD
1000
1500
2000
2500
3000
3500
4000
SI, REAL LIFE SIMULATION

FIGURE 40

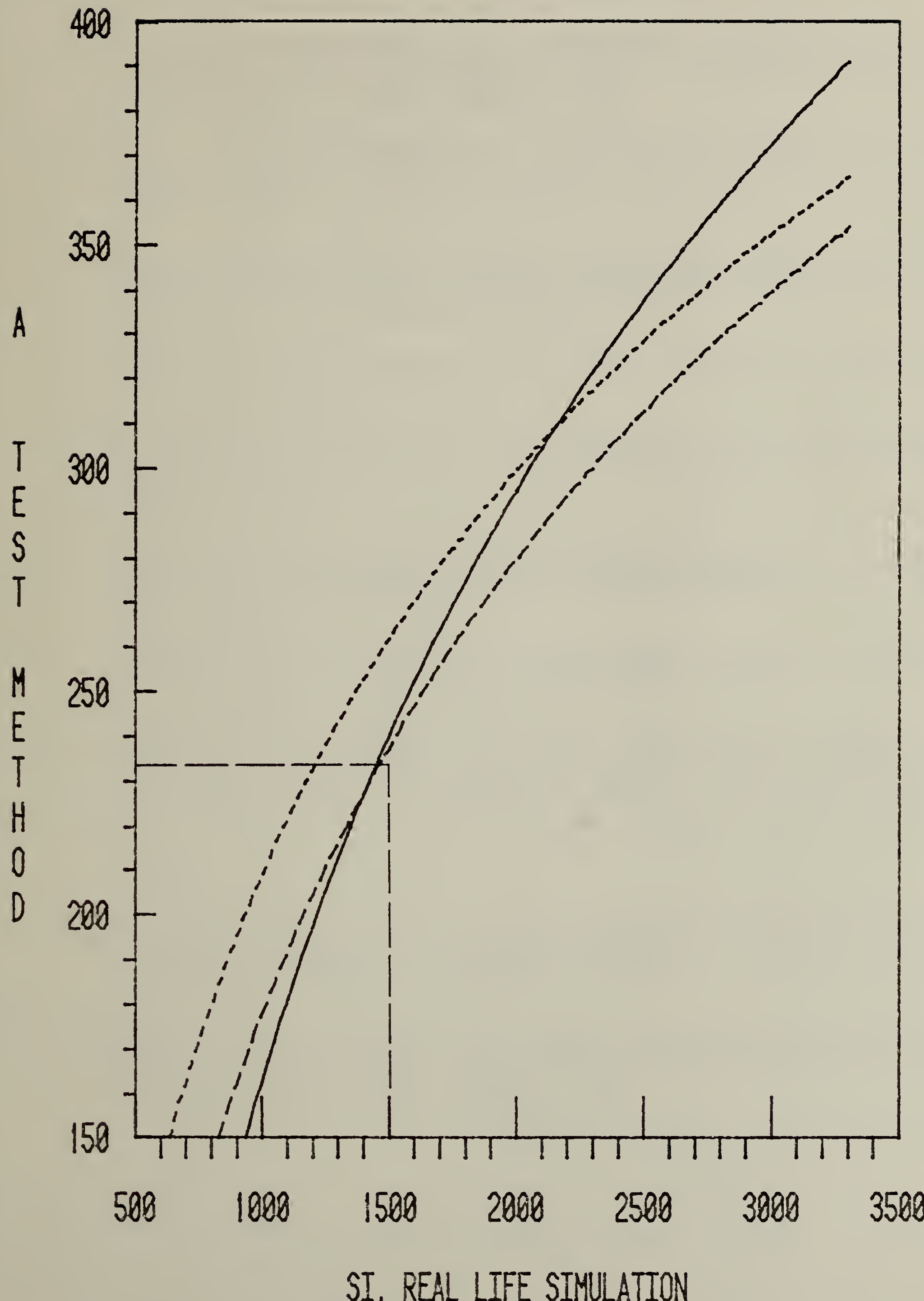
400
350
300
250
200
150
A TEST METHOD
500
1000
1500
2000
2500
3000
3500
SI, REAL LIFE SIMULATION

FIGURE 41

REFERENCES

1. Berger, R.E. and Calvano, N.J., Methodology for Choosing Test Parameters to Evaluate Protective Headgear, National Bureau of Standards, NBSIR78-1547, November 1978.

2. Berger, R.E., Considerations in Developing Test Methods for Protective Headgear, National Bureau of Standards Report, NBSIR76-1107, August 1976.

3. Hodgson, V.R., National Operating Committee on Standards for Athletic Equipment Football Helmet Certification Program, Medicine and Science in Sports, 7 (3) pp. 225-232 (1975).

4. Timoshenko, S. and Goodier, J.N., Theory of Elasticity (2nd Edition) McGraw Hill, New York (1951).

5. Stalnaker, R.L., Fogle, J.L., and McElhaney, J.H., Driving Point Impedance Characteristics of the Head, J. Biomechanics, 4, 127-139 (1971).

6. Gill, S., A Process for the Step-by-Step Integration of Differential Equations in an Automatic Digital Computing Machine, Proc. Cambridge Phil. Soc. 47, p. 96 (1951).

7. Hodgson, V.R. and Thomas, L.M., Head Injury Tolerance, in Aircraft Crashworthiness, K. Saczalski, ed. (1975).

8. Newman, J.A., On the Use of the Head Injury Criterion (HIC) in Protective Headgear Evaluation, Proceedings of the 19th Stapp Car Crash Conference, Society of Automotive Engineers, New York (1975).

9. Nilson, E.N., Cubic Splines on Uniform Meshes, Comm. A.C.M., 13, (4) (1970).

10. Standard Method of Test for Shock Attenuation Characteristics of Protective Headgear for Football, ASTM F429-75, American Society for Testing and Materials, Philadelphia (1975).

11. Mahajan, B.M. and Beine, W.B., Impact Attenuation Performance of Surfaces Installed Under Playground Equipment, National Bureau of Standards, NBSIR79-1707, February 1979.

ACKNOWLEDGMENT

I thank Bill Beine for his essential contributions in data reduction, statistical analysis, and effective graphical presentations.

NBS-114A (REV. 9-78)

U.S. DEPT. OF COMM. BIBLIOGRAPHIC DATA SHEET	1. PUBLICATION OR REPORT NO. NBSIR80-1987	2. Gov't. Accession No.	3. Recipient's Accession No.

4. TITLE AND SUBTITLE	5. Publication Date
A Mathematical Model for Use in Evaluating and Developing Impact Test Methods for Protective Headgear	March 1980
	6. Performing Organization Code
7. AUTHOR(S) Robert E. Berger	8. Performing Organ. Report No.
9. PERFORMING ORGANIZATION NAME AND ADDRESS NATIONAL BUREAU OF STANDARDS DEPARTMENT OF COMMERCE WASHINGTON, DC 20234	10. Project/Task/Work Unit No. 11. Contract/Grant No.
12. SPONSORING ORGANIZATION NAME AND COMPLETE ADDRESS (Street, City, State, ZIP) National Bureau of Standards Department of Commerce Washington, D.C. 20234	13. Type of Report & Period Covered 14. Sponsoring Agency Code

15. SUPPLEMENTARY NOTES

☐ Document describes a computer program; SF-185, FIPS Software Summary, is attached.

16. ABSTRACT *(A 200-word or less factual summary of most significant information. If document includes a significant bibliography or literature survey, mention it here.)*

A lumped parameter mathematical model was developed to connect injury parameters in real life head impact environments to output parameters of test methods for evaluating protective headgear. Analytical/experimental schemes were developed for mathematically representing the parameters that characterize each of the three distinct elements of the model: the head or headform, the impact surface, the helmet. A comparison of the model output to experimental results showed a satisfactory agreement. The model was shown to be useful in determining test method pass/fail criteria which correspond to the threshold of injury in the real life situation.

17. KEY WORDS *(six to twelve entries; alphabetical order; capitalize only the first letter of the first key word unless a proper name; separated by semicolons)*

Drop test parameter; head injury; helmet; injury criteria; mathematical model; test methods

18. AVAILABILITY ☒ Unlimited	19. SECURITY CLASS (THIS REPORT)	21. NO. OF PRINTED PAGES
☐ For Official Distribution. Do Not Release to NTIS	UNCLASSIFIED	74
☐ Order From Sup. of Doc., U.S. Government Printing Office, Washington, DC 20402, SD Stock No. SN003-003-	20. SECURITY CLASS (THIS PAGE)	22. Price
☒ Order From National Technical Information Service (NTIS), Springfield, VA. 22161	UNCLASSIFIED	$7.00

USCOMM-DC